



Search for a CP-odd Higgs boson decaying into a heavy CP-even Higgs boson and a Z boson in the $\ell^+\ell^-t\bar{t}$ and $\nu\bar{\nu}b\bar{b}$ final states using 140 fb^{-1} of data collected with the ATLAS detector

The ATLAS Collaboration

A search for a heavy CP-odd Higgs boson, A , decaying into a Z boson and a heavy CP-even Higgs boson, H , is presented. It uses the full LHC Run 2 dataset of pp collisions at $\sqrt{s} = 13\text{ TeV}$ collected with the ATLAS detector, corresponding to an integrated luminosity of 140 fb^{-1} . The search for $A \rightarrow ZH$ is performed in the $\ell^+\ell^-t\bar{t}$ and $\nu\bar{\nu}b\bar{b}$ final states and surpasses the reach of previous searches in different final states in the region with $m_H > 350\text{ GeV}$ and $m_A > 800\text{ GeV}$. No significant deviation from the Standard Model expectation is found. Upper limits are placed on the production cross-section times the decay branching ratios. Limits with less model dependence are also presented as functions of the reconstructed $m(t\bar{t})$ and $m(b\bar{b})$ distributions in the $\ell^+\ell^-t\bar{t}$ and $\nu\bar{\nu}b\bar{b}$ channels, respectively. In addition, the results are interpreted in the context of two-Higgs-doublet models.

Contents

1	Introduction	2
2	ATLAS detector	4
3	Data and simulated event samples	5
4	Object reconstruction	6
5	Event selection and background estimation	7
5.1	$\ell^+\ell^-t\bar{t}$ selection	8
5.2	$\nu\bar{\nu}b\bar{b}$ selection	10
6	Systematic uncertainties	12
7	Statistical analysis	13
8	Results	15
8.1	Upper limits on the production cross-section for $A \rightarrow ZH \rightarrow \ell^+\ell^-t\bar{t}/\nu\bar{\nu}b\bar{b}$	18
8.2	Interpretation in the context of 2HDM	20
8.3	Model-independent limits	23
9	Conclusion	24
	Upper limits on the production cross sections for additional $\tan\beta$ values	26

1 Introduction

The discovery of a Higgs boson at the Large Hadron Collider (LHC) [1, 2] raised the question of whether this particle is part of an extended scalar sector, a scenario which arises in several models that attempt to explain the shortcomings of the Standard Model (SM), such as the hierarchy problem, the excess of matter over antimatter in the observable universe and the existence of dark matter. This question has motivated experimental searches for extended scalar sectors at the LHC [3]. A simple such extension that has received a lot of attention is the two-Higgs-doublet model (2HDM) [4, 5]. The 2HDM is popular due to its very rich phenomenology and the fact that it is motivated by several new physics scenarios such as supersymmetry [6], dark matter [7, 8] and axion [9] models, electroweak baryogenesis [10] and neutrino mass models [11].

A second Higgs doublet leads to five Higgs bosons after electroweak symmetry breaking. The phenomenology depends on many parameters, including the masses of the Higgs bosons and the parameters of the Higgs potential. Phenomenological studies often assume CP-conservation and discrete symmetries that eliminate quartic terms odd in either of the doublets [12]. This leads to two CP-even Higgs bosons, h and H , with $m_h < m_H$, one CP-odd boson, A , and two charged scalars, H^\pm . This model has seven free parameters, usually taken to be the masses of the Higgs bosons (m_h, m_H, m_A, m_{H^\pm}), the ratio of the vacuum expectation values of the two doublets ($\tan\beta$), the potential parameter (m_{12}), and the mixing angle (α) of

the CP-even Higgs bosons. It is usually assumed that the h boson is the Higgs boson that was discovered at the LHC and has $m_h \simeq 125$ GeV. In this scenario, h has the same couplings to fermions and vector bosons as the SM Higgs boson at lowest order in the limit that $\cos(\beta - \alpha) = 0$, known as the alignment limit.

Precision electroweak measurements [13] suggest that the masses of two of the heavy Higgs bosons in the 2HDM are degenerate. This has motivated many LHC searches, such as for the $A \rightarrow Zh$ process [14, 15], where $m_A = m_H$ is assumed when interpreting the results. The scenario $m_A \neq m_H$ has strong motivation from electroweak baryogenesis models [16–20]; in particular, $m_A > m_H$ is favoured [17] for a strong first-order phase transition to have occurred in the early universe. The A boson mass is also constrained to be not far above 1 TeV [16, 21], whereas the h boson is required to have properties similar to those of a SM Higgs boson and hence it is compatible with the Higgs boson that was observed at the LHC [17].

In such a scenario, the most promising experimental signature is an A boson produced either via gluon–gluon fusion (ggF, Figure 1(a)) or in association with b -quarks (bbA, Figure 1(b)), with a subsequent decay into ZH , which dominates when the mass difference $m_A - m_H$ becomes large. The signature of the $A \rightarrow ZH$ process has been sought at the LHC in final states where the Z boson decays leptonically ($Z \rightarrow \ell^+\ell^-$) and the H boson decays into $b\bar{b}$, WW or $\tau\tau$ [22–24]. These final states, although very sensitive, cannot probe the parameter space in which $m_H > 2m_{\text{top}}$, where the $H \rightarrow t\bar{t}$ decay becomes dominant. This parameter space was probed recently with $A \rightarrow ZH$ and $H \rightarrow hh$ [25], but this decay chain is not sensitive in the alignment limit.

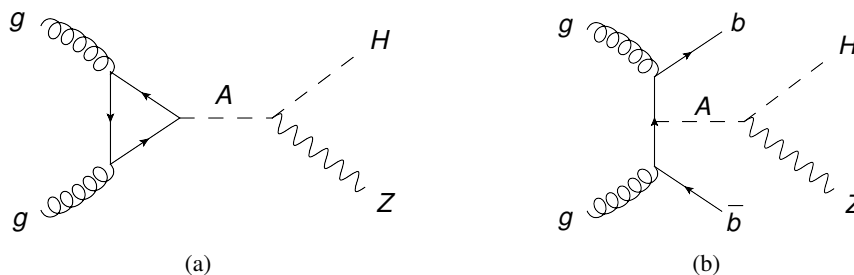


Figure 1: Feynman diagrams for the ggF (a) and bbA (b) production modes. The searches presented in this paper target final states in which the H boson decays into $t\bar{t}$ or $b\bar{b}$ and the Z boson decays into $\ell^+\ell^-$ or $\nu\bar{\nu}$.

The first search presented in this paper aims to cover this unexplored phase space by searching for $A \rightarrow ZH$ in the $\ell^+\ell^-t\bar{t}$ final state. Top-quark pairs ($t\bar{t}$) in which one top-quark decays semileptonically and the other decays hadronically are considered. This leads to a signature with three leptons (electrons or muons) and at least four jets, two of which are expected to have originated from b -quarks.

In addition, a search for $A \rightarrow ZH$ with the Z boson decaying into neutrinos and the H boson decaying into a pair of b -quarks is performed. This constitutes the first search at the LHC for $b\bar{b}$ resonances with a mass up to 2 TeV produced in association with missing transverse momentum, and complements the sensitivity of the $\ell^+\ell^-b\bar{b}$ search [22] at high m_A , due to the higher branching ratio of the Z boson decay into neutrinos [14]. Moreover, this search could also be reinterpreted in the context of hierarchical 2HDMs with extra mediators coupling to dark matter [8], thus also complementing the existing searches [26] in the high m_H regime.

2 ATLAS detector

The ATLAS detector [27] at the LHC covers nearly the entire solid angle around the collision point.¹ It consists of an inner tracking detector surrounded by a thin superconducting solenoid, electromagnetic and hadron calorimeters, and a muon spectrometer incorporating three large superconducting air-core toroidal magnets.

The inner-detector system (ID) is immersed in a 2 T axial magnetic field and provides charged-particle tracking in the range $|\eta| < 2.5$. The high-granularity silicon pixel detector covers the vertex region and typically provides four measurements per track, the first hit normally being in the insertable B-layer installed before Run 2 [28, 29]. It is followed by the silicon microstrip tracker, which usually provides eight measurements per track. These silicon detectors are complemented by the transition radiation tracker (TRT), which enables radially extended track reconstruction up to $|\eta| = 2.0$. The TRT also provides electron identification information based on the fraction of hits (typically 30 in total) above a higher energy-deposit threshold corresponding to transition radiation.

The calorimeter system covers the pseudorapidity range $|\eta| < 4.9$. Within the region $|\eta| < 3.2$, electromagnetic calorimetry is provided by barrel and endcap high-granularity lead/liquid-argon (LAr) calorimeters, with an additional thin LAr presampler covering $|\eta| < 1.8$ to correct for energy loss in material upstream of the calorimeters. Hadron calorimetry is provided by the steel/scintillator-tile calorimeter, segmented into three barrel structures within $|\eta| < 1.7$, and two copper/LAr hadron endcap calorimeters. The solid angle coverage is completed with forward copper/LAr and tungsten/LAr calorimeter modules optimised for electromagnetic and hadronic energy measurements respectively.

The muon spectrometer (MS) comprises separate trigger and high-precision tracking chambers measuring the deflection of muons in a magnetic field generated by the superconducting air-core toroidal magnets. The field integral of the toroids ranges between 2.0 and 6.0 T m across most of the detector. Three layers of precision chambers, each consisting of layers of monitored drift tubes, cover the region $|\eta| < 2.7$, complemented by cathode-strip chambers in the forward region, where the background is highest. The muon trigger system covers the range $|\eta| < 2.4$ with resistive-plate chambers in the barrel, and thin-gap chambers in the endcap regions.

Interesting events are selected by the first-level trigger system implemented in custom hardware, followed by selections made by algorithms implemented in software in the high-level trigger [30]. The first-level trigger accepts events from the 40 MHz bunch crossings at a rate below 100 kHz, which the high-level trigger reduces in order to record events to disk at about 1 kHz.

An extensive software suite [31] is used in data simulation, in the reconstruction and analysis of real and simulated data, in detector operations, and in the trigger and data acquisition systems of the experiment.

¹ ATLAS uses a right-handed coordinate system with its origin at the nominal interaction point (IP) in the centre of the detector and the z -axis along the beam pipe. The x -axis points from the IP to the centre of the LHC ring, and the y -axis points upwards. Cylindrical coordinates (r, ϕ) are used in the transverse plane, ϕ being the azimuthal angle around the z -axis. The pseudorapidity is defined in terms of the polar angle θ as $\eta = -\ln \tan(\theta/2)$. Angular distance is measured in units of $\Delta R \equiv \sqrt{(\Delta\eta)^2 + (\Delta\phi)^2}$.

3 Data and simulated event samples

The search presented here uses 140 fb^{-1} of proton–proton collision data at a centre-of-mass energy (\sqrt{s}) of 13 TeV recorded by the ATLAS detector during the years 2015–2018 (Run 2). All events were required to pass basic data-quality requirements which ensure that all components of the ATLAS detector were functioning correctly [32].

For the analysis targeting the $\ell^+ \ell^- t \bar{t}$ final state, events were recorded using a logical OR of single-electron triggers with transverse momentum (p_T) thresholds varying from 24 to 26 GeV or single-muon triggers with p_T thresholds varying from 20 to 26 GeV and a combination of quality and isolation requirements. Offline, the leptons were required to be geometrically matched to the corresponding trigger object and to have a p_T threshold 1–2 GeV above the high-level trigger threshold to operate in the region where the trigger reaches its maximum efficiency. For the analysis targeting the $\nu \bar{\nu} b \bar{b}$ final state, events were recorded by the missing transverse momentum (E_T^{miss}) triggers with thresholds varying between 70 and 110 GeV, which become fully efficient for an offline E_T^{miss} value of approximately 200 GeV. The trigger efficiencies in simulation are corrected to match those observed in data. For the E_T^{miss} triggers, this is done following the procedure in Ref. [33]. Events with one or two leptons that are used to define background-enriched control regions in the $\nu \bar{\nu} b \bar{b}$ channel are selected with the same single-lepton triggers as in the $\ell^+ \ell^- t \bar{t}$ channel.

Simulated signal events were generated with MADGRAPH5_AMC@NLO (MG5AMC) 2.3.3 [34], requiring an s -channel A boson that decays into a Z boson and H boson, and using the UFO model provided in Ref. [8] to calculate the loop-induced ggF process with a finite m_{top} value.² Both the ggF and bbA production modes (shown in Figure 1) were generated at leading order (LO) in QCD for various combinations of (m_A, m_H) using the NNPDF3.0NLO set of parton distribution functions (PDF) [35], with the former including contributions from top-quark loop-induced processes but neglecting contributions from bottom-loop induced processes, which have a negligible impact on the kinematic distributions. The ggF samples were generated at $\tan \beta = 1$ and the bbA production samples were generated at $\tan \beta = 5$. Simulated events with different values of $\tan \beta$ were obtained via matrix-element reweighting [36]. The decay widths of the A and H bosons were calculated by MG5AMC at LO and finite-width effects were included in the simulation. The decays of the Z and H bosons were simulated using MADSPIN [37, 38]. PYTHIA 8.244 [39] was used to model the parton shower and hadronisation, using the A14 [40] set of tuned parameters (tune). Non-resonant diagrams, in which the ZH final state is produced through a top-quark box were found to have a negligible impact and thus were not included in the simulation. The interference between the resonant diagram shown in Figure 1 and the non-resonant box diagrams, and also the SM $t \bar{t} Z$ process, was studied using the UFO model provided in Ref. [41] and found to be negligible. The generation of events in the $\nu \bar{\nu} b \bar{b}$ final state required $E_T^{\text{miss}} > 100 \text{ GeV}$, which increased the efficiency of the simulation by improving the acceptance. Simulated events in the $\ell^+ \ell^- t \bar{t}$ final state were filtered to select events with at least one top-quark decaying semileptonically, with no kinematic requirements on the generator-level leptons.

Simulated events for the background processes were generated as shown in Table 1. The decays of bottom and charm hadrons were simulated using EVTGEN 1.6.0 [42], except for the samples generated using SHERPA [43], in which case these decays were generated within SHERPA.

The effect of multiple interactions in the same and neighbouring bunch crossings (pile-up) in all simulated samples was modelled by overlaying each hard-scattering event with simulated inelastic proton–proton

² This UFO model contains a priori an extra CP-odd Higgs boson a that mixes with the CP-odd Higgs boson A of the 2HDM with a mixing angle $\sin \theta$. This is completely decoupled in the signal generation by setting $\sin \theta = 0$, thereby effectively yielding a 2HDM with five physical Higgs bosons.

Table 1: List of generators used for the simulation of different processes. (N)(N)LO or (N)NLL refers to (next-to-)(next-to-)leading order or (next-to-)next-to-leading-logarithm accuracy in the perturbative expansion of the cross-sections, while EW refers to the inclusion of electroweak corrections at the order indicated. For all samples using the A14 or AZNLO tune, the NNPDF2.3_{LO} [48] or CTEQ6L1 [49] PDF set was used, respectively. The diagram removal (DR) and diagram subtraction (DS) schemes [50] were used to remove the overlap between the $t\bar{t}Z/tWZ$ and $t\bar{t}/tW$ processes, respectively. V denotes a W or Z boson.

Process	Matrix element	QCD order	PDF	Parton shower	Tune	Cross-section	Special settings
$t\bar{t}$	POWHEG v2 [51–54]	NLO	NNPDF3.0 _{NLO} [35]	PYTHIA 8.230 [39]	A14 [40]	NNLO+NNLL QCD [55–61]	$h_{\text{damp}} = 1.5m_{\text{top}}$
tW	POWHEG v2 [52–54, 62]	NLO	NNPDF3.0 _{NLO} [35]	PYTHIA 8.230 [39]	A14 [40]	NLO+NNLL QCD [63, 64]	DS scheme [50]
Single top t -channel	POWHEG v2 [52–54, 65]	NLO	NNPDF3.0 _{NLO} [35]	PYTHIA 8.230 [39]	A14 [40]	NLO QCD [66, 67]	4-flavour scheme
Single top s -channel	POWHEG v2 [52–54, 65]	NLO	NNPDF3.0 _{NLO} [35]	PYTHIA 8.230 [39]	A14 [40]	NLO QCD [66, 67]	5-flavour scheme
V +jets	SHERPA 2.2.1 [68]	0,1 jets @ NLO 2,3,4 jets @ LO	NNPDF3.0 _{NNLO} [35]	SHERPA [43]	default	NNLO [69]	MEPS@NLO [70–73]
Diboson $q\bar{q} \rightarrow VV$	SHERPA 2.2.1 [68]	0,1 jets @ NLO 2,3 jets @ LO	NNPDF3.0 _{NNLO} [35]	SHERPA [43]	default	NLO QCD	MEPS@NLO [70–73]
Diboson $gg \rightarrow VV$	SHERPA 2.2.2 [68]	0,1 jets @ LO	NNPDF3.0 _{NNLO} [35]	SHERPA [43]	default	NLO QCD	MEPS@NLO [70–73]
$q\bar{q} \rightarrow Vh$	POWHEG v2 [54]	NLO	NNPDF3.0 _{NLO} [35]	PYTHIA 8.212 [39]	AZNLO [74]	NNLO QCD + NLO EW [77–83]	MinLO [75, 76]
$gg \rightarrow Zh$	POWHEG v2 [54]	NLO	NNPDF3.0 _{NLO} [35]	PYTHIA 8.212 [39]	AZNLO [74]	NLO+NNLL QCD [84–86]	-
$t\bar{t}V$	MG5AMC 2.3.3 [34]	NLO	NNPDF3.0 _{NLO} [35]	PYTHIA 8.210 [39]	A14 [40]	NLO QCD + NLO EW [87]	$t\bar{t}l\bar{l}$ scaled by $\mathcal{O}(\alpha_s^3\alpha)$ off-shell correction
$t\bar{t}H$	POWHEG v2 [51–54, 88]	NLO	NNPDF3.0 _{NLO} [35]	PYTHIA 8.230 [39]	A14 [40]	NLO QCD + NLO EW [87]	-
tZq	MG5AMC 2.3.3 [34]	NLO	NNPDF3.0 _{NLO} [35]	PYTHIA 8.230 [39]	A14 [40]	NLO QCD	4-flavour scheme, off-shell effects, top decays in MadSpin [37, 38]
$t\bar{t}t\bar{t}$ $t\bar{t}WW$	MG5AMC 2.3.2 [34]	LO	NNPDF3.1 _{LO} [35]	PYTHIA 8.186 [44]	A14 [40]	LO QCD	top decays in MadSpin [37, 38]
tWZ	MG5AMC 2.6.2 [34]	LO	NNPDF3.1 _{LO} [35]	PYTHIA 8.235 [39]	A14 [40]	LO QCD	top decays in MadSpin [37, 38], DR scheme [50]
VVV	SHERPA 2.2.2 [68]	0 jets @ NLO 1,2 jets @ LO	NNPDF3.0 _{NNLO} [35]	SHERPA [43]	default	NLO QCD	-

events generated with PYTHIA 8.186 [44] using the NNPDF2.3_{LO} PDF set and the A3 tune [45]. The simulated events were weighted to reproduce the distribution of the average number of interactions per bunch crossing observed in the data. All generated background samples were passed through the GEANT4-based [46] detector simulation [47] of the ATLAS detector. The ATLFast-II simulation [47] was used for the signal samples. The simulated events were reconstructed in the same way as the data (see Section 4).

4 Object reconstruction

Tracks measured in the ID are used to reconstruct interaction vertices [89]. The one with the highest sum of squared transverse momenta of associated tracks is selected as the primary vertex and its position is taken as the proton–proton collision point in the reconstruction of physics objects.

Electrons are reconstructed from a track matched to a cluster built from energy deposits in the calorimeter [90]. They are identified using a multivariate likelihood technique [91], using the ‘loose’ working point (WP) for the $\nu\bar{\nu}b\bar{b}$ channel and the ‘medium’ WP for the $\ell^+\ell^-t\bar{t}$ channel, and they are required to fulfil loose calorimeter isolation criteria. Electrons must have $p_{\text{T}} > 7$ GeV and $|\eta| < 2.47$. To ensure that they are

compatible with the primary vertex, the track associated with the electron candidate is required to have $\sigma(d_0) < 5$ and $|z_0 \sin \theta| < 0.5$ mm, where $\sigma(d_0)$ is the significance of the transverse impact parameter, z_0 is the longitudinal impact parameter and θ is the polar angle of the track.

Muons are reconstructed by matching track segments in the MS to a track in the ID [92]. They are identified by using selections on the quality of the tracks and the compatibility of the ID and MS measurements, and they are required to satisfy the ‘loose’ identification WP and loose isolation criteria combining calorimeter and track information [92]. Muons are required to have $p_T > 7$ GeV, $|\eta| < 2.5$, $\sigma(d_0) < 3$ and $|z_0 \sin \theta| < 0.5$ mm.

Hadronically decaying τ -leptons are reconstructed from calorimeter-cell energy clusters [93] formed by the anti- k_t algorithm [94, 95] with a radius parameter of $R = 0.4$. Either one or three tracks must lie within a cone of size $\Delta R = 0.2$ around the direction of the hadronically decaying τ candidate, which is identified using a recurrent neural network [96] and the ‘loose’ WP. The τ -lepton candidates must have $p_T > 15$ GeV and $|\eta| < 2.5$, excluding the calorimeter barrel/endcap transition region ($1.37 \leq |\eta| \leq 1.52$).

Jets are reconstructed from particle-flow objects formed from ID tracks and calorimeter energy clusters [97] by using the anti- k_t algorithm with a radius parameter of $R = 0.4$. Jets with $|\eta| < 2.5$ ($2.5 < |\eta| < 4.5$) are classified as central (forward) jets and are required to have $p_T > 20$ (30) GeV. Central jets with $20 \text{ GeV} < p_T < 60 \text{ GeV}$ and $|\eta| < 2.4$ are required to pass the ‘tight’ jet vertex tagger (JVT) [98] WP that suppresses jets originating from pile-up interactions.

Jets containing b -hadrons, hereafter referred to as b -jets, are identified using the DL1r tagger [99]. A WP corresponding to a 77% efficiency in simulated inclusive $t\bar{t}$ events is used for the $\ell^+\ell^-t\bar{t}$ channel, while a WP corresponding to a 70% efficiency is used for the $\nu\bar{\nu}b\bar{b}$ channel. The decays of the b -hadrons can produce muons which are vetoed when building particle-flow objects and therefore are not included in the energy of the reconstructed jets. To correct for this effect, the four-momentum of the closest non-isolated muon that satisfies $\Delta R(b\text{-jet}, \mu) < \min(0.4, 0.04 + 10/p_T(\mu) [\text{GeV}])$ is added to the four-momentum of the b -jet. The corrected four-momentum is used when defining the event selection criteria described in the following section.

The event’s missing transverse momentum, \vec{E}_T^{miss} (or E_T^{miss} for its modulus), is defined as the negative vector sum of the transverse momenta of all the observable electron, muon and jet objects described above, plus a soft term comprising ID tracks that are matched to the primary vertex but not to any of the already included objects [100]. An E_T^{miss} significance variable (S_{MET}) which is sensitive to fake- E_T^{miss} effects is defined using the expected resolutions of all objects used in the E_T^{miss} reconstruction and the correlations between them [101].

An overlap removal procedure is applied to avoid any double-counting between the reconstructed leptons, including the hadronically decaying τ -leptons, and jets [33].

5 Event selection and background estimation

The final state resulting from the $A \rightarrow Z(\rightarrow \ell^+\ell^-)H(\rightarrow t\bar{t})$ signal process, where one top-quark decays semileptonically and the other decays hadronically, is expected to contain three high- p_T leptons, two of which should have an invariant mass close to the Z boson mass, m_Z , and a resonant $t\bar{t}$ pair. The main backgrounds expected in the $\ell^+\ell^-t\bar{t}$ channel consist of $t\bar{t}Z$ events, which have a non-resonant $m(t\bar{t})$

spectrum, and events with a jet misidentified as a lepton which mostly arise from the $t\bar{t}$ process with both top quarks decaying semileptonically.

The $A \rightarrow Z(\rightarrow \nu\bar{\nu})H(\rightarrow b\bar{b})$ signal process leads to a final state with large $E_{\text{T}}^{\text{miss}}$, no leptons, at least two b -jets and a resonant $m(b\bar{b})$ spectrum. The main backgrounds in the $\nu\bar{\nu}b\bar{b}$ channel arise from Z +heavy-flavour (denoted by Zhf)³ and $t\bar{t}$ processes.

Differences between the signal and background processes in lepton multiplicity, flavour, charge and kinematics are exploited to define background-enriched control regions that can be used to constrain the main backgrounds, as described in the following sections.

A common preselection is applied to the $\ell^+\ell^-t\bar{t}$ and $\nu\bar{\nu}b\bar{b}$ channels to reject events without a reconstructed primary vertex or events containing jets with properties consistent with beam-induced background processes, cosmic-ray showers or noisy calorimeter cells [102]. The subsequent channel-specific selections are described in the following sections.

5.1 $\ell^+\ell^-t\bar{t}$ selection

In the $\ell^+\ell^-t\bar{t}$ channel, the dominant background consists of $t\bar{t}Z$ events, which, unlike signal events, produce a non-resonant $m(t\bar{t})$ spectrum. Another major background consists of $t\bar{t}$ events with two prompt leptons from the top-quark decays and an extra lepton which is expected to originate from b -hadron decays in 60% of cases or a jet misidentified as a lepton in the remaining 40% of cases. Other backgrounds arise from multi-boson events and events with a single top quark produced in association with vector bosons; these backgrounds generally have lower lepton p_{T} , a non-resonant $m(t\bar{t})$ spectrum, and can be accompanied by Z bosons. Events are therefore separated into signal (SR), control (CR) and validation (VR) regions using a combination of requirements on the following three kinematic quantities: the p_{T} of the third-highest- p_{T} lepton ($p_{\text{T}}(\ell_3)$), the mass of the Z boson candidate (m_Z^{cand}) and the invariant mass of the H boson candidate (m_H^{cand}), as defined below.

Events in all regions are required to have exactly three leptons (electrons or muons), leading to the four flavour combinations eee , $ee\mu$, $\mu\mu e$, and $\mu\mu\mu$. The leptons must have $p_{\text{T}} > 7$ GeV, with the highest- p_{T} lepton having $p_{\text{T}} > 27$ GeV. Furthermore, only events with at least four jets and exactly two b -tagged jets are retained.⁴ The events which do not contain any pairs of leptons with opposite-sign charges and the same flavour (OSSF), namely the $e^\pm e^\pm \mu^\mp$ and $\mu^\pm \mu^\pm e^\mp$ combinations, are selected for the same-sign (ss) region, which serves as the $t\bar{t}$ CR. Events with at least one OSSF lepton pair are considered further in the selection of the SR and other CRs and VRs.

The following regions are defined by requirements on $p_{\text{T}}(\ell_3)$: the region with $p_{\text{T}}(\ell_3) > 13$ GeV (denoted by L3hi) is enriched in signal events, whereas the region with $7 \text{ GeV} < p_{\text{T}}(\ell_3) < 13$ GeV (denoted by L3lo) is enriched in background events.

The Z candidate is defined as the OSSF lepton pair whose invariant mass is closest to m_Z [103], and only events with $|m_Z^{\text{cand}} - m_Z| < 20$ GeV are retained. Events that satisfy $|m_Z^{\text{cand}} - m_Z| < 10$ GeV define the

³ Jets in simulated events are labelled as b/c -jets if a b/c -hadron with $p_{\text{T}} > 5$ GeV is found within a cone of size $\Delta R = 0.3$ around the jet axis, or as light jets (l -jets) otherwise. In the $\nu\bar{\nu}b\bar{b}$ channel the W/Z +jets events are divided according to the true flavour of the jets that constitute the Higgs boson candidate, into heavy flavour, consisting of bb , bc , bl and cc , and light flavour, consisting of cl and ll . These components are denoted in the following by Vhf and Vlf, respectively.

⁴ For the bbA production mode, it was found that the majority of events with three or more b -jets ($\gtrsim 60\%$) are reconstructed in the 2- b -tag region, since the additional b -jets are soft and forward.

Zin region, where more signal events are expected, and the remaining events define the Zout region. In the ss region, the Z candidate is reconstructed from the pair of leptons with same-sign charges and the same flavour, and only events with $|m_Z^{\text{cand}} - m_Z| < 20$ GeV are selected.

A combination of the $p_T(\ell_3)$ and m_Z^{cand} requirements allows the definition of several regions, enriched in either signal or background events. The signal events generally populate the L3hi_Zin region. Two signal-depleted regions are also defined: L3lo_Zin, with roughly equal contributions from Zhf, $t\bar{t}$ and $t\bar{t}Z$ background processes, and L3hi_Zout, with a relatively large contribution from $t\bar{t}$ and $t\bar{t}Z$ background processes. These signal-depleted regions cannot be used as CRs to simultaneously constrain the normalisation of the Zhf, $t\bar{t}$ and $t\bar{t}Z$ backgrounds because they receive fairly similar background contributions and have a limited number of events. They are therefore only used as VRs to verify that the fit model (described in Section 7) can describe the data in regions that are kinematically close to the SR.

The semileptonically decaying top-quark candidate (t_{lep}) is reconstructed from the lepton that is not used in the reconstruction of the Z candidate, the b -jet which is the closest in ΔR to this lepton, and \vec{E}_T^{miss} . To improve the resolution in $m_{t_{\text{lep}}}$, the longitudinal-momentum component of the neutrino from the t_{lep} decay is calculated by constraining the mass of the lepton–neutrino system to be equal to the W boson mass, m_W .⁵ The hadronically decaying top-quark candidate (t_{had}) is reconstructed from the light-jet pair with mass m_{jj} closest to m_W and the b -jet that is not used in the t_{lep} reconstruction. To improve the resolution in $m_{t_{\text{had}}}$, the four-momenta of the light-jet pair that constitutes the hadronic W candidate are rescaled by m_W/m_{jj} .

The H candidate is defined as the sum of the four-momenta of t_{lep} and t_{had} , while the A candidate is reconstructed as the sum of the four-momenta of the H candidate and the Z candidate. The fact that the H and Z candidates for signal events are produced by the decay of a resonance constrains the kinematic properties of these candidates; the constraints depend on the m_A and m_H values of the signal hypothesis. In particular, the H candidate is expected to be produced more centrally than background events. It is found that requiring the pseudorapidity of the H candidate in the rest frame of the A candidate to satisfy $|\eta_{H\text{-cand}}^{ZH\text{-r.fr.}}| < 2.2 + 0.0004 \cdot m(t\bar{t})$ [GeV] $- 0.0011 \cdot m(\ell^+\ell^-t\bar{t})$ [GeV] provides the optimal sensitivity across the whole (m_A, m_H) plane. The parameters of the linear function defining this requirement are determined by a fit to the values of the $|\eta_{H\text{-cand}}^{ZH\text{-r.fr.}}|$ cut that maximise the expected significance for each (m_A, m_H) hypothesis.

The presence of a signal would manifest itself as a resonance in the $m(t\bar{t})$ and $m(\ell^+\ell^-t\bar{t})$ distributions, as well as in the distribution of the mass difference $\Delta m = m(\ell^+\ell^-t\bar{t}) - m(t\bar{t})$ [41]. The region that is expected to contain most of the signal events for a given mass hypothesis m_H is constructed using a sliding window defined by the condition $|m(t\bar{t}) - m_H| < N \cdot \sigma$, where $\sigma \approx 0.16 \cdot m_H$ is the resolution in $m(t\bar{t})$ and $N = 2$ (1.5) for $m_H < (\geq) 500$ GeV, and this region is referred to as the Hin SR. The sideband regions with a lower or higher $m(t\bar{t})$ value define the Hlo and Hhi CRs, which are used to constrain the normalisation of the simulated $t\bar{t}Z$ sample. The N factor, which defines the width of the signal region, is optimised to achieve the highest signal significance.

The four-momentum vector of the H candidate is rescaled by $m_H/m(t\bar{t})$ to improve the resolution in $m(\ell^+\ell^-t\bar{t})$. The rescaling is performed only in the SR, where the resonance is expected, and is applied to both the simulated events and data events. After this rescaling, the resolution in $m(\ell^+\ell^-t\bar{t})$ improves by as much as a factor of three, particularly for signal hypotheses with small $m_A - m_H$ values, and ranges from 3% to 20% for small and large $m_A - m_H$ values, respectively.

⁵ In the resulting quadratic equation, the neutrino p_z is taken from the real component in the case of complex solutions or the smaller component of the two solutions if both solutions are real.

The fraction of signal events passing the full event selection varies from 2% to 3.5%, depending on the mass hypothesis, and the fraction increases slightly with increasing m_H .

A summary of the selection criteria that define the different regions considered in the statistical analysis is given in Table 2.

Table 2: Event selection for the $\ell^+ \ell^- t\bar{t}$ channel. The SR, CR and VR symbols next to the region name indicate that this region is used as a signal, control or validation region in the fit, respectively.

Requirement	Regions				
	ss (CR)	L3hi_Zout (VR)	L3hi_Zin		L3lo_Zin (VR)
			Hlo / Hhi (CR)	Hin (SR)	
Number of leptons $p_T(\ell_1)$ Number of jets Number of b -jets $ \eta_{H\text{-cand}}^{ZH\text{-r.fr.}} $			3 > 27 GeV		
			≥ 4		
			2		
			$< 2.2 + 0.0004 \cdot m(t\bar{t})[\text{GeV}] - 0.0011 \cdot m(\ell^+ \ell^- t\bar{t})[\text{GeV}]$		
$p_T(\ell_3)$			> 13 GeV		> 7 GeV & < 13 GeV
Lepton flavour	$e e \mu / \mu \mu e$		$e e e / e e \mu / \mu \mu e / \mu \mu \mu$		
OSSF lepton pairs	0		≥ 1		
$ m_Z^{\text{cand}} - m_Z $	< 20 GeV	> 10 GeV & < 20 GeV	< 10 GeV		
$ m(t\bar{t}) - m_H $	$m_H < 500 \text{ GeV}$ $m_H \geq 500 \text{ GeV}$	-	> $0.32 \cdot m_H$ > $0.24 \cdot m_H$	< $0.32 \cdot m_H$ < $0.24 \cdot m_H$	-

5.2 $\nu\bar{\nu}b\bar{b}$ selection

In the $\nu\bar{\nu}b\bar{b}$ channel, the events are split into regions with different lepton multiplicities. The signal is expected to manifest in the region with no leptons. A region consisting of exactly two leptons of the same flavour (2L),⁶ enriched in Zhf events, and a region with one electron and one muon ($e\mu$), enriched in $t\bar{t}$ events, are used to constrain the corresponding background normalisations. Finally, a region with exactly one lepton (1L) is used as a VR. The SR, CR and VR regions are further divided into regions with exactly two and at least three b -jets, which target the ggF and bbA production modes, respectively.

In events with at least one lepton, the highest- p_T lepton is required to have $p_T(\ell_1) > 27 \text{ GeV}$. Events in all regions are required to have $p_T(V) > 150 \text{ GeV}$ (V denotes a Z or W boson), where $p_T(V) = E_T^{\text{miss}}$ in the region with no leptons, $p_T(V) = |\vec{p}_T(\ell) + \vec{E}_T^{\text{miss}}|$ in the 1L region and $p_T(V) = |\vec{p}_T(\ell_1) + \vec{p}_T(\ell_2)|$ in the 2L and $e\mu$ regions. Events are also required to have at least two b -jets. A veto on events with more than five jets or events containing any hadronically decaying τ -lepton (τ^{had}) candidates is applied to suppress the $t\bar{t}$ background.

To suppress the background from multi-jet events, only events in which the smallest azimuthal angle between \vec{E}_T^{miss} and any jet, $\min_i \Delta\phi(\vec{E}_T^{\text{miss}}, \vec{p}_i^{\text{jet}})$, is larger than $\pi/10$ are selected. This background is further suppressed by selecting events with $\mathcal{S}_{\text{MET}} > 3$ ($\mathcal{S}_{\text{MET}} > 10$) in the region with one (zero) lepton(s). These selection criteria are found to reduce the multi-jet contamination to a negligible level. In contrast, a selection $\mathcal{S}_{\text{MET}} < 5$ is applied in the 2L region to reduce the contamination from the $t\bar{t}$ background and maximise the purity in the Zhf background in this CR. The purity of the Zhf background in the 2L region is further increased by retaining only events that satisfy $|m_Z^{\text{cand}} - m_Z| < 10 \text{ GeV}$.

⁶ In principle, the 2L region could also contain signal from the $A \rightarrow ZH \rightarrow \ell^+ \ell^- b\bar{b}$ process. Based on the constraints on the cross-section for this process derived in Ref. [22] and given that the 2L region is included in the statistical analysis as a single bin (see Section 7) it has been estimated that the impact of such a signal contamination in the 2L control region would be smaller than 3%, with a negligible impact on the analysis, and is therefore neglected.

The H candidate is reconstructed from the two highest- p_T b -jets and only events with $m(b\bar{b}) > 50$ GeV are retained. The ΔR between the b -jets forming the H candidate is required to be smaller than 3.3 (3.5) for events with exactly two (at least three) b -jets.

To further suppress the $t\bar{t}$ background in events with no leptons, two top-quark-mass proxy variables are defined as follows [26]:

$$m_{\text{top}}^{\text{near/far}} = \sqrt{2p_{T,b_{\text{near/far}}} E_T^{\text{miss}} \left[1 - \cos \Delta\phi \left(\vec{p}_{T,b_{\text{near/far}}}, \vec{E}_T^{\text{miss}} \right) \right]},$$

where near (far) refers to the H candidate's b -jet that is nearer to (farther from) the \vec{E}_T^{miss} in azimuthal angle. The b -jet closer to \vec{E}_T^{miss} in azimuthal angle is used for the calculation of $m_{\text{top}}^{\text{near}}$, whereas the b -jet farther from \vec{E}_T^{miss} is used for $m_{\text{top}}^{\text{far}}$. Events are retained only if $m_{\text{top}}^{\text{near}} > 180$ GeV and $m_{\text{top}}^{\text{far}} > 200$ GeV.

The presence of a signal would manifest as a broad resonance in the distribution of the A candidate transverse mass ($m_T(VH)$) in the final state with no leptons. The region which is expected to contain most of the signal events for a given mass hypothesis m_H is constructed using a sliding window defined by the condition $|m(b\bar{b}) - m_H| < 2 \cdot \sigma$, where $\sigma = 0.1 \cdot m_H$ is the resolution in $m(b\bar{b})$. The adjacent regions with a lower or higher $m(b\bar{b})$ define the Hlo and Hhi regions, which are used as CRs in the statistical analysis. The Hlo and Hhi regions contain events from a mix of background processes, so they constrain all the background processes present there, rather than a specific one.

The four-momentum vector of the H candidate is rescaled by $m_H/m(b\bar{b})$ to improve the resolution in $m_T(VH)$. The rescaling is performed only in the SR, where the resonance is expected, and is applied to both the simulated events and data events. The resolution in $m_T(VH)$ after this rescaling ranges from 8% for signal hypotheses with high m_H and low $m_A - m_H$ values, to 27% for signal hypotheses with low m_H and high $m_A - m_H$ values.

The fraction of signal events passing the full event selection varies from less than 1% for signal events with low $m_A - m_H$, which also have low E_T^{miss} , to about 21% for signal events with high $m_A - m_H$.

A summary of the selection requirements applied in the SR, VRs and CRs is shown in Table 3.

Table 3: Event selection for the $\nu\bar{\nu}b\bar{b}$ channel. The SR, CR and VR symbols next to the region name indicate that this region is used as a signal, control or validation region in the fit, respectively.

Requirement	Regions			
	2L (CR)	$e\mu$ (CR)	1L (VR)	0L
				Hlo / Hhi (CR)
Number of jets	2–5			
Number of b -jets	≥ 2			
$m(b\bar{b})$	> 50 GeV			
Number of τ^{had}	0			
$p_{\text{T}}(V)$	> 150 GeV			
$\min_i \Delta\phi(\vec{E}_{\text{T}}^{\text{miss}}, \vec{p}_i^{\text{jet}})$	$> \pi/10$			
$\Delta R(b_1, b_2)$	< 3.3 (2 b -jets)			
	< 3.5 (≥ 3 b -jets)			
Number of leptons	2		1	0
Lepton flavour	$ee/\mu\mu$	$e\mu$	e/μ	-
$p_{\text{T}}(\ell_1)$	> 27 GeV			-
$ m_{\text{Z}}^{\text{cand}} - m_{\text{Z}} $	< 10 GeV	-		
S_{MET}	< 5	-	> 3	> 10
$m_{\text{top}}^{\text{near}}$	-			> 180 GeV
$m_{\text{top}}^{\text{far}}$	-			> 200 GeV
$ m(b\bar{b}) - m_{\text{H}} $	-		$> 0.2 \cdot m_{\text{H}}$	$< 0.2 \cdot m_{\text{H}}$

6 Systematic uncertainties

Experimental uncertainties from detector effects and theoretical uncertainties related to the modelling of the simulated signal and background processes affect the normalisation and shape of the final discriminating variable (see Section 7) as well as the relative normalisation of events in the SR and CRs.

Uncertainties arising from the calibration of the jet energy scale and resolution are derived as functions of the jet p_{T} and η [104]. Uncertainties arising from the identification of b -jets are derived in Refs. [99, 105, 106]. Uncertainties related to the reconstruction and identification of leptons are derived in Refs. [90, 92]. Uncertainties in the reconstruction of $E_{\text{T}}^{\text{miss}}$ are taken into account as described in Ref. [107]. The number of pile-up collisions in simulation is reweighted to match the data and a 4% variation of this reweighting factor is assigned as an uncertainty. The uncertainty in the total integrated luminosity is 0.83% [108], obtained using the LUCID-2 detector [109] for the primary luminosity measurements.

For the V +jets and diboson processes, uncertainties are estimated by comparing the nominal SHERPA samples with alternative samples simulated with MG5AMC 2.2.2 interfaced to PYTHIA 8.186 and including up to four jets in the matrix element calculated at LO accuracy in QCD. Uncertainties related to multi-jet merging and resummation are calculated by varying the associated scales in SHERPA.

For the $t\bar{t}Z$ process, the uncertainty related to the modelling of the parton shower is obtained by comparing the nominal sample with a sample simulated with MG5AMC 2.3.3 interfaced to HERWIG 7.13 [110]. An additional uncertainty related to the modelling of initial- and final-state radiation is obtained using the associated eigentune of the A14 tune [40].

For the $t\bar{t}$ process, an uncertainty related to the NLO matching is obtained by comparing the nominal sample with a sample simulated with MG5AMC 2.6.0 interfaced to PYTHIA 8.230, while the parton shower uncertainty is obtained by comparison with a sample simulated with POWHEG+HERWIG 7.04 [111, 112]. The initial- and final-state radiation uncertainties are obtained by varying the renormalisation scale in the

initial- and final-state emissions by a factor of two. The downward variation of the renormalisation scale in initial-state emissions is accompanied by an upward variation of the h_{damp} parameter by a factor of two.

For the tW process, an additional uncertainty related to the removal of the overlap with the $t\bar{t}$ process is obtained by comparing the nominal sample evaluated using the diagram subtraction technique with a sample which uses the diagram removal technique.

For all simulated samples, the uncertainties due to missing higher orders in QCD are estimated by independent variations of the renormalisation and factorisation scales by a factor of two, while the PDF and α_s uncertainties are calculated using the PDF4LHC prescription [113].

Systematic uncertainties for background processes that contribute less than 1% to the total background are neglected.

Statistical uncertainties are dominant in the $\ell^+\ell^-t\bar{t}$ channel for all (m_A, m_H) hypotheses, while in the $\nu\bar{\nu}b\bar{b}$ analysis the systematic uncertainties dominate. The dominant systematic uncertainties in the $\nu\bar{\nu}b\bar{b}$ channel are related to the modelling of the Zhf and Whf background processes as well as to the jet energy scale and resolution.

The relative contributions from the different sources of uncertainty for representative (m_A, m_H) hypotheses in the two channels are shown in Table 4. The fractional impact is calculated by considering the square of the uncertainty in the signal strength parameter (μ) arising from a group of uncertainties (as listed in the left column of the table), divided by the square of the total uncertainty in μ . The value of μ used is determined by the fit to data. Due to correlations, the sum of the impacts of different systematic uncertainties may not be equal to the total impact of all systematic uncertainties. Statistical uncertainties include the uncertainties due to the size of the data sample and the uncertainties associated with the background process normalisations which are free to float in the fit. The row ‘‘MC sample size’’ refers to the systematic uncertainty due to the finite number of generated events in the simulation.

7 Statistical analysis

To extract the final result of the search presented here, a binned profile likelihood fit [114] to the data is used. The likelihood function $\mathcal{L}(\mu, \theta)$ is constructed from a product of Poisson probabilities $\text{Pois}(N_{\text{obs}}|\mu s + b)$ for observing N_{obs} data events when μs signal and b background events are expected in each bin of the fitted distribution. It contains the parameter-of-interest μ , which is a factor multiplying the nominal signal cross-section and is extracted by maximising the likelihood. Background processes whose event yields are constrained using data have freely floating normalisations in the likelihood function (see Table 4). The uncertainties due to the limited number of simulated background events are incorporated in the likelihood as nuisance parameters (NP) using Poisson probability density functions following a simplified version of the Beeston–Barlow technique [115].

The rest of the systematic uncertainties are incorporated in the fit as NP, constrained using Gaussian probability density functions. These include (i) the NP corresponding to the normalisation uncertainty in the measured phase space, added for each background sample whose normalisation is not left to float freely in the fit, (ii) the NP corresponding to the uncertainty in the acceptance difference between the different regions considered in the fit and (iii) the NP corresponding to the uncertainty in the distribution shape of the fitted final discriminating variable.

Table 4: Fractional squared uncertainty in μ from the different sources of uncertainty for different (m_A, m_H) values in the $\ell^+\ell^-t\bar{t}$ and $\nu\bar{\nu}b\bar{b}$ channels.

Source of uncertainty	Fractional squared uncertainty in μ				
	$\ell^+\ell^-t\bar{t}$ signals (m_A, m_H) [GeV]		$\nu\bar{\nu}b\bar{b}$ signals (m_A, m_H) [GeV]		
	(700, 500)	(1200, 800)	(400, 130)	(700, 300)	(1200, 800)
Total statistical uncertainty	0.91	0.90	0.19	0.27	0.48
Total systematic uncertainty	0.09	0.10	0.81	0.73	0.52
Statistical uncertainties					
Data statistics	0.40	0.72	0.16	0.24	0.48
$t\bar{t}Z$ normalisation	0.36	0.14	neglected		
Zhf normalisation	not free to float, included in ‘Other’		0.01	0.05	0.12
$t\bar{t}$ normalisation	0.01	0.02	0.06	0.01	0.01
Systematic uncertainties					
Jets	0.02	0.01	0.15	0.10	0.10
b -tagging	< 0.01	< 0.01	0.02	< 0.01	0.05
E_T^{miss} soft-term and pile-up	< 0.01	< 0.01	0.01	0.01	< 0.01
Luminosity	< 0.01	< 0.01	< 0.01	< 0.01	< 0.01
Other experimental sources	< 0.01	< 0.01	< 0.01	< 0.01	< 0.01
$t\bar{t}Z$ modelling	0.03	0.05	not applied		
$t\bar{t}$ modelling	0.01	0.02	0.05	0.01	0.01
Zhf modelling	included in ‘Other’		0.21	0.47	0.30
Whf modelling	neglected		0.14	0.04	0.10
tW modelling	neglected		0.02	0.03	< 0.01
Other modelling sources	0.01	0.02	0.08	0.01	< 0.01
Signal modelling	< 0.01	< 0.01	< 0.01	< 0.01	< 0.01
MC sample size	0.01	0.01	0.05	0.05	0.05

In the $\ell^+\ell^-t\bar{t}$ channel, the normalisation of the $t\bar{t}$ background is constrained by using the ss region, and the normalisation of the $t\bar{t}Z$ background is constrained by using the $Hl0$ and Hhi regions, so these normalisations are allowed to float freely in the fit. A simultaneous fit is performed to the data yields in the ss , $Hl0$ and Hhi CRs and to the Δm distribution in the Hin SR, which is the final discriminating variable for this channel.

In the $\nu\bar{\nu}b\bar{b}$ channel, the normalisations of the $t\bar{t}$ and Zhf background processes are allowed to float freely in the likelihood function, since they are constrained by using the $e\mu$ and 2L regions, respectively. Due to a known mismodelling of Zhf events [14, 26, 33], which is expected to be more severe in the ≥ 3 - b -tag region, two decorrelated normalisation factors are used for the Zhf background in the 2- b -tag and ≥ 3 - b -tag regions. The $t\bar{t}$ events populating the ≥ 3 - b -tag region can arise either from events with at least three real b -jets, via $t\bar{t} + (g \rightarrow b\bar{b})$, or from the misidentification of a c -jet originating from a W boson produced in the top-quark decays. The contributions of the two processes depend on $m(b\bar{b})$, with the former dominating in the high $m(b\bar{b})$ region. To account for the different underlying processes, two decorrelated normalisation factors are applied to the $t\bar{t}$ background in the 2- b -tag and ≥ 3 - b -tag regions. A simultaneous fit of the $m_T(VH)$ distribution, which is the final discriminating variable for this channel, is performed in the 2L, $e\mu$, $Hl0$ and Hhi CRs and the Hin SR including both the 2- b -tag and ≥ 3 - b -tag regions. Eight bins of the $m_T(VH)$ distribution are used in the 2L 2- b -tag region, but only two bins in the $e\mu$ region and a single bin in the 2L ≥ 3 - b -tag, $Hl0$ and Hhi regions.

Since a large number of events satisfy the selection criteria, both the significance of any excess and the upper limits are calculated in the asymptotic approximation [114]. Upper limits on μ are extracted using the profile-likelihood test statistic and the CL_s prescription [116] by performing fits for multiple (m_A, m_H)

values. All upper limits mentioned in Section 8 correspond to a confidence level (CL) of 95%.

8 Results

No significant deviation from the background-only hypothesis is observed in the likelihood fits. The largest excess over the SM background prediction, amounting to a local significance of 2.85σ , is observed in the $\ell^+ \ell^- t \bar{t}$ channel, for the signal hypothesis corresponding to $(m_A, m_H) = (650, 450)$ GeV. The global significance for the $\ell^+ \ell^- t \bar{t}$ channel is estimated following Refs. [117, 118] to be 2.35σ .

The yields and post-fit distributions presented here are obtained from background-only fits to the data in the SR and CRs. The constraints from these fits are also applied to the VRs to gauge whether the fit can describe the data in regions that are kinematically close to the SR and CRs but are not included in the fits. Representative yields in the SR, CRs and VRs are shown in Figure 2 and Tables 5 to 7. Representative distributions of the fit discriminant and the mass of the H candidate in the SR are shown in Figures 3 and 4.

Table 5: Yields in the $\ell^+ \ell^- t \bar{t}$ channel obtained from the background-only fit to data using Hin450 as the signal region. The indicated uncertainties include statistical and systematic components. The value next to the region name refers to the m_H hypothesis.

	L3hi_Zin			ss (CR)	(VR)	(VR)
	Hlo450 (CR)	Hin450 (SR)	Hhi450 (CR)		L3hi_Zout	L3lo_Zin
$t \bar{t} Z$	5.1 ± 0.9	200 ± 22	113 ± 13	2.3 ± 0.6	29.0 ± 3.2	30.8 ± 3.4
$t \bar{t}$	1.2 ± 0.8	29 ± 9	16 ± 6	40 ± 7	46 ± 14	54 ± 17
$t W Z$	0.40 ± 0.14	12 ± 4	10 ± 4	0.13 ± 0.04	1.6 ± 0.5	2.2 ± 0.7
$t Z q$	0.6 ± 0.4	13 ± 8	10 ± 6	0.046 ± 0.032	1.8 ± 1.2	2.4 ± 1.6
$VV + VVV$	1.5 ± 0.5	15 ± 4	11.1 ± 3.5	0.034 ± 0.013	2.3 ± 0.6	3.1 ± 0.9
Z	1.5 ± 1.1	11 ± 4	3.9 ± 1.6	0.025 ± 0.010	3.7 ± 1.4	39 ± 15
$t \bar{t} W + t \bar{t} H + t \bar{t} W W + t \bar{t} t \bar{t}$	0.16 ± 0.05	6.8 ± 0.9	4.9 ± 0.9	7.4 ± 1.8	8.4 ± 1.8	1.63 ± 0.27
Total background	10.5 ± 1.5	285 ± 15	169 ± 10	50 ± 7	93 ± 13	133 ± 21
Data	7	303	153	49	84	119

Table 6: Yields in the 2- b -tag regions of the $\nu \bar{\nu} b \bar{b}$ channel obtained from the background-only fit to data using Hin300 as the signal region. The indicated uncertainties include statistical and systematic components. The value next to the region name refers to the m_H hypothesis.

	0L			2L (CR)	$e\mu$ (CR)	1L (VR)
	Hlo300 (CR)	Hin300 (SR)	Hhi300 (CR)			
$t \bar{t}$	3800 ± 400	600 ± 80	290 ± 40	370 ± 60	8700 ± 500	336000 ± 28000
Single-top (s -, t -chan)	93 ± 18	26 ± 4	16.7 ± 3.1	0.70 ± 0.15	12.4 ± 0.7	16700 ± 1100
Single-top $t W$	600 ± 400	160 ± 90	90 ± 60	43 ± 23	800 ± 500	23000 ± 12000
Whf	2800 ± 900	330 ± 100	230 ± 70	2.8 ± 1.0	29 ± 9	21000 ± 7000
Zhf	8500 ± 900	2200 ± 120	1620 ± 90	5370 ± 120	18.1 ± 1.3	1070 ± 90
Vlf	44 ± 8	10.8 ± 1.7	12.3 ± 2.3	23 ± 5	0.35 ± 0.08	330 ± 60
$VHbb$	210 ± 130	0.8 ± 0.5	0.48 ± 0.31	60 ± 40	0.37 ± 0.23	350 ± 220
VV	770 ± 150	15.4 ± 1.7	12.3 ± 1.6	207 ± 24	1.63 ± 0.20	1260 ± 140
Total background	16960 ± 170	3350 ± 50	2270 ± 50	6080 ± 90	9620 ± 110	400000 ± 26000
Data	16961	3389	2266	6037	9618	415808

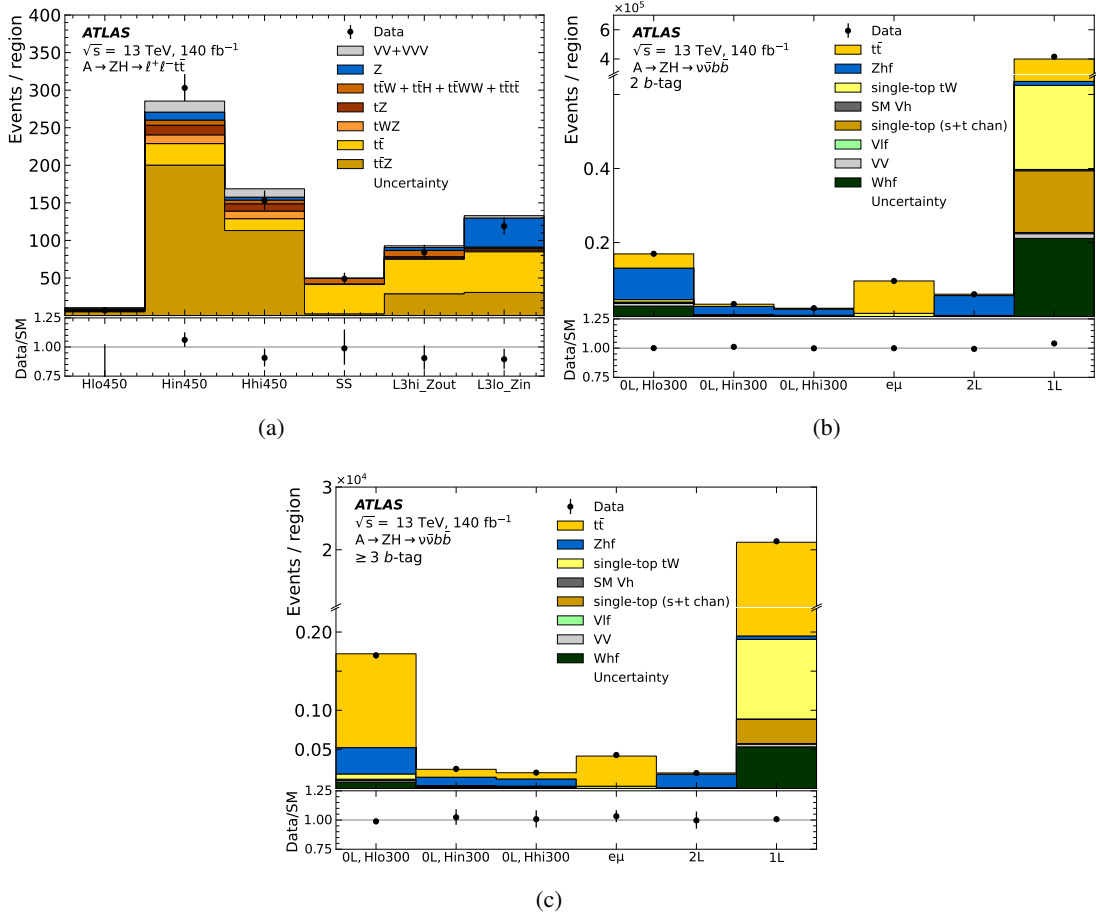


Figure 2: Yields in the SR, CRs and VRs used in the $\ell^+\ell^-t\bar{t}$ channel (a) and in the 2- b -tag (b) and ≥ 3 - b -tag (c) regions of the $\nu\bar{\nu}b\bar{b}$ channel. The yields are obtained from a background-only fit to data. The region names are defined in Tables 2 and 3. The value next to the region name refers to the m_H hypothesis. The data are represented as black points and the associated error bars represent the statistical uncertainty. The hatched band indicates the combined statistical and systematic uncertainty for the sum of backgrounds.

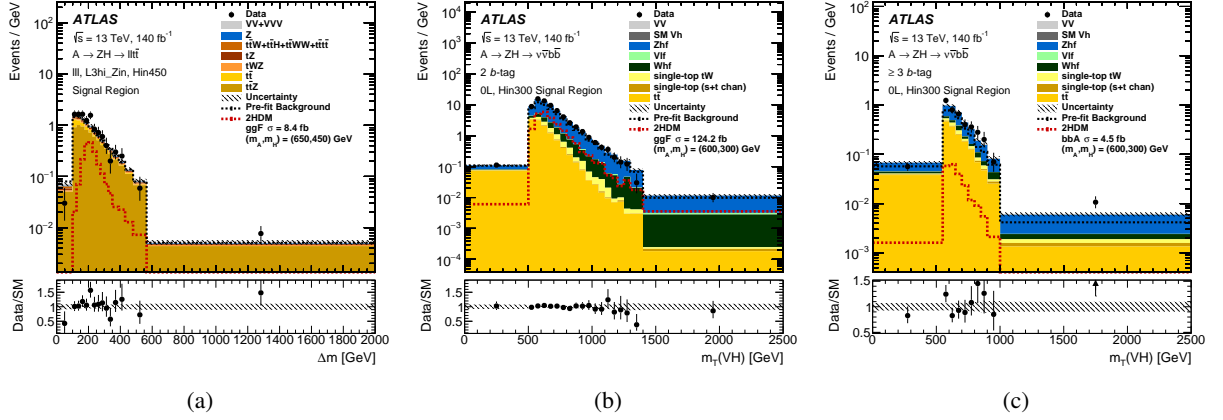


Figure 3: The distribution of the fit discriminant $\Delta m = m(\ell^+\ell^-\bar{t}\bar{t}) - m(\bar{t}\bar{t})$ in the SR of the $\ell^+\ell^-\bar{t}\bar{t}$ channel for the $m_H = 450$ GeV hypothesis (a). The distribution of the fit discriminant $m_T(VH)$ in the SR of the $\nu\bar{b}\bar{b}$ channel in the 2- b -tag (b) and ≥ 3 - b -tag (c) region, for the $m_H = 300$ GeV hypothesis. The background yields are obtained from a background-only fit to data. Signal distributions corresponding to ggF or bbA production normalised to the theory cross-section are shown for comparison. The data are represented as black points and the associated error bars represent the statistical uncertainty. The hatched band indicates the combined statistical and systematic uncertainty for the sum of backgrounds. The quantity on the vertical axis is the number of events divided by the bin width in GeV.

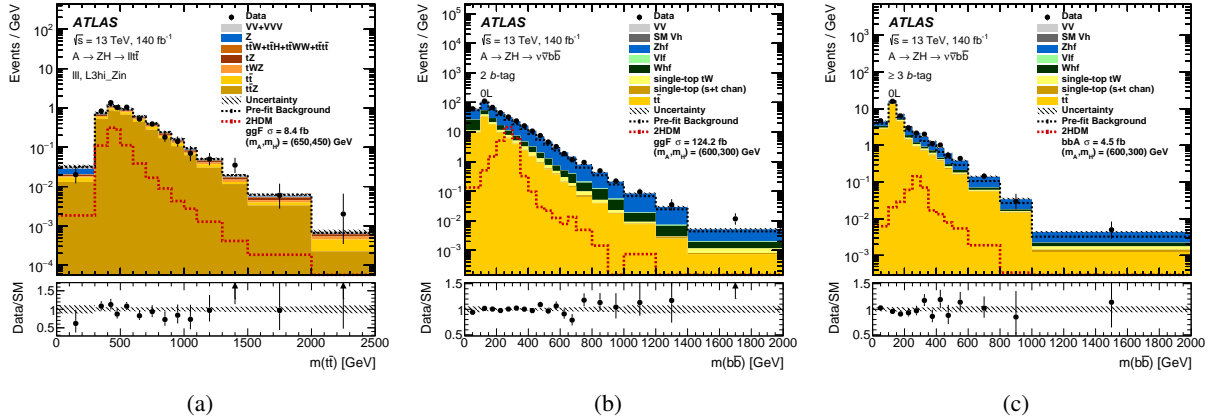


Figure 4: The $m(\bar{t}\bar{t})$ distribution in the L3hi_Zin region of the $\ell^+\ell^-\bar{t}\bar{t}$ channel (a) and the $m(\bar{b}\bar{b})$ distribution in the $\nu\bar{b}\bar{b}$ channel in the 2- b -tag (b) and ≥ 3 - b -tag (c) $\mathcal{O}L$ region. The background yields are obtained from a background-only fit to data. Signal distributions corresponding to ggF or bbA production normalised to the theory cross-section are shown for comparison. The data are represented as black points and the associated error bars represent the statistical uncertainty. The hatched band indicates the combined statistical and systematic uncertainty for the sum of backgrounds. The quantity on the vertical axis is the number of events divided by the bin width in GeV.

Table 7: Yields in the ≥ 3 - b -tag regions of the $\nu\bar{\nu}b\bar{b}$ channel obtained from the background-only fit to data using Hin300 as the signal region. The indicated uncertainties include statistical and systematic components. The value next to the region name refers to the m_H hypothesis.

	0L			2L (CR)	e μ (CR)	1L (VR)
	Hlo300 (CR)	Hin300 (SR)	Hhi300 (CR)			
$t\bar{t}$	1200 \pm 70	101 \pm 8	80 \pm 9	16.9 \pm 3.1	385 \pm 26	19300 \pm 1400
Single-top (s -, t -chan)	11.0 \pm 1.2	3.9 \pm 0.5	4.0 \pm 0.4	–	0.28 \pm 0.10	310 \pm 27
Single-top tW	70 \pm 50	13 \pm 8	8 \pm 7	1.2 \pm 0.8	27 \pm 19	1000 \pm 700
Whf	82 \pm 28	18 \pm 6	14 \pm 5	0.13 \pm 0.04	1.2 \pm 0.4	530 \pm 170
Zhf	340 \pm 50	106 \pm 10	91 \pm 10	173 \pm 13	0.60 \pm 0.16	43 \pm 5
Vlf	0.73 \pm 0.33	0.14 \pm 0.05	0.17 \pm 0.04	0.0040 \pm 0.0020	–	6.9 \pm 2.8
VHbb	3.7 \pm 2.4	0.48 \pm 0.31	0.42 \pm 0.27	1.1 \pm 0.7	0.010 \pm 0.007	5.3 \pm 3.4
VV	21 \pm 4	3.7 \pm 0.5	3.3 \pm 0.4	6.6 \pm 0.9	0.037 \pm 0.018	35 \pm 4
Total background	1720 \pm 40	245 \pm 9	201 \pm 8	199 \pm 12	415 \pm 19	21200 \pm 1300
Data	1702	251	203	198	428	21356

The normalisation factors in the $\ell^+\ell^-t\bar{t}$ channel are found to be compatible with unity for the $t\bar{t}Z$ background, while for the $t\bar{t}$ background they range from 1.5 to 1.8 for the different m_H hypotheses with an uncertainty of 0.5. The $t\bar{t}$ normalisation factor is higher than unity due to mismodelling of $t\bar{t}$ events with a non-prompt or misidentified lepton; this has been verified with a data-driven method. In the $\nu\bar{\nu}b\bar{b}$ channel, the normalisation factors for the $t\bar{t}$ background are compatible with unity, while for the Zhf background they are in the range 1.2–1.3 with an uncertainty of 0.1 in the 2- b -tag region and in the range 1.4–1.7 with an uncertainty of 0.2 in the ≥ 3 - b -tag regions. The Zhf normalisation factors are higher than unity due to mismodelling of the Zhf process in SHERPA [14, 26, 33]. In the $\ell^+\ell^-t\bar{t}$ channel, the $t\bar{t}$ template corresponds to $t\bar{t}$ events with two prompt leptons and one non-prompt or misidentified lepton, while in the $\nu\bar{\nu}b\bar{b}$ channel it corresponds to $t\bar{t}$ events with two prompt leptons, so the two normalisation factors obtained above are not comparable.

8.1 Upper limits on the production cross-section for $A \rightarrow ZH \rightarrow \ell^+\ell^-t\bar{t}/\nu\bar{\nu}b\bar{b}$

Upper limits on the production cross-section for the A boson times the decay branching ratios, $B(A \rightarrow ZH) \times B(H \rightarrow t\bar{t})$ in the $\ell^+\ell^-t\bar{t}$ channel and $B(A \rightarrow ZH) \times B(H \rightarrow b\bar{b})$ in the $\nu\bar{\nu}b\bar{b}$ channel, are derived for the ggF and bbA production modes and are shown in Figures 5 and 6. While the limits generally depend on the natural width of the A and H bosons, for the parameter space that is relevant for this search only the width of the A boson matters, with the width of the H boson always being very small compared to the experimental resolution. The width of the A boson increases as $m_A - m_H$ increases and is roughly independent of $\tan\beta$ for $\tan\beta \gtrsim 5$ but becomes larger for smaller values of $\tan\beta$ (i.e. $\tan\beta \lesssim 5$). This implies that the limits provided in Figures 5 and 6 for $\tan\beta = 10$ are generally applicable for $\tan\beta \gtrsim 5$, while the limits provided for $\tan\beta = 1$ are not applicable for other $\tan\beta$ values. Upper limits for other $\tan\beta$ values are provided in Figures 9 to 12 in the Appendix. Limits for intermediate $\tan\beta$ values can be obtained by interpolating between the limits for the given $\tan\beta$ values.

To obtain more realistic limits, instead of using narrow-width A bosons, the signals are generated with a natural width that corresponds to the prediction of the 2HDM for $\tan\beta = 1$ in ggF production and $\tan\beta = 10$ in bbA production. For the 2HDM benchmarks considered and the parameter space that is relevant for this search (see Section 8.2), the $\tan\beta$ and Higgs boson mass values are enough to define the A boson width. The choice $\tan\beta = 10$ is made for bbA production because at this value this production

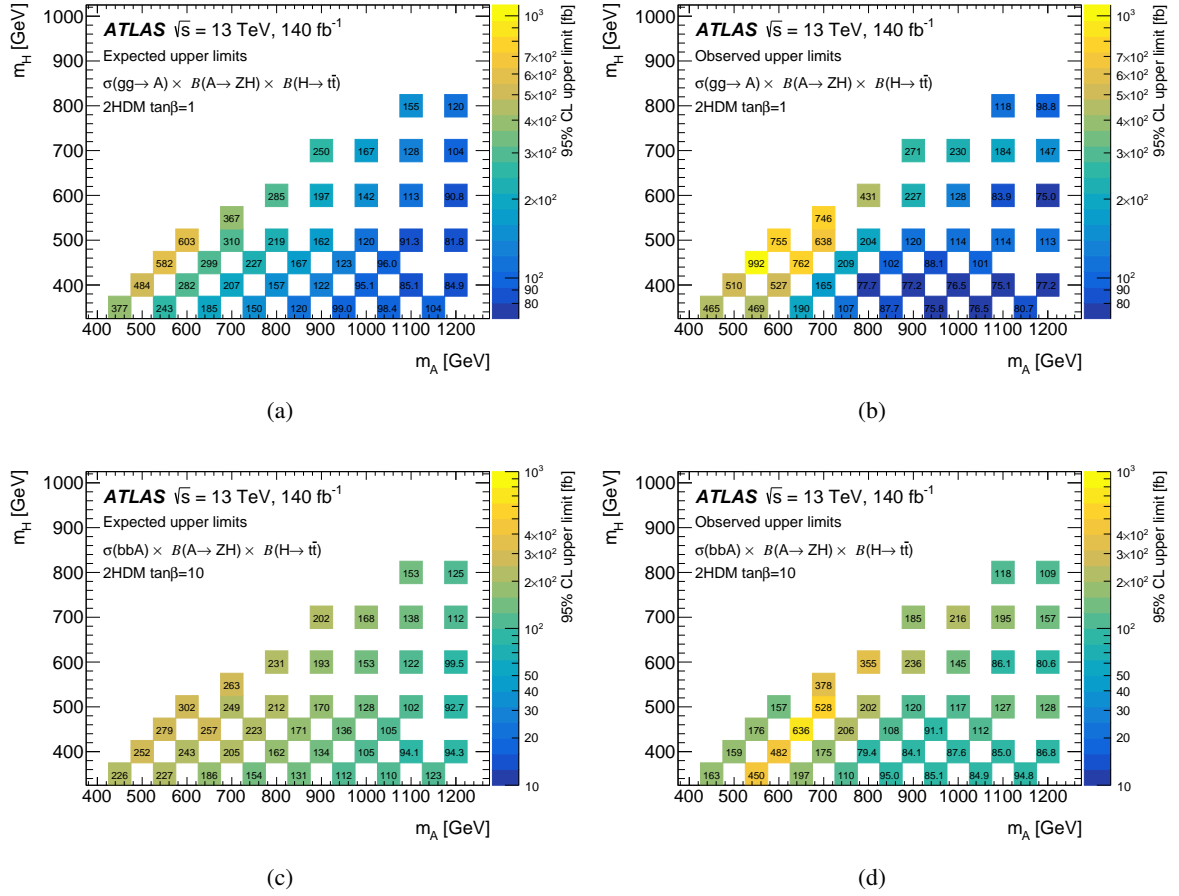


Figure 5: Expected (a,c) and observed (b,d) upper limits at 95% CL on $\sigma(gg \rightarrow A) \times B(A \rightarrow ZH) \times B(H \rightarrow t\bar{t})$ (a,b) and $\sigma(b\bar{b}A) \times B(A \rightarrow ZH) \times B(H \rightarrow t\bar{t})$ (c,d) in the (m_A, m_H) plane. The limits are shown for either $\tan\beta = 1$ or $\tan\beta = 10$ in ggF or bbA production, respectively. The $\tan\beta$ value is relevant only for the choice of A boson width.

mechanism is dominant in the benchmark models discussed in Section 8.2 (Type-II and flipped 2HDM). In the 2HDM benchmarks considered here, the width of the A boson relative to its mass is a few percent for low m_A values and increases at high m_A . For example, for the m_A range shown in Figures 5(a) and 5(b) for the $\ell^+\ell^-t\bar{t}$ channel, the A boson width ranges from 4.3% to 37% of its mass.

The observed upper limit in the $\ell^+\ell^-t\bar{t}$ channel in the case of ggF production varies from 75.0 fb for $(m_A, m_H) = (1200, 600)$ GeV to 992 fb for $(m_A, m_H) = (550, 450)$ GeV; this is to be compared with the respective expected limits of 90.8 fb and 582 fb. The observed upper limit in the $\ell^+\ell^-t\bar{t}$ channel in the case of bbA production varies from 79.4 fb for $(m_A, m_H) = (800, 400)$ GeV to 636 fb for $(m_A, m_H) = (650, 450)$ GeV; this is to be compared with the respective expected limits of 162 fb and 257 fb. Similarly, for the $\nu\bar{\nu}b\bar{b}$ channel, the observed upper limit in the case of ggF production varies from 6.2 fb for $(m_A, m_H) = (1200, 300)$ GeV to 3700 fb for $(m_A, m_H) = (350, 150)$ GeV; this is to be compared with the respective expected limits of 10.6 fb and 3520 fb. Finally, for the $\nu\bar{\nu}b\bar{b}$ channel, the observed upper limit in the case of bbA production varies from 3.62 fb for $(m_A, m_H) = (1200, 200)$ GeV to 1750 fb for $(m_A, m_H) = (350, 150)$ GeV; this is to be compared with the respective expected limits of 9.92 fb and 1910 fb.

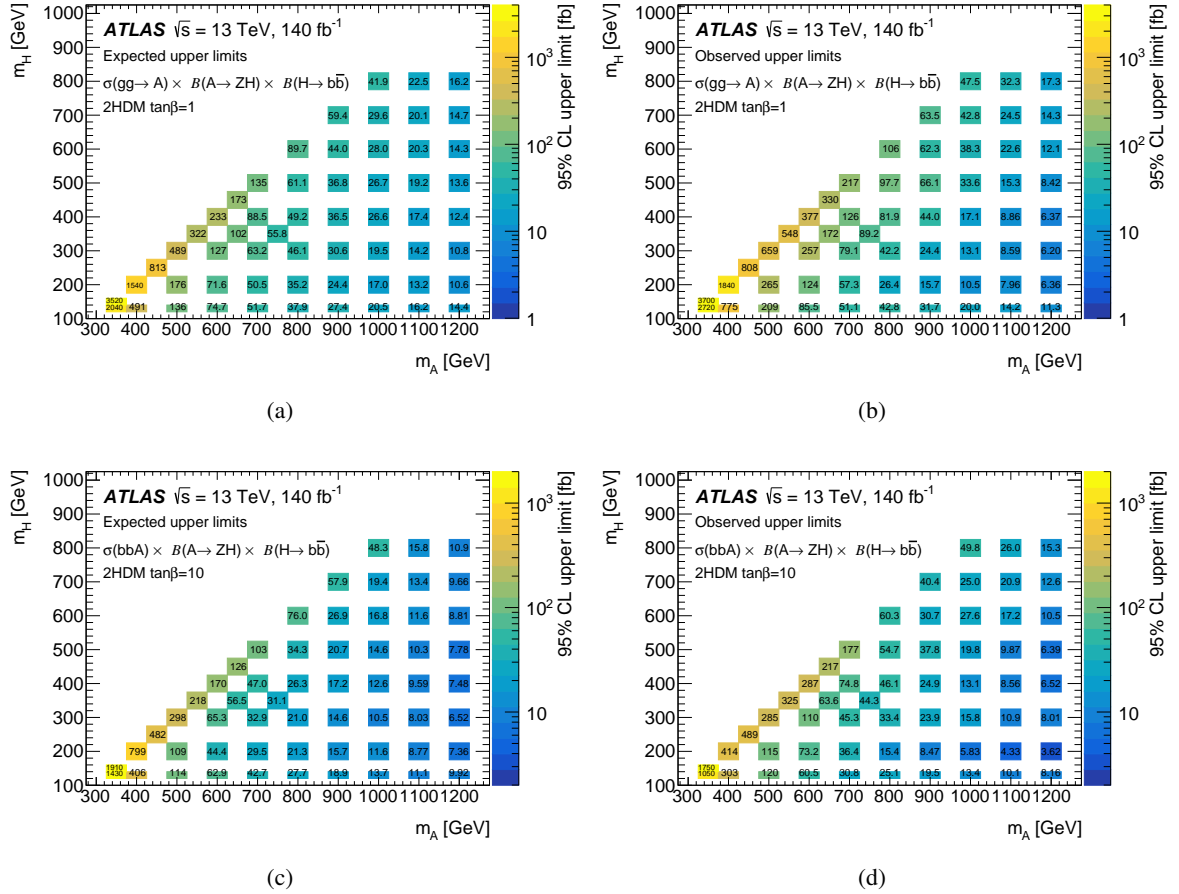


Figure 6: Expected (a,c) and observed (b,d) upper limits at 95% CL on $\sigma(gg \rightarrow A) \times B(A \rightarrow ZH) \times B(H \rightarrow b\bar{b})$ (a,b) and $\sigma(b\bar{b}A) \times B(A \rightarrow ZH) \times B(H \rightarrow b\bar{b})$ (c,d) in the (m_A, m_H) plane. The limits are shown for either $\tan\beta = 1$ or $\tan\beta = 10$ in ggF or bbA production, respectively. The $\tan\beta$ value is relevant only for the choice of A boson width.

8.2 Interpretation in the context of 2HDM

The upper limits shown in Section 8.1 are interpreted in the context of the CP-conserving 2HDM. For this interpretation, several assumptions are made to reduce the number of free parameters in the model. The H^\pm bosons are assumed to have the same mass as the A boson, whereas $m_H < m_A$ is assumed for the masses of the A and H bosons. The 2HDM parameter m_{12}^2 is fixed to $m_A^2 \tan\beta / (1 + \tan^2\beta)$. The h boson is assumed to have a mass of 125 GeV and its couplings to fermions and vector bosons are set to be the same as those of the SM Higgs boson at lowest order by choosing $\cos(\beta - \alpha) = 0$. The widths of the A and H bosons are taken from the predictions of the 2HDM. These assumptions leave three free parameters: m_A , m_H and $\tan\beta$. In addition, there are four possible arrangements of the Yukawa couplings, which are known as type-I, type-II, lepton specific and flipped 2HDM. For the parameter space that is relevant for this search, the widths of the A and H bosons differ very little across the different 2HDM types in comparison with the experimental mass resolution. In the same parameter space, the A boson width is larger than the H boson width, so the quoted limits from this search cannot be interpreted as limits for the $H \rightarrow ZA$ process. The cross-sections for A boson production in the 2HDM are calculated with corrections up to NNLO in

QCD for ggF and bbA production in the five-flavour scheme as implemented in SusHi [119–122]. For bbA production, a cross-section in the four-flavour scheme is also calculated as described in Refs. [123, 124] and the results are combined with the five-flavour scheme calculation following Ref. [125]. The Higgs boson branching ratios are calculated using 2HDMC [126]. The procedure used to calculate the cross-sections and branching ratios, as well as to choose the 2HDM parameter values, follows Ref. [87].

The upper limits are interpreted as constraints in the (m_A, m_H) plane for several $\tan\beta$ values. The widths of the A and H bosons change as a function of $\tan\beta$ and these variations are taken into account when calculating the constraints. The results are quoted only for cases in which the width of the A boson is no more than 25% of m_A . Figures 7(a) and 7(b) show the constraints from the $\ell^+\ell^-t\bar{t}$ channel for the type-I and type-II 2HDM, respectively. Constraints from this channel for the lepton-specific 2HDM are very similar to type-I. Constraints from the $\nu\bar{\nu}b\bar{b}$ channel are shown in Figure 7(c) for the type-I 2HDM, and in Figures 7(d) and 7(e) for the type-II 2HDM. These results extend the reach of the $A \rightarrow ZH \rightarrow \ell\ell b\bar{b}$ search reported in Ref. [22], especially in parts of the parameter space with $m_H > 350$ GeV and $m_A > 800$ GeV.

The fact that the observed exclusion limit for the $\ell^+\ell^-t\bar{t}$ channel is smaller than the expected exclusion limit in the region around $(m_A, m_H) = (650, 450)$ GeV in Figures 7(a) and 7(b) is a consequence of the small data excess observed in Figure 3(a). Similarly, in the $\nu\bar{\nu}b\bar{b}$ channel, at low $\tan\beta$ in Figure 7(d) the expected and observed limits diverge because of a small excess of events for $550 \text{ GeV} \lesssim m_T(VH) \lesssim 650 \text{ GeV}$. Finally, differences seen between the limits at high $\tan\beta$ are affected by small excesses or deficits in the data; in particular, the smaller observed exclusion limit in the region with $(m_A, m_H) = (600, 300)$ GeV is due to the excess observed in Figure 3(c).

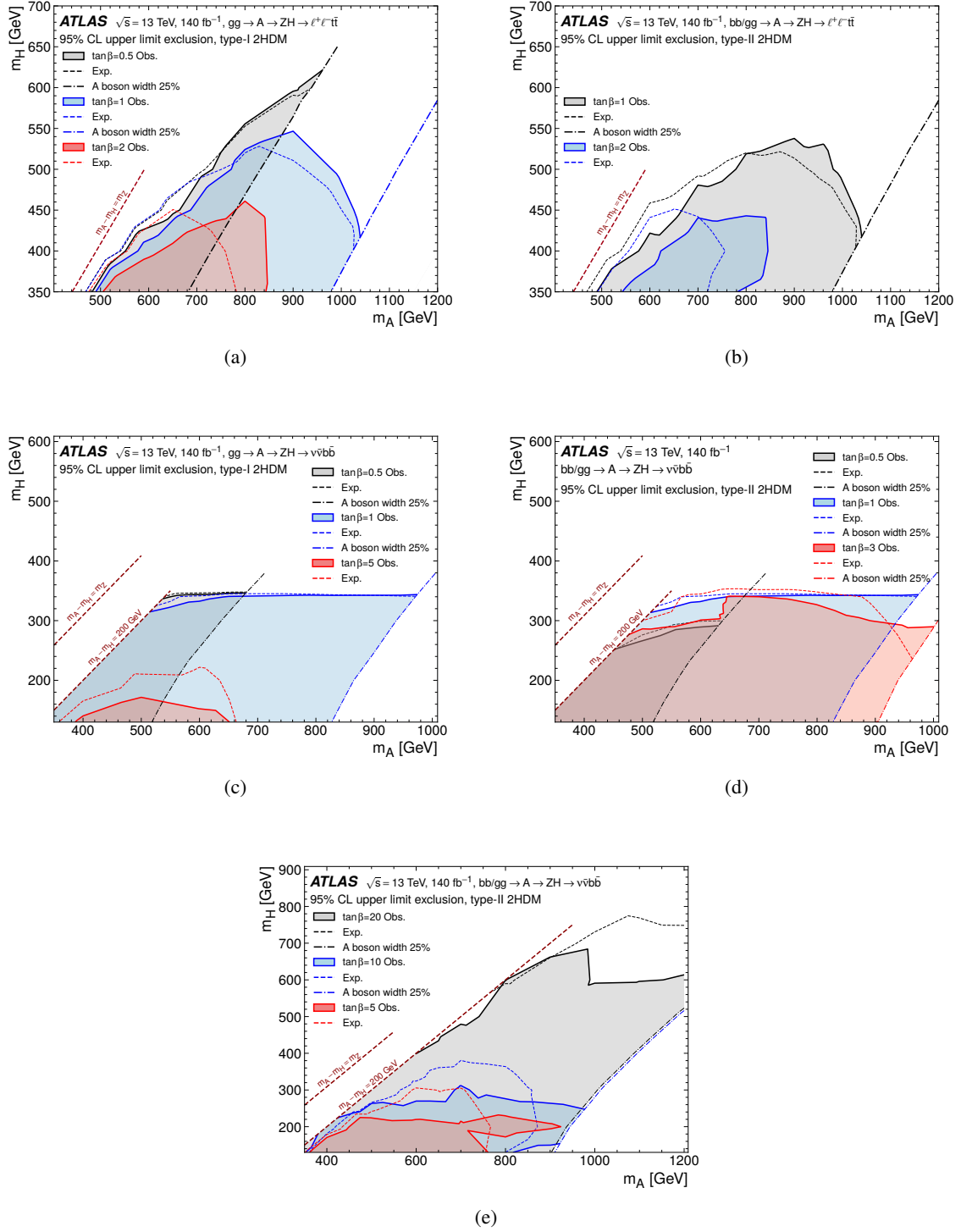


Figure 7: Observed and expected 95% CL exclusion regions in the (m_A, m_H) plane for various $\tan\beta$ values for the $\ell^+ \ell^- t \bar{t}$ channel, type-I (a) and type-II (b) 2HDM, and $\nu\nu b\bar{b}$ channel, type-I (c) and type-II (d,e) 2HDM. The line at $m_A - m_H = 200$ GeV shown in (c–e) corresponds to the edge of the analysis sensitivity due to the E_T^{miss} requirement.

8.3 Model-independent limits

The upper limits presented above are based on the assumption that the Z and H candidates in the final state are produced resonantly and therefore have a significant model dependence. In addition to the 2HDM interpretation, limits with less model dependence are derived with a slight modification of the fit model as follows. Assuming that a resonance X that decays into a $t\bar{t}$ or $b\bar{b}$ pair is produced in association with a Z boson, the number of signal events that will be recorded by the detector in a given bin of the reconstructed $m(t\bar{t})$ or $m(b\bar{b})$ distribution will be equal to the integrated luminosity times the ‘visible cross-section’ $\sigma_{\text{vis}}(Z(\ell\ell)X(t\bar{t}))$ or $\sigma_{\text{vis}}(Z(\nu\bar{\nu})X(b\bar{b}))$.

Upper limits at 95% CL are placed on $\sigma_{\text{vis}}(Z(\ell\ell)X(t\bar{t}))$ and $\sigma_{\text{vis}}(Z(\nu\bar{\nu})X(b\bar{b}))$ using the fit model described in Section 7, except that the $m(t\bar{t})$ or $m(b\bar{b})$ distributions for the events that pass the SR selection are fitted using three bins. The signal template is constructed by adding a single signal event in the central bin of the $m(t\bar{t})$ or $m(b\bar{b})$ distribution, with the adjacent bins used as CRs. The corresponding ss region or $e\mu$ and 2L regions are also used as CRs in this fit without any modification. Using the $m(t\bar{t})$ or $m(b\bar{b})$ distributions instead of the Δm or $m_{\text{T}}(VH)$ distributions in the fit ensures that the limit thus obtained is independent of how the Z and H candidates are produced, and using a large bin that contains all of the signal events ensures that the limit does not depend strongly on the lineshape of the $t\bar{t}$ or $b\bar{b}$ resonance.⁷

To obtain the upper limits on the visible cross-section as functions of $m(t\bar{t})$ and $m(b\bar{b})$, multiple independent fits are performed, each time using different SRs, defined by the bin edges shown in Figure 8. These limits can be used to estimate sensitivities for theories involving high-mass $t\bar{t}$ or $b\bar{b}$ resonances, by comparing the upper limit shown in Figure 8 with the visible cross-section predicted by a specific theory, given by

$$\sigma_{\text{vis}}^{\text{theory}} = \sigma_{\text{theory}} \times B \times (\mathcal{A} \cdot \epsilon)_{m(t\bar{t})/m(b\bar{b})},$$

where σ_{theory} is the inclusive signal cross-section, B is the product of the branching ratios for the decay chain and $(\mathcal{A} \cdot \epsilon)_{m(t\bar{t})/m(b\bar{b})}$ is the acceptance times efficiency for reconstructing a signal-model event in a given bin of the $m(b\bar{b})$ or $m(t\bar{t})$ distribution. The use of the limits shown in Figure 8 requires the value of $(\mathcal{A} \cdot \epsilon)_{m(t\bar{t})/m(b\bar{b})}$ for a given signal model to be obtained from a Monte Carlo ‘truth’-level analysis that reproduces the event selection described in Section 5, incorporating the detector effects, for example via fast simulation packages such as DELPHES [127] or smearing routines such as the ones provided in the RIVET framework [128, 129]. The applicability of these limits is not guaranteed outside the phase space in which $(\mathcal{A} \cdot \epsilon)$ values are provided, or when the derived $(\mathcal{A} \cdot \epsilon)$ values differ significantly from the values provided in this publication.

⁷ For signals that predict a $t\bar{t}$ or $b\bar{b}$ resonance with a mass that lies between the bin edges in Figure 8, the limits from all bins in which the signal contributes have to be combined, taking into account their respective acceptances.

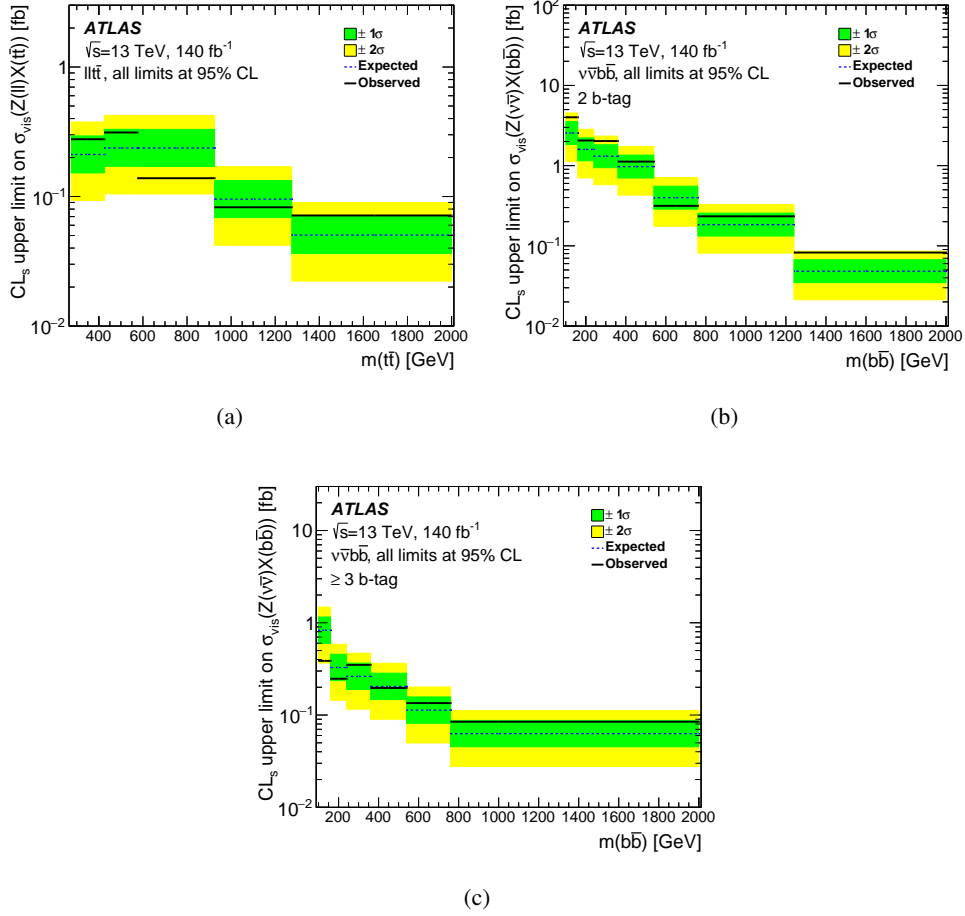


Figure 8: Observed (solid line) and expected (dashed line) 95% CL upper limits on $\sigma_{\text{vis}}(Z(\ell\ell)X(t\bar{t}))$ (a) and $\sigma_{\text{vis}}(Z(\nu\bar{\nu})X(b\bar{b}))$ obtained from the 2- b -tag (b) and ≥ 3 - b -tag (c) regions. The limits are obtained in bins of reconstructed $m(t\bar{t})$ and $m(b\bar{b})$. The green and yellow bands correspond to the $\pm 1\sigma$ and $\pm 2\sigma$ intervals for the expected upper limits, respectively.

9 Conclusion

A search for the decay of a heavy CP-odd Higgs boson A into a heavy CP-even Higgs boson H is presented, using the full LHC Run 2 dataset of 13 TeV proton–proton collisions corresponding to an integrated luminosity of 140 fb^{-1} recorded by the ATLAS detector. Two channels are considered in the present search. The $\ell^+\ell^-\bar{t}\bar{t}$ channel, which probes H boson decays into a pair of top quarks and Z boson decays into a pair of charged leptons, provides sensitivity in the $m_H > 350$ GeV region. The $\nu\bar{\nu}b\bar{b}$ channel, which probes H boson decays into a pair of b -quarks and Z boson decays into neutrinos, extends the sensitivity of previous searches in parts of the parameter space with $m_A > 800$ GeV and $m_H < 350$ GeV.

No significant excess over the SM background prediction is observed. Upper limits are set at the 95% confidence level on the production cross-section times the decay branching ratios. These results are interpreted in the context of the two-Higgs-doublet models and yield an exclusion range significantly larger than those obtained by previous searches sensitive to this parameter space. In addition, upper limits are

quoted as a function of reconstructed $m(t\bar{t})$ and $m(b\bar{b})$, assuming the production of a $t\bar{t}$ or $b\bar{b}$ resonance.

Acknowledgements

We thank CERN for the very successful operation of the LHC, as well as the support staff from our institutions without whom ATLAS could not be operated efficiently.

We acknowledge the support of ANPCyT, Argentina; YerPhI, Armenia; ARC, Australia; BMWFW and FWF, Austria; ANAS, Azerbaijan; CNPq and FAPESP, Brazil; NSERC, NRC and CFI, Canada; CERN; ANID, Chile; CAS, MOST and NSFC, China; Minciencias, Colombia; MEYS CR, Czech Republic; DNRF and DNSRC, Denmark; IN2P3-CNRS and CEA-DRF/IRFU, France; SRNSFG, Georgia; BMBF, HGF and MPG, Germany; GSRI, Greece; RGC and Hong Kong SAR, China; ISF and Benoziyo Center, Israel; INFN, Italy; MEXT and JSPS, Japan; CNRST, Morocco; NWO, Netherlands; RCN, Norway; MEiN, Poland; FCT, Portugal; MNE/IFA, Romania; MESTD, Serbia; MSSR, Slovakia; ARRS and MIZŠ, Slovenia; DSI/NRF, South Africa; MICINN, Spain; SRC and Wallenberg Foundation, Sweden; SERI, SNSF and Cantons of Bern and Geneva, Switzerland; MOST, Taiwan; TENMAK, Türkiye; STFC, United Kingdom; DOE and NSF, United States of America. In addition, individual groups and members have received support from BCKDF, CANARIE, Compute Canada and CRC, Canada; PRIMUS 21/SCI/017 and UNCE SCI/013, Czech Republic; COST, ERC, ERDF, Horizon 2020, ICSC-NextGenerationEU and Marie Skłodowska-Curie Actions, European Union; Investissements d’Avenir Labex, Investissements d’Avenir IDEX and ANR, France; DFG and AvH Foundation, Germany; Herakleitos, Thales and Aristeia programmes co-financed by EU-ESF and the Greek NSRF, Greece; BSF-NSF and MINERVA, Israel; Norwegian Financial Mechanism 2014-2021, Norway; NCN and NAWA, Poland; La Caixa Banking Foundation, CERCA Programme Generalitat de Catalunya and PROMETEO and GenT Programmes Generalitat Valenciana, Spain; Göran Gustafssons Stiftelse, Sweden; The Royal Society and Leverhulme Trust, United Kingdom.

The crucial computing support from all WLCG partners is acknowledged gratefully, in particular from CERN, the ATLAS Tier-1 facilities at TRIUMF (Canada), NDGF (Denmark, Norway, Sweden), CC-IN2P3 (France), KIT/GridKA (Germany), INFN-CNAF (Italy), NL-T1 (Netherlands), PIC (Spain), ASGC (Taiwan), RAL (UK) and BNL (USA), the Tier-2 facilities worldwide and large non-WLCG resource providers. Major contributors of computing resources are listed in Ref. [130].

Upper limits on the production cross sections for additional $\tan \beta$ values

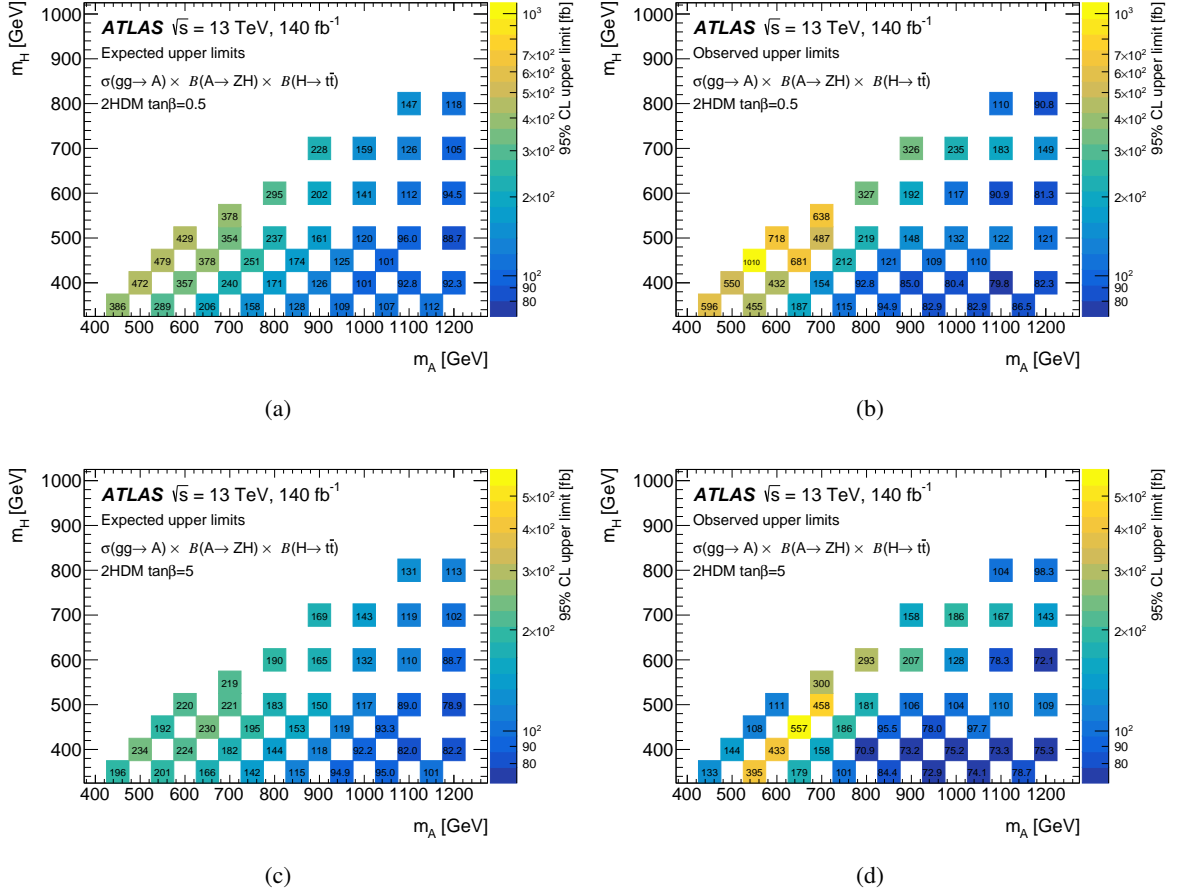


Figure 9: Expected and observed upper limits at 95% CL on $\sigma(gg \rightarrow A) \times B(A \rightarrow ZH) \times B(H \rightarrow t\bar{t})$. The limits are shown for $\tan \beta = 0.5$ (a,b) and $\tan \beta = 5$ (c,d). The $\tan \beta$ value is relevant only for the choice of A boson width.

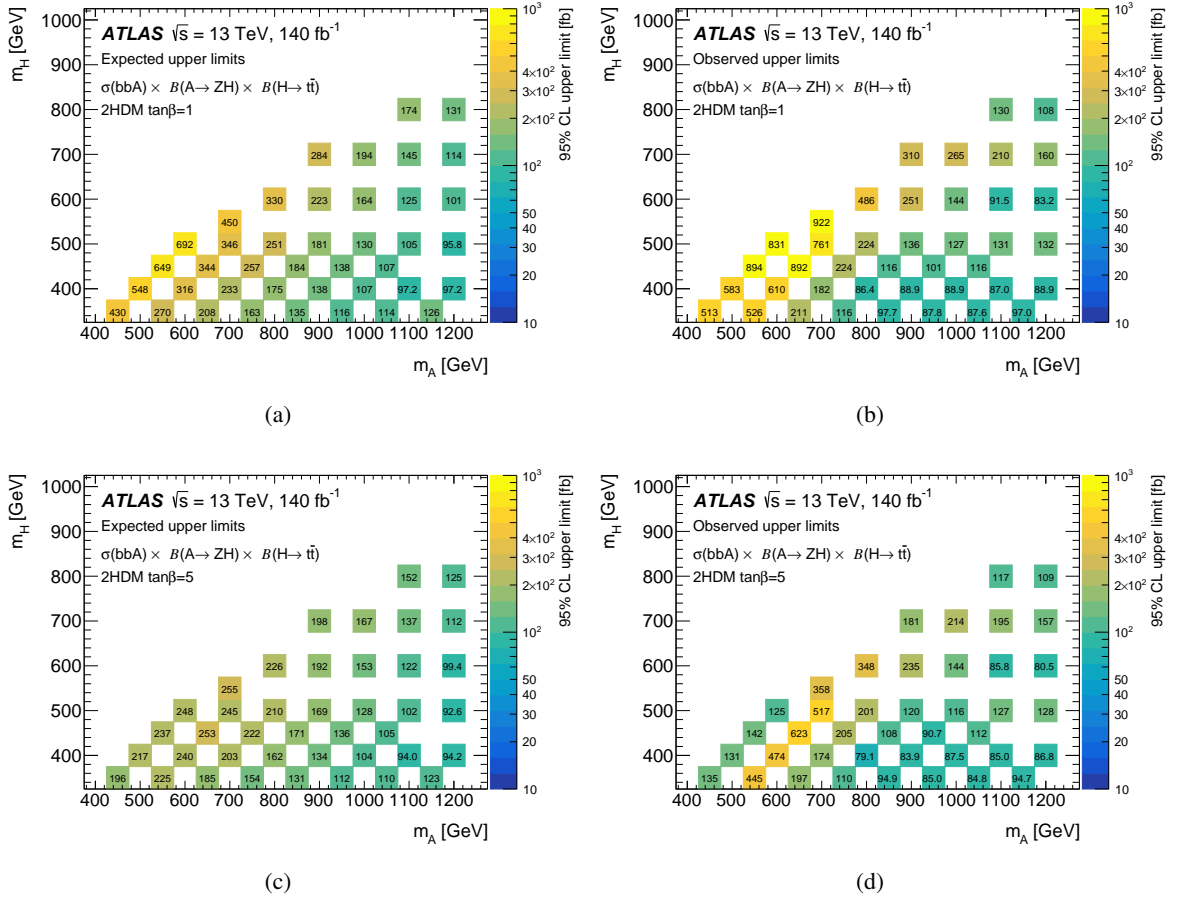


Figure 10: Expected and observed upper limits at 95% CL on $\sigma(b\bar{b}A) \times B(A \rightarrow ZH) \times B(H \rightarrow t\bar{t})$. The limits are shown for $\tan\beta = 1$ (a,b) and $\tan\beta = 5$ (c,d). The $\tan\beta$ value is relevant only for the choice of A boson width.

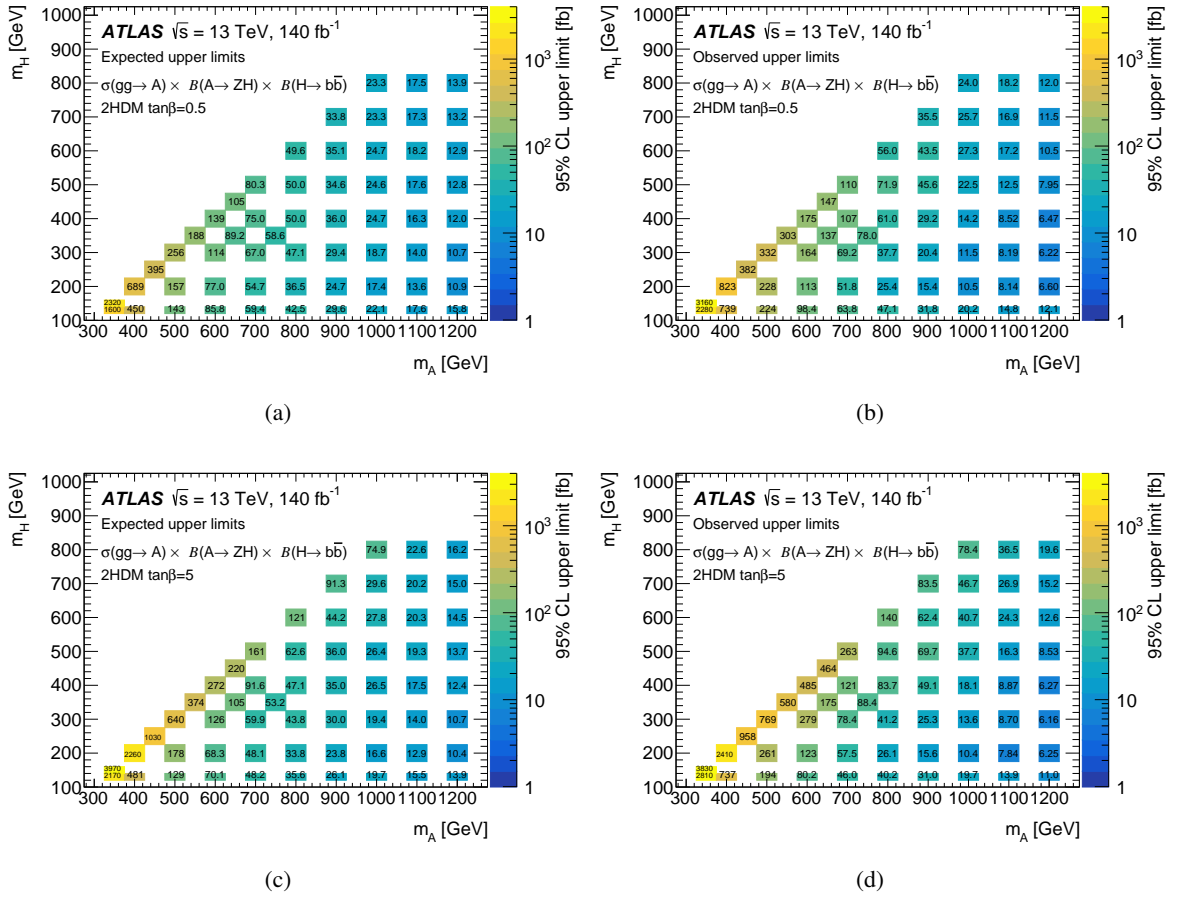


Figure 11: Expected and observed upper limits at 95% CL on $\sigma(gg \rightarrow A) \times B(A \rightarrow ZH) \times B(H \rightarrow b\bar{b})$. The limits are shown for $\tan\beta = 0.5$ (a,b) and $\tan\beta = 5$ (c,d). The $\tan\beta$ value is relevant only for the choice of A boson width.

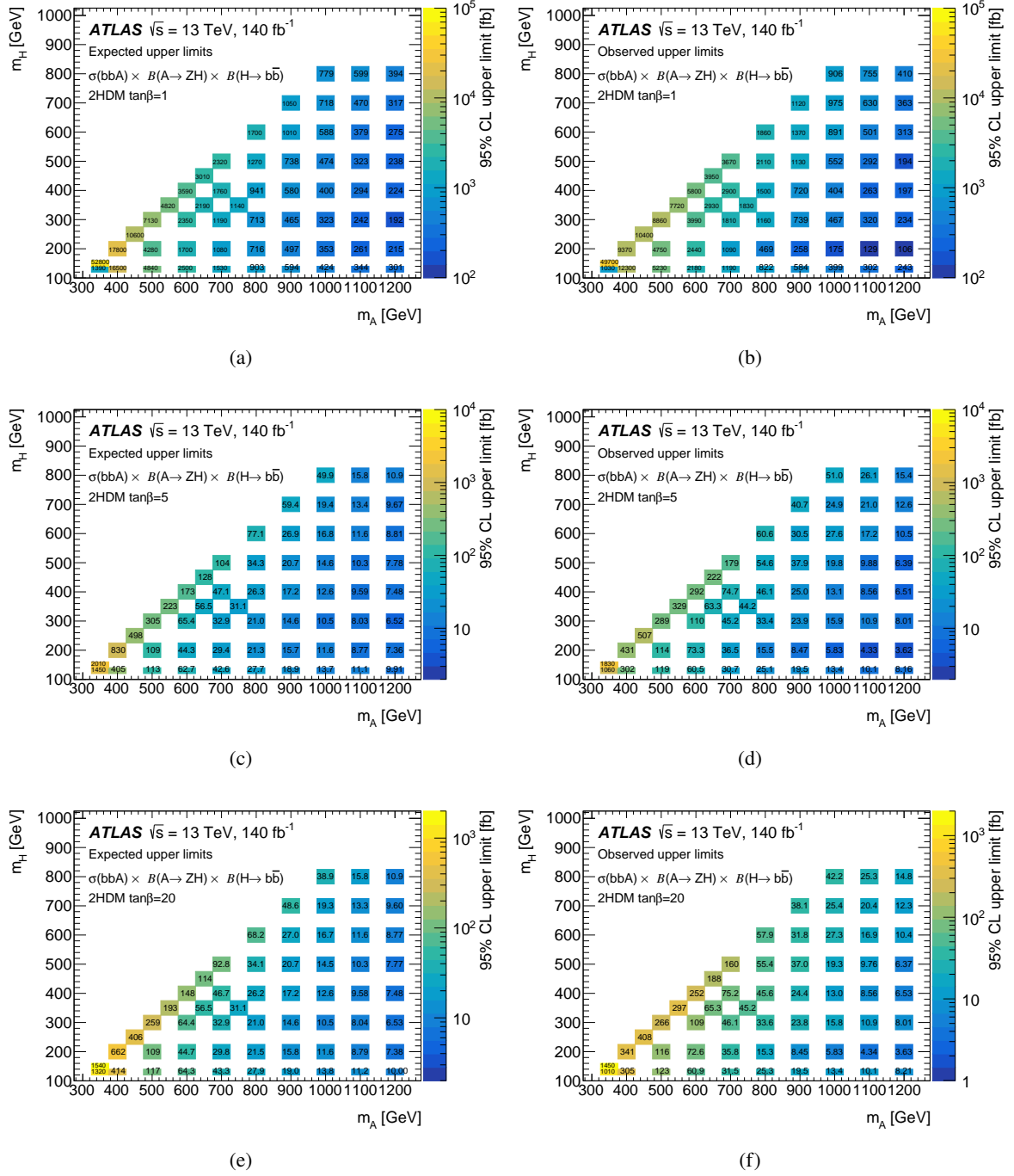


Figure 12: Expected and observed upper limits at 95% CL on $\sigma(b\bar{b}A) \times B(A \rightarrow ZH) \times B(H \rightarrow b\bar{b})$. The limits are shown for $\tan\beta = 1$ (a,b), $\tan\beta = 5$ (c,d) and $\tan\beta = 20$ (e,f). The $\tan\beta$ value is relevant only for the choice of A boson width.

References

- [1] ATLAS Collaboration, *Observation of a new particle in the search for the Standard Model Higgs boson with the ATLAS detector at the LHC*, *Phys. Lett. B* **716** (2012) 1, arXiv: [1207.7214 \[hep-ex\]](#).
- [2] CMS Collaboration, *Observation of a new boson at a mass of 125 GeV with the CMS experiment at the LHC*, *Phys. Lett. B* **716** (2012) 30, arXiv: [1207.7235 \[hep-ex\]](#).
- [3] A. Ferrari and N. Rompotis, *Exploration of Extended Higgs Sectors with Run-2 Proton–Proton Collision Data at the LHC*, *Symmetry* **13** (2021) 2144, Erratum: *Symmetry* **14** (2022) 1546.
- [4] T. D. Lee, *A Theory of Spontaneous T Violation*, *Phys. Rev. D* **8** (1973) 1226.
- [5] G. C. Branco et al., *Theory and phenomenology of two-Higgs-doublet models*, *Phys. Rept.* **516** (2012) 1, arXiv: [1106.0034 \[hep-ph\]](#).
- [6] A. Djouadi, *The anatomy of electroweak symmetry breaking Tome II: The Higgs bosons in the Minimal Supersymmetric Model*, *Phys. Rept.* **459** (2008) 1, arXiv: [hep-ph/0503173](#).
- [7] J. Abdallah et al., *Simplified models for dark matter searches at the LHC*, *Physics of the Dark Universe* **9-10** (2015) 8, arXiv: [1506.03116 \[hep-ph\]](#).
- [8] M. Bauer, U. Haisch and F. Kahlhoefer, *Simplified dark matter models with two Higgs doublets: I. Pseudoscalar mediators*, *JHEP* **05** (2017) 138, arXiv: [1701.07427 \[hep-ph\]](#).
- [9] J. E. Kim and G. Carosi, *Axions and the strong CP problem*, *Rev. Mod. Phys.* **82** (2010) 557, arXiv: [0807.3125 \[hep-ph\]](#), Erratum: *Rev.Mod.Phys.* **91** (2019) 049902.
- [10] A. G. Cohen, D. B. Kaplan and A. E. Nelson, *Progress in Electroweak Baryogenesis*, *Ann. Rev. Nucl. Part. Sci.* **43** (1993) 27, arXiv: [hep-ph/9302210](#).
- [11] S. F. King, *Neutrino mass models*, *Rept. Prog. Phys.* **67** (2003) 107, arXiv: [hep-ph/0310204](#).
- [12] J. F. Gunion and H. E. Haber, *CP-conserving two-Higgs-doublet model: The approach to the decoupling limit*, *Phys. Rev. D* **67** (2003) 075019, arXiv: [hep-ph/0207010](#).
- [13] The Gfitter Group, *Update of the global electroweak fit and constraints on two-Higgs-doublet models*, *Eur. Phys. J. C* **78** (2018) 675, arXiv: [1803.01853 \[hep-ph\]](#).
- [14] ATLAS Collaboration, *Search for heavy resonances decaying into a Z or W boson and a Higgs boson in final states with leptons and b-jets in 139 fb⁻¹ of pp collisions at $\sqrt{s} = 13$ TeV with the ATLAS detector*, *JHEP* **06** (2023) 016, arXiv: [2207.00230 \[hep-ex\]](#).
- [15] CMS Collaboration, *Search for heavy resonances decaying into a vector boson and a Higgs boson in final states with charged leptons, neutrinos, and b quarks*, *Phys. Lett. B* **768** (2017) 137, arXiv: [1610.08066 \[hep-ex\]](#).
- [16] G. C. Dorsch, S. J. Huber and J. M. No, *A strong electroweak phase transition in the 2HDM after LHC8*, *JHEP* **10** (2013) 029, arXiv: [1305.6610 \[hep-ph\]](#).

- [17] G. C. Dorsch, S. J. Huber, K. Mimasu and J. M. No, *Echoes of the Electroweak Phase Transition: Discovering a Second Higgs Doublet through $A_0 \rightarrow ZH_0$* , *Phys. Rev. Lett.* **113** (2014) 211802, arXiv: 1405.5537 [hep-ph].
- [18] N. Turok and J. Zadrozny, *Electroweak baryogenesis in the two-doublet model*, *Nucl. Phys. B* **358** (1991) 471.
- [19] L. Fromme, S. J. Huber and M. Seniuch, *Baryogenesis in the two-Higgs doublet model*, *JHEP* **11** (2006) 038, arXiv: hep-ph/0605242.
- [20] P. Basler, M. Krause, M. Mühlleitner, J. Wittbrodt and A. Wlotzka, *Strong first order electroweak phase transition in the CP-conserving 2HDM revisited*, *JHEP* **02** (2017) 121, arXiv: 1612.04086 [hep-ph].
- [21] W. Su, A. G. Williams and M. Zhang, *Strong first order electroweak phase transition in 2HDM confronting future Z & Higgs factories*, *JHEP* **04** (2021) 219, arXiv: 2011.04540 [hep-ph].
- [22] ATLAS Collaboration, *Search for a heavy Higgs boson decaying into a Z boson and another heavy Higgs boson in the $\ell\ell b\bar{b}$ and $\ell\ell WW$ final states in pp collisions at $\sqrt{s} = 13$ TeV with the ATLAS detector*, *Eur. Phys. J. C* **81** (2020) 396, arXiv: 2011.05639 [hep-ex].
- [23] CMS Collaboration, *Search for neutral resonances decaying into a Z boson and a pair of b jets or τ leptons*, *Phys. Lett. B* **759** (2016) 369, arXiv: 1603.02991 [hep-ex].
- [24] CMS Collaboration, *Search for new neutral Higgs bosons through the $H \rightarrow ZA \rightarrow \ell^+ \ell^- b\bar{b}$ process in pp collisions at $\sqrt{s} = 13$ TeV*, *JHEP* **03** (2020) 055, arXiv: 1911.03781 [hep-ex].
- [25] ATLAS Collaboration, *Search for Higgs boson pair production in association with a vector boson in pp collisions at $\sqrt{s} = 13$ TeV with the ATLAS detector*, *Eur. Phys. J. C* **83** (2022) 519, arXiv: 2210.05415 [hep-ex].
- [26] ATLAS Collaboration, *Search for dark matter produced in association with a Standard Model Higgs boson decaying into b-quarks using the full Run 2 dataset from the ATLAS detector*, *JHEP* **11** (2021) 209, arXiv: 2108.13391 [hep-ex].
- [27] ATLAS Collaboration, *The ATLAS Experiment at the CERN Large Hadron Collider*, *JINST* **3** (2008) S08003.
- [28] ATLAS Collaboration, *ATLAS Insertable B-Layer: Technical Design Report*, ATLAS-TDR-19; CERN-LHCC-2010-013, 2010, URL: <https://cds.cern.ch/record/1291633>, Addendum: ATLAS-TDR-19-ADD-1; CERN-LHCC-2012-009, 2012, URL: <https://cds.cern.ch/record/1451888>.
- [29] B. Abbott et al., *Production and integration of the ATLAS Insertable B-Layer*, *JINST* **13** (2018) T05008, arXiv: 1803.00844 [physics.ins-det].
- [30] ATLAS Collaboration, *Performance of the ATLAS trigger system in 2015*, *Eur. Phys. J. C* **77** (2017) 317, arXiv: 1611.09661 [hep-ex].
- [31] ATLAS Collaboration, *The ATLAS Collaboration Software and Firmware*, ATL-SOFT-PUB-2021-001, 2021, URL: <https://cds.cern.ch/record/2767187>.
- [32] ATLAS Collaboration, *ATLAS data quality operations and performance for 2015–2018 data-taking*, *JINST* **15** (2020) P04003, arXiv: 1911.04632 [physics.ins-det].

- [33] ATLAS Collaboration, *Measurements of WH and ZH production in the $H \rightarrow b\bar{b}$ decay channel in pp collisions at 13 TeV with the ATLAS detector*, *Eur. Phys. J. C* **81** (2021) 178, arXiv: [2007.02873 \[hep-ex\]](#).
- [34] J. Alwall et al., *The automated computation of tree-level and next-to-leading order differential cross sections, and their matching to parton shower simulations*, *JHEP* **07** (2014) 079, arXiv: [1405.0301 \[hep-ph\]](#).
- [35] The NNPDF Collaboration, R. D. Ball et al., *Parton distributions for the LHC run II*, *JHEP* **04** (2015) 040, arXiv: [1410.8849 \[hep-ph\]](#).
- [36] P. Artoisenet, V. Lemaître, F. Maltoni and O. Mattelaer, *Automation of the matrix element reweighting method*, *JHEP* **12** (2010) 068, arXiv: [1007.3300 \[hep-ph\]](#).
- [37] S. Frixione, E. Laenen, P. Motylinski and B. R. Webber, *Angular correlations of lepton pairs from vector boson and top quark decays in Monte Carlo simulations*, *JHEP* **04** (2007) 081, arXiv: [hep-ph/0702198](#).
- [38] P. Artoisenet, R. Frederix, O. Mattelaer and R. Rietkerk, *Automatic spin-entangled decays of heavy resonances in Monte Carlo simulations*, *JHEP* **03** (2013) 015, arXiv: [1212.3460 \[hep-ph\]](#).
- [39] T. Sjöstrand et al., *An introduction to PYTHIA 8.2*, *Comput. Phys. Commun.* **191** (2015) 159, arXiv: [1410.3012 \[hep-ph\]](#).
- [40] ATLAS Collaboration, *ATLAS Pythia 8 tunes to 7 TeV data*, ATL-PHYS-PUB-2014-021, 2014, URL: <https://cds.cern.ch/record/1966419>.
- [41] U. Haisch and G. Poleseello, *Searching for heavy Higgs bosons in the $t\bar{t}Z$ and tbW final states*, *JHEP* **09** (2018) 151, arXiv: [1807.07734 \[hep-ph\]](#).
- [42] D. J. Lange, *The EvtGen particle decay simulation package*, *Nucl. Instrum. Meth. A* **462** (2001) 152.
- [43] S. Schumann and F. Krauss, *A parton shower algorithm based on Catani–Seymour dipole factorisation*, *JHEP* **03** (2008) 038, arXiv: [0709.1027 \[hep-ph\]](#).
- [44] T. Sjöstrand, S. Mrenna and P. Skands, *A brief introduction to PYTHIA 8.1*, *Comput. Phys. Commun.* **178** (2008) 852, arXiv: [0710.3820 \[hep-ph\]](#).
- [45] ATLAS Collaboration, *The Pythia 8 A3 tune description of ATLAS minimum bias and inelastic measurements incorporating the Donnachie–Landshoff diffractive model*, ATL-PHYS-PUB-2016-017, 2016, URL: <https://cds.cern.ch/record/2206965>.
- [46] S. Agostinelli et al., *GEANT4 – a simulation toolkit*, *Nucl. Instrum. Meth. A* **506** (2003) 250.
- [47] ATLAS Collaboration, *The ATLAS Simulation Infrastructure*, *Eur. Phys. J. C* **70** (2010) 823, arXiv: [1005.4568 \[physics.ins-det\]](#).
- [48] NNPDF Collaboration, R. D. Ball et al., *Parton distributions with LHC data*, *Nucl. Phys. B* **867** (2013) 244, arXiv: [1207.1303 \[hep-ph\]](#).
- [49] J. Pumplin et al., *New Generation of Parton Distributions with Uncertainties from Global QCD Analysis*, *JHEP* **07** (2002) 012, arXiv: [hep-ph/0201195](#).

- [50] S. Frixione, E. Laenen, P. Motylinski, C. White and B. R. Webber, *Single-top hadroproduction in association with a W boson*, **JHEP** **07** (2008) 029, arXiv: [0805.3067 \[hep-ph\]](#).
- [51] S. Frixione, G. Ridolfi and P. Nason, *A positive-weight next-to-leading-order Monte Carlo for heavy flavour hadroproduction*, **JHEP** **09** (2007) 126, arXiv: [0707.3088 \[hep-ph\]](#).
- [52] P. Nason, *A new method for combining NLO QCD with shower Monte Carlo algorithms*, **JHEP** **11** (2004) 040, arXiv: [hep-ph/0409146](#).
- [53] S. Frixione, P. Nason and C. Oleari, *Matching NLO QCD computations with parton shower simulations: the POWHEG method*, **JHEP** **11** (2007) 070, arXiv: [0709.2092 \[hep-ph\]](#).
- [54] S. Alioli, P. Nason, C. Oleari and E. Re, *A general framework for implementing NLO calculations in shower Monte Carlo programs: the POWHEG BOX*, **JHEP** **06** (2010) 043, arXiv: [1002.2581 \[hep-ph\]](#).
- [55] M. Beneke, P. Falgari, S. Klein and C. Schwinn, *Hadronic top-quark pair production with NNLL threshold resummation*, **Nucl. Phys. B** **855** (2012) 695, arXiv: [1109.1536 \[hep-ph\]](#).
- [56] M. Cacciari, M. Czakon, M. Mangano, A. Mitov and P. Nason, *Top-pair production at hadron colliders with next-to-next-to-leading logarithmic soft-gluon resummation*, **Phys. Lett. B** **710** (2012) 612, arXiv: [1111.5869 \[hep-ph\]](#).
- [57] P. Bärnreuther, M. Czakon and A. Mitov, *Percent-Level-Precision Physics at the Tevatron: Next-to-Next-to-Leading Order QCD Corrections to $q\bar{q} \rightarrow t\bar{t} + X$* , **Phys. Rev. Lett.** **109** (2012) 132001, arXiv: [1204.5201 \[hep-ph\]](#).
- [58] M. Czakon and A. Mitov, *NNLO corrections to top-pair production at hadron colliders: the all-fermionic scattering channels*, **JHEP** **12** (2012) 054, arXiv: [1207.0236 \[hep-ph\]](#).
- [59] M. Czakon and A. Mitov, *NNLO corrections to top pair production at hadron colliders: the quark-gluon reaction*, **JHEP** **01** (2013) 080, arXiv: [1210.6832 \[hep-ph\]](#).
- [60] M. Czakon, P. Fiedler and A. Mitov, *Total Top-Quark Pair-Production Cross Section at Hadron Colliders Through $O(\alpha_S^4)$* , **Phys. Rev. Lett.** **110** (2013) 252004, arXiv: [1303.6254 \[hep-ph\]](#).
- [61] M. Czakon and A. Mitov, *Top++: A program for the calculation of the top-pair cross-section at hadron colliders*, **Comput. Phys. Commun.** **185** (2014) 2930, arXiv: [1112.5675 \[hep-ph\]](#).
- [62] E. Re, *Single-top Wt -channel production matched with parton showers using the POWHEG method*, **Eur. Phys. J. C** **71** (2011) 1547, arXiv: [1009.2450 \[hep-ph\]](#).
- [63] N. Kidonakis, *Two-loop soft anomalous dimensions for single top quark associated production with a W^- or H^-* , **Phys. Rev. D** **82** (2010) 054018, arXiv: [1005.4451 \[hep-ph\]](#).
- [64] N. Kidonakis, ‘Top Quark Production’, *Proceedings, Helmholtz International Summer School on Physics of Heavy Quarks and Hadrons (HQ 2013)* (JINR, Dubna, Russia, 15th–28th July 2013) 139, arXiv: [1311.0283 \[hep-ph\]](#).

- [65] R. Frederix, E. Re and P. Torrielli, *Single-top t -channel hadroproduction in the four-flavour scheme with POWHEG and aMC@NLO*, *JHEP* **09** (2012) 130, arXiv: [1207.5391 \[hep-ph\]](#).
- [66] M. Aliev et al., *HATHOR – HAdronic Top and Heavy quarks crOss section calculatoR*, *Comput. Phys. Commun.* **182** (2011) 1034, arXiv: [1007.1327 \[hep-ph\]](#).
- [67] P. Kant et al., *HatHor for single top-quark production: Updated predictions and uncertainty estimates for single top-quark production in hadronic collisions*, *Comput. Phys. Commun.* **191** (2015) 74, arXiv: [1406.4403 \[hep-ph\]](#).
- [68] E. Bothmann et al., *Event generation with Sherpa 2.2*, *SciPost Phys.* **7** (2019) 034, arXiv: [1905.09127 \[hep-ph\]](#).
- [69] C. Anastasiou, L. Dixon, K. Melnikov and F. Petriello, *High-precision QCD at hadron colliders: Electroweak gauge boson rapidity distributions at next-to-next-to leading order*, *Phys. Rev. D* **69** (2004) 094008, arXiv: [hep-ph/0312266](#).
- [70] S. Höche, F. Krauss, M. Schönherr and F. Siegert, *A critical appraisal of NLO+PS matching methods*, *JHEP* **09** (2012) 049, arXiv: [1111.1220 \[hep-ph\]](#).
- [71] S. Höche, F. Krauss, M. Schönherr and F. Siegert, *QCD matrix elements + parton showers. The NLO case*, *JHEP* **04** (2013) 027, arXiv: [1207.5030 \[hep-ph\]](#).
- [72] S. Catani, F. Krauss, B. R. Webber and R. Kuhn, *QCD Matrix Elements + Parton Showers*, *JHEP* **11** (2001) 063, arXiv: [hep-ph/0109231](#).
- [73] S. Höche, F. Krauss, S. Schumann and F. Siegert, *QCD matrix elements and truncated showers*, *JHEP* **05** (2009) 053, arXiv: [0903.1219 \[hep-ph\]](#).
- [74] ATLAS Collaboration, *Measurement of the Z/γ^* boson transverse momentum distribution in pp collisions at $\sqrt{s} = 7$ TeV with the ATLAS detector*, *JHEP* **09** (2014) 145, arXiv: [1406.3660 \[hep-ex\]](#).
- [75] K. Hamilton, P. Nason and G. Zanderighi, *MINLO: multi-scale improved NLO*, *JHEP* **10** (2012) 155, arXiv: [1206.3572 \[hep-ph\]](#).
- [76] G. Luisoni, P. Nason, C. Oleari and F. Tramontano, *$HW^\pm/HZ + 0$ and 1 jet at NLO with the POWHEG BOX interfaced to GoSam and their merging within MinLO*, *JHEP* **10** (2013) 083, arXiv: [1306.2542 \[hep-ph\]](#).
- [77] M. L. Ciccolini, S. Dittmaier and M. Krämer, *Electroweak radiative corrections to associated WH and ZH production at hadron colliders*, *Phys. Rev. D* **68** (2003) 073003, arXiv: [hep-ph/0306234 \[hep-ph\]](#).
- [78] O. Brein, A. Djouadi and R. Harlander, *NNLO QCD corrections to the Higgs-strahlung processes at hadron colliders*, *Phys. Lett. B* **579** (2004) 149, arXiv: [hep-ph/0307206](#).
- [79] G. Ferrera, M. Grazzini and F. Tramontano, *Associated Higgs-W-Boson Production at Hadron Colliders: A Fully Exclusive QCD Calculation at NNLO*, *Phys. Rev. Lett.* **107** (2011) 152003, arXiv: [1107.1164 \[hep-ph\]](#).
- [80] O. Brein, R. V. Harlander, M. Wiesemann and T. Zirke, *Top-quark mediated effects in hadronic Higgs-Strahlung*, *Eur. Phys. J. C* **72** (2012) 1868, arXiv: [1111.0761 \[hep-ph\]](#).

- [81] G. Ferrera, M. Grazzini and F. Tramontano, *Higher-order QCD effects for associated WH production and decay at the LHC*, [JHEP **04** \(2014\) 039](#), arXiv: [1312.1669 \[hep-ph\]](#).
- [82] G. Ferrera, M. Grazzini and F. Tramontano, *Associated ZH production at hadron colliders: The fully differential NNLO QCD calculation*, [Phys. Lett. B **740** \(2015\) 51](#), arXiv: [1407.4747 \[hep-ph\]](#).
- [83] J. M. Campbell, R. K. Ellis and C. Williams, *Associated production of a Higgs boson at NNLO*, [JHEP **06** \(2016\) 179](#), arXiv: [1601.00658 \[hep-ph\]](#).
- [84] L. Altenkamp, S. Dittmaier, R. V. Harlander, H. Rzehak and T. J. E. Zirke, *Gluon-induced Higgs-strahlung at next-to-leading order QCD*, [JHEP **02** \(2013\) 078](#), arXiv: [1211.5015 \[hep-ph\]](#).
- [85] R. V. Harlander, A. Kulesza, V. Theeuwes and T. Zirke, *Soft gluon resummation for gluon-induced Higgs Strahlung*, [JHEP **11** \(2014\) 082](#), arXiv: [1410.0217 \[hep-ph\]](#).
- [86] O. Brein, R. V. Harlander and T. J. E. Zirke, *vh@nnlo – Higgs Strahlung at hadron colliders*, [Comput. Phys. Commun. **184** \(2013\) 998](#), arXiv: [1210.5347 \[hep-ph\]](#).
- [87] D. de Florian et al., *Handbook of LHC Higgs Cross Sections: 4. Deciphering the Nature of the Higgs Sector*, (2016), arXiv: [1610.07922 \[hep-ph\]](#).
- [88] H. B. Hartanto, B. Jäger, L. Reina and D. Wackerth, *Higgs boson production in association with top quarks in the POWHEG BOX*, [Phys. Rev. D **91** \(2015\) 094003](#), arXiv: [1501.04498 \[hep-ph\]](#).
- [89] ATLAS Collaboration, *Vertex Reconstruction Performance of the ATLAS Detector at $\sqrt{s} = 13$ TeV*, ATL-PHYS-PUB-2015-026, 2015, URL: <https://cds.cern.ch/record/2037717>.
- [90] ATLAS Collaboration, *Electron and photon performance measurements with the ATLAS detector using the 2015–2017 LHC proton–proton collision data*, [JINST **14** \(2019\) P12006](#), arXiv: [1908.00005 \[hep-ex\]](#).
- [91] ATLAS Collaboration, *Electron reconstruction and identification in the ATLAS experiment using the 2015 and 2016 LHC proton–proton collision data at $\sqrt{s} = 13$ TeV*, [Eur. Phys. J. C **79** \(2019\) 639](#), arXiv: [1902.04655 \[physics.ins-det\]](#).
- [92] ATLAS Collaboration, *Muon reconstruction and identification efficiency in ATLAS using the full Run 2 pp collision data set at $\sqrt{s} = 13$ TeV*, [Eur. Phys. J. C **81** \(2021\) 578](#), arXiv: [2012.00578 \[hep-ex\]](#).
- [93] ATLAS Collaboration, *Reconstruction, Energy Calibration, and Identification of Hadronically Decaying Tau Leptons in the ATLAS Experiment for Run-2 of the LHC*, ATL-PHYS-PUB-2015-045, 2015, URL: <https://cds.cern.ch/record/2064383>.
- [94] M. Cacciari, G. P. Salam and G. Soyez, *The anti- k_t jet clustering algorithm*, [JHEP **04** \(2008\) 063](#), arXiv: [0802.1189 \[hep-ph\]](#).
- [95] M. Cacciari, G. P. Salam and G. Soyez, *FastJet user manual*, [Eur. Phys. J. C **72** \(2012\) 1896](#), arXiv: [1111.6097 \[hep-ph\]](#).
- [96] ATLAS Collaboration, *Identification of hadronic tau lepton decays using neural networks in the ATLAS experiment*, ATL-PHYS-PUB-2019-033, 2019, URL: <https://cds.cern.ch/record/2688062>.

- [97] ATLAS Collaboration, *Jet reconstruction and performance using particle flow with the ATLAS Detector*, *Eur. Phys. J. C* **77** (2017) 466, arXiv: [1703.10485 \[hep-ex\]](#).
- [98] ATLAS Collaboration, *Performance of pile-up mitigation techniques for jets in pp collisions at $\sqrt{s} = 8$ TeV using the ATLAS detector*, *Eur. Phys. J. C* **76** (2016) 581, arXiv: [1510.03823 \[hep-ex\]](#).
- [99] ATLAS Collaboration, *ATLAS b-jet identification performance and efficiency measurement with $t\bar{t}$ events in pp collisions at $\sqrt{s} = 13$ TeV*, *Eur. Phys. J. C* **79** (2019) 970, arXiv: [1907.05120 \[hep-ex\]](#).
- [100] ATLAS Collaboration, *E_T^{miss} performance in the ATLAS detector using 2015–2016 LHC pp collisions*, ATLAS-CONF-2018-023, 2018, URL: <https://cds.cern.ch/record/2625233>.
- [101] ATLAS Collaboration, *Object-based missing transverse momentum significance in the ATLAS Detector*, ATLAS-CONF-2018-038, 2018, URL: <https://cds.cern.ch/record/2630948>.
- [102] ATLAS Collaboration, *Selection of jets produced in 13 TeV proton–proton collisions with the ATLAS detector*, ATLAS-CONF-2015-029, 2015, URL: <https://cds.cern.ch/record/2037702>.
- [103] Particle Data Group, P. Zyla et al., *Review of Particle Physics*, *PTEP* **2020** (2020) 083C01.
- [104] ATLAS Collaboration, *Jet energy scale and resolution measured in proton–proton collisions at $\sqrt{s} = 13$ TeV with the ATLAS detector*, *Eur. Phys. J. C* **81** (2021) 689, arXiv: [2007.02645 \[hep-ex\]](#).
- [105] ATLAS Collaboration, *Measurement of the c-jet mistagging efficiency in $t\bar{t}$ events using pp collision data at $\sqrt{s} = 13$ TeV collected with the ATLAS detector*, *Eur. Phys. J. C* **82** (2022) 95, arXiv: [2109.10627 \[hep-ex\]](#).
- [106] ATLAS Collaboration, *Calibration of light-flavour b-jet mistagging rates using ATLAS proton–proton collision data at $\sqrt{s} = 13$ TeV*, ATLAS-CONF-2018-006, 2018, URL: <https://cds.cern.ch/record/2314418>.
- [107] ATLAS Collaboration, *Performance of missing transverse momentum reconstruction with the ATLAS detector using proton-proton collisions at $\sqrt{s} = 13$ TeV*, *Eur. Phys. J. C* **78** (2018) 903, arXiv: [1802.08168 \[hep-ex\]](#).
- [108] ATLAS Collaboration, *Luminosity determination in pp collisions at $\sqrt{s} = 13$ TeV using the ATLAS detector at the LHC*, (2022), arXiv: [2212.09379 \[hep-ex\]](#).
- [109] G. Avoni et al., *The new LUCID-2 detector for luminosity measurement and monitoring in ATLAS*, *JINST* **13** (2018) P07017.
- [110] J. Bellm et al., *Herwig 7.1 Release Note*, (2017), arXiv: [1705.06919 \[hep-ph\]](#).
- [111] M. Bähr et al., *Herwig++ physics and manual*, *Eur. Phys. J. C* **58** (2008) 639, arXiv: [0803.0883 \[hep-ph\]](#).
- [112] J. Bellm et al., *Herwig 7.0/Herwig++ 3.0 release note*, *Eur. Phys. J. C* **76** (2016) 196, arXiv: [1512.01178 \[hep-ph\]](#).

- [113] J. Butterworth et al., *PDF4LHC recommendations for LHC Run II*, *J. Phys. G* **43** (2016) 023001, arXiv: [1510.03865 \[hep-ph\]](#).
- [114] G. Cowan, K. Cranmer, E. Gross and O. Vitells, *Asymptotic formulae for likelihood-based tests of new physics*, *Eur. Phys. J. C* **71** (2011) 1554, arXiv: [1007.1727 \[physics.data-an\]](#), Erratum: *Eur. Phys. J. C* **73** (2013) 2501.
- [115] R. Barlow and C. Beeston, *Fitting using finite Monte Carlo samples*, *Comput. Phys. Commun.* **77** (1993) 219.
- [116] A. L. Read, *Presentation of search results: the CL_s technique*, *J. Phys. G* **28** (2002) 2693.
- [117] O. Vitells and E. Gross, *Estimating the significance of a signal in a multi-dimensional search*, *Astropart. Phys.* **35** (2011) 230, arXiv: [1105.4355 \[astro-ph.IM\]](#).
- [118] E. Gross and O. Vitells, *Trial factors for the look elsewhere effect in high energy physics*, *Eur. Phys. J. C* **70** (2010) 525, arXiv: [1005.1891 \[physics.data-an\]](#).
- [119] R. V. Harlander, S. Liebler and H. Mantler, *SusHi: A program for the calculation of Higgs production in gluon fusion and bottom-quark annihilation in the Standard Model and the MSSM*, *Comput. Phys. Commun.* **184** (2013) 1605, arXiv: [1212.3249 \[hep-ph\]](#).
- [120] R. V. Harlander and P. Kant, *Higgs production and decay: analytic results at next-to-leading-order QCD*, *JHEP* **12** (2005) 015, arXiv: [hep-ph/0509189](#).
- [121] R. V. Harlander and W. B. Kilgore, *Higgs boson production in bottom quark fusion at next-to-next-to leading order*, *Phys. Rev. D* **68** (2003) 013001, arXiv: [hep-ph/0304035](#).
- [122] R. V. Harlander and W. B. Kilgore, *Next-to-Next-to-Leading Order Higgs Production at Hadron Colliders*, *Phys. Rev. Lett.* **88** (2002) 201801, arXiv: [hep-ph/0201206](#).
- [123] S. Dawson, C. B. Jackson, L. Reina and D. Wackerroth, *Exclusive Higgs boson production with bottom quarks at hadron colliders*, *Phys. Rev. D* **69** (2004) 074027, arXiv: [hep-ph/0311067](#).
- [124] S. Dittmaier, M. Krämer and M. Spira, *Higgs radiation off bottom quarks at the Fermilab Tevatron and the CERN LHC*, *Phys. Rev. D* **70** (2004) 074010, arXiv: [hep-ph/0309204](#).
- [125] R. Harlander, M. Krämer and M. Schumacher, *Bottom-quark associated Higgs-boson production: reconciling the four- and five-flavour scheme approach*, (2011), arXiv: [1112.3478 \[hep-ph\]](#).
- [126] D. Eriksson, J. Rathsman and O. Stål, *2HDMC – two-Higgs-doublet model calculator*, *Comput. Phys. Commun.* **181** (2010) 189, arXiv: [0902.0851 \[hep-ph\]](#).
- [127] DELPHES 3 Collaboration, *DELPHES 3: A modular framework for fast simulation of a generic collider experiment*, *JHEP* **02** (2014) 057, arXiv: [1307.6346 \[hep-ex\]](#).
- [128] A. Buckley, D. Kar and K. Nordström, *Fast simulation of detector effects in Rivet*, *SciPost Phys.* **8** (2020) 025, arXiv: [1910.01637 \[hep-ph\]](#).
- [129] C. Bierlich et al., *Robust Independent Validation of Experiment and Theory: Rivet version 3*, *SciPost Phys.* **8** (2020) 026, arXiv: [1912.05451 \[hep-ph\]](#).

- [130] ATLAS Collaboration, *ATLAS Computing Acknowledgements*, ATL-SOFT-PUB-2023-001, 2023,
URL: <https://cds.cern.ch/record/2869272>.

The ATLAS Collaboration

G. Aad ¹⁰², B. Abbott ¹²⁰, K. Abeling ⁵⁵, N.J. Abicht ⁴⁹, S.H. Abidi ²⁹, A. Abouhorma ^{35e}, H. Abramowicz ¹⁵¹, H. Abreu ¹⁵⁰, Y. Abulaiti ¹¹⁷, B.S. Acharya ^{69a,69b,m}, C. Adam Bourdarios ⁴, L. Adamczyk ^{86a}, S.V. Addepalli ²⁶, M.J. Addison ¹⁰¹, J. Adelman ¹¹⁵, A. Adiguzel ^{21c}, T. Adye ¹³⁴, A.A. Affolder ¹³⁶, Y. Afik ³⁶, M.N. Agaras ¹³, J. Agarwala ^{73a,73b}, A. Aggarwal ¹⁰⁰, C. Agheorghiesei ^{27c}, A. Ahmad ³⁶, F. Ahmadov ^{38,y}, W.S. Ahmed ¹⁰⁴, S. Ahuja ⁹⁵, X. Ai ^{62a}, G. Aielli ^{76a,76b}, A. Aikot ¹⁶³, M. Ait Tamlihat ^{35e}, B. Aitbenchikh ^{35a}, I. Aizenberg ¹⁶⁹, M. Akbiyik ¹⁰⁰, T.P.A. Åkesson ⁹⁸, A.V. Akimov ³⁷, D. Akiyama ¹⁶⁸, N.N. Akolkar ²⁴, S. Aktas ^{21a}, K. Al Houry ⁴¹, G.L. Alberghi ^{23b}, J. Albert ¹⁶⁵, P. Albicocco ⁵³, G.L. Albouy ⁶⁰, S. Alderweireldt ⁵², M. Aleksa ³⁶, I.N. Aleksandrov ³⁸, C. Alexa ^{27b}, T. Alexopoulos ¹⁰, F. Alfonsi ^{23b}, M. Algren ⁵⁶, M. Alhroob ¹²⁰, B. Ali ¹³², H.M.J. Ali ⁹¹, S. Ali ¹⁴⁸, S.W. Alibocus ⁹², M. Aliev ¹⁴⁵, G. Alimonti ^{71a}, W. Alkakh ⁵⁵, C. Allaire ⁶⁶, B.M.M. Allbrooke ¹⁴⁶, J.F. Allen ⁵², C.A. Allendes Flores ^{137f}, P.P. Allport ²⁰, A. Aloisio ^{72a,72b}, F. Alonso ⁹⁰, C. Alpigiani ¹³⁸, M. Alvarez Estevez ⁹⁹, A. Alvarez Fernandez ¹⁰⁰, M. Alves Cardoso ⁵⁶, M.G. Alviggi ^{72a,72b}, M. Aly ¹⁰¹, Y. Amaral Coutinho ^{83b}, A. Ambler ¹⁰⁴, C. Amelung ³⁶, M. Amerl ¹⁰¹, C.G. Ames ¹⁰⁹, D. Amidei ¹⁰⁶, S.P. Amor Dos Santos ^{130a}, K.R. Amos ¹⁶³, V. Ananiev ¹²⁵, C. Anastopoulos ¹³⁹, T. Andeen ¹¹, J.K. Anders ³⁶, S.Y. Andreev ^{47a,47b}, A. Andreatta ^{71a,71b}, S. Angelidakis ⁹, A. Angerami ^{41,ab}, A.V. Anisenkov ³⁷, A. Annovi ^{74a}, C. Antel ⁵⁶, M.T. Anthony ¹³⁹, E. Antipov ¹⁴⁵, M. Antonelli ⁵³, F. Anulli ^{75a}, M. Aoki ⁸⁴, T. Aoki ¹⁵³, J.A. Aparisi Pozo ¹⁶³, M.A. Aparo ¹⁴⁶, L. Aperio Bella ⁴⁸, C. Appelt ¹⁸, A. Apyan ²⁶, N. Aranzabal ³⁶, S.J. Arbiol Val ⁸⁷, C. Arcangeletti ⁵³, A.T.H. Arce ⁵¹, E. Arena ⁹², J-F. Arguin ¹⁰⁸, S. Argyropoulos ⁵⁴, J.-H. Arling ⁴⁸, O. Arnaez ⁴, H. Arnold ¹¹⁴, G. Artoni ^{75a,75b}, H. Asada ¹¹¹, K. Asai ¹¹⁸, S. Asai ¹⁵³, N.A. Asbah ⁶¹, K. Assamagan ²⁹, R. Astalos ^{28a}, S. Atashi ¹⁶⁰, R.J. Atkin ^{33a}, M. Atkinson ¹⁶², H. Atmani ^{35f}, P.A. Atlasiddha ¹²⁸, K. Augsten ¹³², S. Auricchio ^{72a,72b}, A.D. Auriol ²⁰, V.A. Austrup ¹⁰¹, G. Avolio ³⁶, K. Axiotis ⁵⁶, G. Azuelos ^{108,af}, D. Babal ^{28b}, H. Bachacou ¹³⁵, K. Bachas ^{152,p}, A. Bachi ³⁴, F. Backman ^{47a,47b}, A. Badea ⁶¹, T.M. Baer ¹⁰⁶, P. Bagnaia ^{75a,75b}, M. Bahmani ¹⁸, A.J. Bailey ¹⁶³, V.R. Bailey ¹⁶², J.T. Baines ¹³⁴, L. Baines ⁹⁴, O.K. Baker ¹⁷², E. Bakos ¹⁵, D. Bakshi Gupta ⁸, V. Balakrishnan ¹²⁰, R. Balasubramanian ¹¹⁴, E.M. Baldin ³⁷, P. Balek ^{86a}, E. Ballabene ^{23b,23a}, F. Balli ¹³⁵, L.M. Baltes ^{63a}, W.K. Balunas ³², J. Balz ¹⁰⁰, E. Banas ⁸⁷, M. Bandieramonte ¹²⁹, A. Bandyopadhyay ²⁴, S. Bansal ²⁴, L. Barak ¹⁵¹, M. Barakat ⁴⁸, E.L. Barberio ¹⁰⁵, D. Barberis ^{57b,57a}, M. Barbero ¹⁰², M.Z. Barel ¹¹⁴, K.N. Barends ^{33a}, T. Barillari ¹¹⁰, M-S. Barisits ³⁶, T. Barklow ¹⁴³, P. Baron ¹²², D.A. Baron Moreno ¹⁰¹, A. Baroncelli ^{62a}, G. Barone ²⁹, A.J. Barr ¹²⁶, J.D. Barr ⁹⁶, L. Barranco Navarro ^{47a,47b}, F. Barreiro ⁹⁹, J. Barreiro Guimarães da Costa ^{14a}, U. Barron ¹⁵¹, M.G. Barros Teixeira ^{130a}, S. Barsov ³⁷, F. Bartels ^{63a}, R. Bartoldus ¹⁴³, A.E. Barton ⁹¹, P. Bartos ^{28a}, A. Basan ¹⁰⁰, M. Baselga ⁴⁹, A. Bassalat ^{66,b}, M.J. Basso ^{156a}, C.R. Basson ¹⁰¹, R.L. Bates ⁵⁹, S. Batlamous ^{35e}, J.R. Batley ³², B. Batool ¹⁴¹, M. Battaglia ¹³⁶, D. Battulga ¹⁸, M. Bause ^{75a,75b}, M. Bauer ³⁶, P. Bauer ²⁴, L.T. Bazzano Hurrell ³⁰, J.B. Beacham ⁵¹, T. Beau ¹²⁷, J.Y. Beauchamp ⁹⁰, P.H. Beauchemin ¹⁵⁸, F. Becherer ⁵⁴, P. Bechtel ²⁴, H.P. Beck ^{19,o}, K. Becker ¹⁶⁷, A.J. Beddall ⁸², V.A. Bednyakov ³⁸, C.P. Bee ¹⁴⁵, L.J. Beemster ¹⁵, T.A. Beermann ³⁶, M. Begalli ^{83d}, M. Begel ²⁹, A. Behera ¹⁴⁵, J.K. Behr ⁴⁸, J.F. Beirer ³⁶, F. Beisiegel ²⁴, M. Belfkir ¹⁵⁹, G. Bella ¹⁵¹, L. Bellagamba ^{23b}, A. Bellerive ³⁴, P. Bellos ²⁰, K. Beloborodov ³⁷, D. Benchechroun ^{35a}, F. Bendebba ^{35a}, Y. Benhammou ¹⁵¹, M. Benoit ²⁹, J.R. Bensinger ²⁶, S. Bentvelsen ¹¹⁴, L. Beresford ⁴⁸, M. Beretta ⁵³,

E. Bergeaas Kuutmann [id](#)¹⁶¹, N. Berger [id](#)⁴, B. Bergmann [id](#)¹³², J. Beringer [id](#)^{17a}, G. Bernardi [id](#)⁵,
 C. Bernius [id](#)¹⁴³, F.U. Bernlochner [id](#)²⁴, F. Bernon [id](#)^{36,102}, A. Berrocal Guardia [id](#)¹³, T. Berry [id](#)⁹⁵,
 P. Berta [id](#)¹³³, A. Berthold [id](#)⁵⁰, I.A. Bertram [id](#)⁹¹, S. Bethke [id](#)¹¹⁰, A. Betti [id](#)^{75a,75b}, A.J. Bevan [id](#)⁹⁴,
 N.K. Bhalla [id](#)⁵⁴, M. Bhamjee [id](#)^{33c}, S. Bhatta [id](#)¹⁴⁵, D.S. Bhattacharya [id](#)¹⁶⁶, P. Bhattacharai [id](#)¹⁴³,
 V.S. Bhopatkar [id](#)¹²¹, R. Bi [id](#)^{29,ai}, R.M. Bianchi [id](#)¹²⁹, G. Bianco [id](#)^{23b,23a}, O. Biebel [id](#)¹⁰⁹, R. Bielski [id](#)¹²³,
 M. Biglietti [id](#)^{77a}, M. Bindi [id](#)⁵⁵, A. Bingul [id](#)^{21b}, C. Bini [id](#)^{75a,75b}, A. Biondini [id](#)⁹², C.J. Birch-sykes [id](#)¹⁰¹,
 G.A. Bird [id](#)^{20,134}, M. Birman [id](#)¹⁶⁹, M. Biros [id](#)¹³³, S. Biryukov [id](#)¹⁴⁶, T. Bisanz [id](#)⁴⁹, E. Bisceglie [id](#)^{43b,43a},
 J.P. Biswal [id](#)¹³⁴, D. Biswas [id](#)¹⁴¹, A. Bitadze [id](#)¹⁰¹, K. Bjørke [id](#)¹²⁵, I. Bloch [id](#)⁴⁸, A. Blue [id](#)⁵⁹,
 U. Blumenschein [id](#)⁹⁴, J. Blumenthal [id](#)¹⁰⁰, G.J. Bobbink [id](#)¹¹⁴, V.S. Bobrovnikov [id](#)³⁷, M. Boehler [id](#)⁵⁴,
 B. Boehm [id](#)¹⁶⁶, D. Bogavac [id](#)³⁶, A.G. Bogdanchikov [id](#)³⁷, C. Bohm [id](#)^{47a}, V. Boisvert [id](#)⁹⁵, P. Bokan [id](#)⁴⁸,
 T. Bold [id](#)^{86a}, M. Bomben [id](#)⁵, M. Bona [id](#)⁹⁴, M. Boonekamp [id](#)¹³⁵, C.D. Booth [id](#)⁹⁵, A.G. Borbély [id](#)⁵⁹,
 I.S. Bordulev [id](#)³⁷, H.M. Borecka-Bielska [id](#)¹⁰⁸, G. Borissov [id](#)⁹¹, D. Bortoletto [id](#)¹²⁶, D. Boscherini [id](#)^{23b},
 M. Bosman [id](#)¹³, J.D. Bossio Sola [id](#)³⁶, K. Bouaouda [id](#)^{35a}, N. Bouchhar [id](#)¹⁶³, J. Boudreau [id](#)¹²⁹,
 E.V. Bouhova-Thacker [id](#)⁹¹, D. Boumediene [id](#)⁴⁰, R. Bouquet [id](#)¹⁶⁵, A. Boveia [id](#)¹¹⁹, J. Boyd [id](#)³⁶,
 D. Boye [id](#)²⁹, I.R. Boyko [id](#)³⁸, J. Bracinek [id](#)²⁰, N. Brahimi [id](#)^{62d}, G. Brandt [id](#)¹⁷¹, O. Brandt [id](#)³²,
 F. Braren [id](#)⁴⁸, B. Brau [id](#)¹⁰³, J.E. Brau [id](#)¹²³, R. Brenner [id](#)¹⁶⁹, L. Brenner [id](#)¹¹⁴, R. Brenner [id](#)¹⁶¹,
 S. Bressler [id](#)¹⁶⁹, D. Britton [id](#)⁵⁹, D. Britzger [id](#)¹¹⁰, I. Brock [id](#)²⁴, G. Brooijmans [id](#)⁴¹, W.K. Brooks [id](#)^{137f},
 E. Brost [id](#)²⁹, L.M. Brown [id](#)¹⁶⁵, L.E. Bruce [id](#)⁶¹, T.L. Bruckler [id](#)¹²⁶, P.A. Bruckman de Renstrom [id](#)⁸⁷,
 B. Brüers [id](#)⁴⁸, A. Bruni [id](#)^{23b}, G. Bruni [id](#)^{23b}, M. Bruschi [id](#)^{23b}, N. Brusino [id](#)^{75a,75b}, T. Buanes [id](#)¹⁶,
 Q. Buat [id](#)¹³⁸, D. Buchin [id](#)¹¹⁰, A.G. Buckley [id](#)⁵⁹, O. Bulekov [id](#)³⁷, B.A. Bullard [id](#)¹⁴³, S. Burdin [id](#)⁹²,
 C.D. Burgard [id](#)⁴⁹, A.M. Burger [id](#)⁴⁰, B. Burghgrave [id](#)⁸, O. Burlayenko [id](#)⁵⁴, J.T.P. Burr [id](#)³²,
 C.D. Burton [id](#)¹¹, J.C. Burzynski [id](#)¹⁴², E.L. Busch [id](#)⁴¹, V. Büscher [id](#)¹⁰⁰, P.J. Bussey [id](#)⁵⁹,
 J.M. Butler [id](#)²⁵, C.M. Buttar [id](#)⁵⁹, J.M. Butterworth [id](#)⁹⁶, W. Buttinger [id](#)¹³⁴, C.J. Buxo Vazquez [id](#)¹⁰⁷,
 A.R. Buzykaev [id](#)³⁷, S. Cabrera Urbán [id](#)¹⁶³, L. Cadamuro [id](#)⁶⁶, D. Caforio [id](#)⁵⁸, H. Cai [id](#)¹²⁹,
 Y. Cai [id](#)^{14a,14e}, Y. Cai [id](#)^{14c}, V.M.M. Cairo [id](#)³⁶, O. Cakir [id](#)^{3a}, N. Calace [id](#)³⁶, P. Calafiura [id](#)^{17a},
 G. Calderini [id](#)¹²⁷, P. Calfayan [id](#)⁶⁸, G. Callea [id](#)⁵⁹, L.P. Caloba [id](#)^{83b}, D. Calvet [id](#)⁴⁰, S. Calvet [id](#)⁴⁰,
 T.P. Calvet [id](#)¹⁰², M. Calvetti [id](#)^{74a,74b}, R. Camacho Toro [id](#)¹²⁷, S. Camarda [id](#)³⁶, D. Camarero Munoz [id](#)²⁶,
 P. Camarri [id](#)^{76a,76b}, M.T. Camerlingo [id](#)^{72a,72b}, D. Cameron [id](#)³⁶, C. Camincher [id](#)¹⁶⁵, M. Campanelli [id](#)⁹⁶,
 A. Camplani [id](#)⁴², V. Canale [id](#)^{72a,72b}, A. Canesse [id](#)¹⁰⁴, J. Cantero [id](#)¹⁶³, Y. Cao [id](#)¹⁶², F. Capocasa [id](#)²⁶,
 M. Capua [id](#)^{43b,43a}, A. Carbone [id](#)^{71a,71b}, R. Cardarelli [id](#)^{76a}, J.C.J. Cardenas [id](#)⁸, F. Cardillo [id](#)¹⁶³,
 G. Carducci [id](#)^{43b,43a}, T. Carli [id](#)³⁶, G. Carlino [id](#)^{72a}, J.I. Carlotto [id](#)¹³, B.T. Carlson [id](#)^{129,q},
 E.M. Carlson [id](#)^{165,156a}, L. Carminati [id](#)^{71a,71b}, A. Carnelli [id](#)¹³⁵, M. Carnesale [id](#)^{75a,75b}, S. Caron [id](#)¹¹³,
 E. Carquin [id](#)^{137f}, S. Carrá [id](#)^{71a}, G. Carratta [id](#)^{23b,23a}, F. Carrio Argos [id](#)^{33g}, J.W.S. Carter [id](#)¹⁵⁵,
 T.M. Carter [id](#)⁵², M.P. Casado [id](#)^{13,i}, M. Caspar [id](#)⁴⁸, F.L. Castillo [id](#)⁴, L. Castillo Garcia [id](#)¹³,
 V. Castillo Gimenez [id](#)¹⁶³, N.F. Castro [id](#)^{130a,130e}, A. Catinaccio [id](#)³⁶, J.R. Catmore [id](#)¹²⁵, V. Cavaliere [id](#)²⁹,
 N. Cavalli [id](#)^{23b,23a}, V. Cavalinni [id](#)^{74a,74b}, Y.C. Cekmecelioglu [id](#)⁴⁸, E. Celebi [id](#)^{21a}, F. Celli [id](#)¹²⁶,
 M.S. Centonze [id](#)^{70a,70b}, V. Cepaitis [id](#)⁵⁶, K. Cerny [id](#)¹²², A.S. Cerqueira [id](#)^{83a}, A. Cerri [id](#)¹⁴⁶,
 L. Cerrito [id](#)^{76a,76b}, F. Cerutti [id](#)^{17a}, B. Cervato [id](#)¹⁴¹, A. Cervelli [id](#)^{23b}, G. Cesarini [id](#)⁵³, S.A. Cetin [id](#)⁸²,
 D. Chakraborty [id](#)¹¹⁵, J. Chan [id](#)¹⁷⁰, W.Y. Chan [id](#)¹⁵³, J.D. Chapman [id](#)³², E. Chapon [id](#)¹³⁵,
 B. Chargeishvili [id](#)^{149b}, D.G. Charlton [id](#)²⁰, T.P. Charman [id](#)⁹⁴, M. Chatterjee [id](#)¹⁹, C. Chauhan [id](#)¹³³,
 S. Chekanov [id](#)⁶, S.V. Chekulaev [id](#)^{156a}, G.A. Chelkov [id](#)^{38,a}, A. Chen [id](#)¹⁰⁶, B. Chen [id](#)¹⁵¹, B. Chen [id](#)¹⁶⁵,
 H. Chen [id](#)^{14c}, H. Chen [id](#)²⁹, J. Chen [id](#)^{62c}, J. Chen [id](#)¹⁴², M. Chen [id](#)¹²⁶, S. Chen [id](#)¹⁵³, S.J. Chen [id](#)^{14c},
 X. Chen [id](#)^{62c,135}, X. Chen [id](#)^{14b,ae}, Y. Chen [id](#)^{62a}, C.L. Cheng [id](#)¹⁷⁰, H.C. Cheng [id](#)^{64a}, S. Cheong [id](#)¹⁴³,
 A. Cheplakov [id](#)³⁸, E. Cheremushkina [id](#)⁴⁸, E. Cherepanova [id](#)¹¹⁴, R. Cherkaoui El Moursli [id](#)^{35e},
 E. Cheu [id](#)⁷, K. Cheung [id](#)⁶⁵, L. Chevalier [id](#)¹³⁵, V. Chiarella [id](#)⁵³, G. Chiarelli [id](#)^{74a}, N. Chiedde [id](#)¹⁰²,
 G. Chiodini [id](#)^{70a}, A.S. Chisholm [id](#)²⁰, A. Chitan [id](#)^{27b}, M. Chitishvili [id](#)¹⁶³, M.V. Chizhov [id](#)³⁸,
 K. Choi [id](#)¹¹, A.R. Chomont [id](#)^{75a,75b}, Y. Chou [id](#)¹⁰³, E.Y.S. Chow [id](#)¹¹³, T. Chowdhury [id](#)^{33g},

K.L. Chu [id](#)¹⁶⁹, M.C. Chu [id](#)^{64a}, X. Chu [id](#)^{14a,14e}, J. Chudoba [id](#)¹³¹, J.J. Chwastowski [id](#)⁸⁷, D. Cieri [id](#)¹¹⁰,
 K.M. Ciesla [id](#)^{86a}, V. Cindro [id](#)⁹³, A. Ciocio [id](#)^{17a}, F. Ciroto [id](#)^{72a,72b}, Z.H. Citron [id](#)^{169,k}, M. Citterio [id](#)^{71a},
 D.A. Ciubotaru [id](#)^{27b}, A. Clark [id](#)⁵⁶, P.J. Clark [id](#)⁵², C. Clarry [id](#)¹⁵⁵, J.M. Clavijo Columbie [id](#)⁴⁸,
 S.E. Clawson [id](#)⁴⁸, C. Clement [id](#)^{47a,47b}, J. Clercx [id](#)⁴⁸, Y. Coadou [id](#)¹⁰², M. Cobal [id](#)^{69a,69c},
 A. Coccaro [id](#)^{57b}, R.F. Coelho Barrue [id](#)^{130a}, R. Coelho Lopes De Sa [id](#)¹⁰³, S. Coelli [id](#)^{71a},
 A.E.C. Coimbra [id](#)^{71a,71b}, B. Cole [id](#)⁴¹, J. Collot [id](#)⁶⁰, P. Conde Muiño [id](#)^{130a,130g}, M.P. Connell [id](#)^{33c},
 S.H. Connell [id](#)^{33c}, I.A. Connelly [id](#)⁵⁹, E.I. Conroy [id](#)¹²⁶, F. Conventi [id](#)^{72a,ag}, H.G. Cooke [id](#)²⁰,
 A.M. Cooper-Sarkar [id](#)¹²⁶, A. Cordeiro Oudot Choi [id](#)¹²⁷, L.D. Corpe [id](#)⁴⁰, M. Corradi [id](#)^{75a,75b},
 F. Corriveau [id](#)^{104,w}, A. Cortes-Gonzalez [id](#)¹⁸, M.J. Costa [id](#)¹⁶³, F. Costanza [id](#)⁴, D. Costanzo [id](#)¹³⁹,
 B.M. Cote [id](#)¹¹⁹, G. Cowan [id](#)⁹⁵, K. Cranmer [id](#)¹⁷⁰, D. Cremonini [id](#)^{23b,23a}, S. Crépe-Renaudin [id](#)⁶⁰,
 F. Crescioli [id](#)¹²⁷, M. Cristinziani [id](#)¹⁴¹, M. Cristoforetti [id](#)^{78a,78b}, V. Croft [id](#)¹¹⁴, J.E. Crosby [id](#)¹²¹,
 G. Crosetti [id](#)^{43b,43a}, A. Cueto [id](#)⁹⁹, T. Cuhadar Donszelmann [id](#)¹⁶⁰, H. Cui [id](#)^{14a,14e}, Z. Cui [id](#)⁷,
 W.R. Cunningham [id](#)⁵⁹, F. Curcio [id](#)^{43b,43a}, P. Czodrowski [id](#)³⁶, M.M. Czurylo [id](#)^{63b},
 M.J. Da Cunha Sargedas De Sousa [id](#)^{57b,57a}, J.V. Da Fonseca Pinto [id](#)^{83b}, C. Da Via [id](#)¹⁰¹,
 W. Dabrowski [id](#)^{86a}, T. Dado [id](#)⁴⁹, S. Dahbi [id](#)^{33g}, T. Dai [id](#)¹⁰⁶, D. Dal Santo [id](#)¹⁹, C. Dallapiccola [id](#)¹⁰³,
 M. Dam [id](#)⁴², G. D'amen [id](#)²⁹, V. D'Amico [id](#)¹⁰⁹, J. Damp [id](#)¹⁰⁰, J.R. Dandoy [id](#)³⁴, M.F. Daneri [id](#)³⁰,
 M. Danninger [id](#)¹⁴², V. Dao [id](#)³⁶, G. Darbo [id](#)^{57b}, S. Darmora [id](#)⁶, S.J. Das [id](#)^{29,ai}, S. D'Auria [id](#)^{71a,71b},
 C. David [id](#)^{156b}, T. Davidek [id](#)¹³³, B. Davis-Purcell [id](#)³⁴, I. Dawson [id](#)⁹⁴, H.A. Day-hall [id](#)¹³², K. De [id](#)⁸,
 R. De Asmundis [id](#)^{72a}, N. De Biase [id](#)⁴⁸, S. De Castro [id](#)^{23b,23a}, N. De Groot [id](#)¹¹³, P. de Jong [id](#)¹¹⁴,
 H. De la Torre [id](#)¹¹⁵, A. De Maria [id](#)^{14c}, A. De Salvo [id](#)^{75a}, U. De Sanctis [id](#)^{76a,76b}, A. De Santo [id](#)¹⁴⁶,
 J.B. De Vivie De Regie [id](#)⁶⁰, D.V. Dedovich [id](#)³⁸, J. Degens [id](#)¹¹⁴, A.M. Deiana [id](#)⁴⁴, F. Del Corso [id](#)^{23b,23a},
 J. Del Peso [id](#)⁹⁹, F. Del Rio [id](#)^{63a}, F. Deliot [id](#)¹³⁵, C.M. Delitzsch [id](#)⁴⁹, M. Della Pietra [id](#)^{72a,72b},
 D. Della Volpe [id](#)⁵⁶, A. Dell'Acqua [id](#)³⁶, L. Dell'Asta [id](#)^{71a,71b}, M. Delmastro [id](#)⁴, P.A. Delsart [id](#)⁶⁰,
 S. Demers [id](#)¹⁷², M. Demichev [id](#)³⁸, S.P. Denisov [id](#)³⁷, L. D'Eramo [id](#)⁴⁰, D. Derendarz [id](#)⁸⁷, F. Derue [id](#)¹²⁷,
 P. Dervan [id](#)⁹², K. Desch [id](#)²⁴, C. Deutsch [id](#)²⁴, F.A. Di Bello [id](#)^{57b,57a}, A. Di Ciaccio [id](#)^{76a,76b},
 L. Di Ciaccio [id](#)⁴, A. Di Domenico [id](#)^{75a,75b}, C. Di Donato [id](#)^{72a,72b}, A. Di Girolamo [id](#)³⁶,
 G. Di Gregorio [id](#)³⁶, A. Di Luca [id](#)^{78a,78b}, B. Di Micco [id](#)^{77a,77b}, R. Di Nardo [id](#)^{77a,77b}, C. Diaconu [id](#)¹⁰²,
 M. Diamantopoulou [id](#)³⁴, F.A. Dias [id](#)¹¹⁴, T. Dias Do Vale [id](#)¹⁴², M.A. Diaz [id](#)^{137a,137b},
 F.G. Diaz Capriles [id](#)²⁴, M. Didenko [id](#)¹⁶³, E.B. Diehl [id](#)¹⁰⁶, L. Diehl [id](#)⁵⁴, S. Díez Cornell [id](#)⁴⁸,
 C. Diez Pardos [id](#)¹⁴¹, C. Dimitriadi [id](#)^{161,24}, A. Dimitrievska [id](#)^{17a}, J. Dingfelder [id](#)²⁴, I-M. Dinu [id](#)^{27b},
 S.J. Dittmeier [id](#)^{63b}, F. Dittus [id](#)³⁶, F. Djama [id](#)¹⁰², T. Djobava [id](#)^{149b}, J.I. Djuvslund [id](#)¹⁶,
 C. Doglioni [id](#)^{101,98}, A. Dohnalova [id](#)^{28a}, J. Dolejsi [id](#)¹³³, Z. Dolezal [id](#)¹³³, K.M. Dona [id](#)³⁹,
 M. Donadelli [id](#)^{83c}, B. Dong [id](#)¹⁰⁷, J. Donini [id](#)⁴⁰, A. D'Onofrio [id](#)^{72a,72b}, M. D'Onofrio [id](#)⁹²,
 J. Dopke [id](#)¹³⁴, A. Doria [id](#)^{72a}, N. Dos Santos Fernandes [id](#)^{130a}, P. Dougan [id](#)¹⁰¹, M.T. Dova [id](#)⁹⁰,
 A.T. Doyle [id](#)⁵⁹, M.A. Draguet [id](#)¹²⁶, E. Dreyer [id](#)¹⁶⁹, I. Drivas-koulouris [id](#)¹⁰, M. Drnevich [id](#)¹¹⁷,
 A.S. Drobac [id](#)¹⁵⁸, M. Drozdova [id](#)⁵⁶, D. Du [id](#)^{62a}, T.A. du Pree [id](#)¹¹⁴, F. Dubinin [id](#)³⁷, M. Dubovsky [id](#)^{28a},
 E. Duchovni [id](#)¹⁶⁹, G. Duckeck [id](#)¹⁰⁹, O.A. Ducu [id](#)^{27b}, D. Duda [id](#)⁵², A. Dudarev [id](#)³⁶, E.R. Duden [id](#)²⁶,
 M. D'uffizi [id](#)¹⁰¹, L. Duflo [id](#)⁶⁶, M. Dührssen [id](#)³⁶, C. Dülsen [id](#)¹⁷¹, A.E. Dumitriu [id](#)^{27b}, M. Dunford [id](#)^{63a},
 S. Dungs [id](#)⁴⁹, K. Dunne [id](#)^{47a,47b}, A. Duperrin [id](#)¹⁰², H. Duran Yildiz [id](#)^{3a}, M. Düren [id](#)⁵⁸,
 A. Durglishvili [id](#)^{149b}, B.L. Dwyer [id](#)¹¹⁵, G.I. Dyckes [id](#)^{17a}, M. Dyndal [id](#)^{86a}, B.S. Dziedzic [id](#)⁸⁷,
 Z.O. Earnshaw [id](#)¹⁴⁶, G.H. Eberwein [id](#)¹²⁶, B. Eckerova [id](#)^{28a}, S. Eggebrecht [id](#)⁵⁵,
 E. Egidio Purcino De Souza [id](#)¹²⁷, L.F. Ehrke [id](#)⁵⁶, G. Eigen [id](#)¹⁶, K. Einsweiler [id](#)^{17a}, T. Ekelof [id](#)¹⁶¹,
 P.A. Ekman [id](#)⁹⁸, S. El Farkh [id](#)^{35b}, Y. El Ghazali [id](#)^{35b}, H. El Jarrari [id](#)³⁶, A. El Moussaouy [id](#)¹⁰⁸,
 V. Ellajosyula [id](#)¹⁶¹, M. Ellert [id](#)¹⁶¹, F. Ellinghaus [id](#)¹⁷¹, N. Ellis [id](#)³⁶, J. Elmsheuser [id](#)²⁹, M. Elsing [id](#)³⁶,
 D. Emelianov [id](#)¹³⁴, Y. Enari [id](#)¹⁵³, I. Ene [id](#)^{17a}, S. Epari [id](#)¹³, J. Erdmann [id](#)⁴⁹, P.A. Erland [id](#)⁸⁷,
 M. Errenst [id](#)¹⁷¹, M. Escalier [id](#)⁶⁶, C. Escobar [id](#)¹⁶³, E. Etzion [id](#)¹⁵¹, G. Evans [id](#)^{130a}, H. Evans [id](#)⁶⁸,
 L.S. Evans [id](#)⁹⁵, M.O. Evans [id](#)¹⁴⁶, A. Ezhilov [id](#)³⁷, S. Ezzarqtouni [id](#)^{35a}, F. Fabbri [id](#)⁵⁹, L. Fabbri [id](#)^{23b,23a},

G. Facini ⁹⁶, V. Fadeyev ¹³⁶, R.M. Fakhruddinov ³⁷, S. Falciano ^{75a}, L.F. Falda Ulhoa Coelho ³⁶, P.J. Falke ²⁴, J. Faltova ¹³³, C. Fan ¹⁶², Y. Fan ^{14a}, Y. Fang ^{14a,14e}, M. Fanti ^{71a,71b}, M. Faraj ^{69a,69b}, Z. Farazpay ⁹⁷, A. Farbin ⁸, A. Farilla ^{77a}, T. Farooque ¹⁰⁷, S.M. Farrington ⁵², F. Fassi ^{35e}, D. Fassouliotis ⁹, M. Faucci Giannelli ^{76a,76b}, W.J. Fawcett ³², L. Fayard ⁶⁶, P. Federic ¹³³, P. Federicova ¹³¹, O.L. Fedin ^{37,a}, G. Fedotov ³⁷, M. Feickert ¹⁷⁰, L. Feligioni ¹⁰², D.E. Fellers ¹²³, C. Feng ^{62b}, M. Feng ^{14b}, Z. Feng ¹¹⁴, M.J. Fenton ¹⁶⁰, A.B. Fenyuk ³⁷, L. Ferencz ⁴⁸, R.A.M. Ferguson ⁹¹, S.I. Fernandez Luengo ^{137f}, P. Fernandez Martinez ¹³, M.J.V. Fernoux ¹⁰², J. Ferrando ⁴⁸, A. Ferrari ¹⁶¹, P. Ferrari ^{114,113}, R. Ferrari ^{73a}, D. Ferrere ⁵⁶, C. Ferretti ¹⁰⁶, F. Fiedler ¹⁰⁰, P. Fiedler ¹³², A. Filipčič ⁹³, E.K. Filmer ¹, F. Filthaut ¹¹³, M.C.N. Fiolhais ^{130a,130c,c}, L. Fiorini ¹⁶³, W.C. Fisher ¹⁰⁷, T. Fitschen ¹⁰¹, P.M. Fitzhugh ¹³⁵, I. Fleck ¹⁴¹, P. Fleischmann ¹⁰⁶, T. Flick ¹⁷¹, M. Flores ^{33d,ac}, L.R. Flores Castillo ^{64a}, L. Flores Sanz De Acedo ³⁶, F.M. Follega ^{78a,78b}, N. Fomin ¹⁶, J.H. Foo ¹⁵⁵, B.C. Forland ⁶⁸, A. Formica ¹³⁵, A.C. Forti ¹⁰¹, E. Fortin ³⁶, A.W. Fortman ⁶¹, M.G. Foti ^{17a}, L. Fountas ^{9,j}, D. Fournier ⁶⁶, H. Fox ⁹¹, P. Francavilla ^{74a,74b}, S. Francescato ⁶¹, S. Franchellucci ⁵⁶, M. Franchini ^{23b,23a}, S. Franchino ^{63a}, D. Francis ³⁶, L. Franco ¹¹³, V. Franco Lima ³⁶, L. Franconi ⁴⁸, M. Franklin ⁶¹, G. Frattari ²⁶, A.C. Freegard ⁹⁴, W.S. Freund ^{83b}, Y.Y. Frid ¹⁵¹, J. Friend ⁵⁹, N. Fritzsche ⁵⁰, A. Froch ⁵⁴, D. Froidevaux ³⁶, J.A. Frost ¹²⁶, Y. Fu ^{62a}, S. Fuenzalida Garrido ^{137f}, M. Fujimoto ¹⁰², K.Y. Fung ^{64a}, E. Furtado De Simas Filho ^{83b}, M. Furukawa ¹⁵³, J. Fuster ¹⁶³, A. Gabrielli ^{23b,23a}, A. Gabrielli ¹⁵⁵, P. Gadow ³⁶, G. Gagliardi ^{57b,57a}, L.G. Gagnon ^{17a}, E.J. Gallas ¹²⁶, B.J. Gallop ¹³⁴, K.K. Gan ¹¹⁹, S. Ganguly ¹⁵³, Y. Gao ⁵², F.M. Garay Walls ^{137a,137b}, B. Garcia ²⁹, C. García ¹⁶³, A. Garcia Alonso ¹¹⁴, A.G. Garcia Caffaro ¹⁷², J.E. García Navarro ¹⁶³, M. Garcia-Sciveres ^{17a}, G.L. Gardner ¹²⁸, R.W. Gardner ³⁹, N. Garelli ¹⁵⁸, D. Garg ⁸⁰, R.B. Garg ^{143,n}, J.M. Gargan ⁵², C.A. Garner ¹⁵⁵, C.M. Garvey ^{33a}, P. Gaspar ^{83b}, V.K. Gassmann ¹⁵⁸, G. Gaudio ^{73a}, V. Gautam ¹³, P. Gauzzi ^{75a,75b}, I.L. Gavrilenko ³⁷, A. Gavriyuk ³⁷, C. Gay ¹⁶⁴, G. Gaycken ⁴⁸, E.N. Gazis ¹⁰, A.A. Geanta ^{27b}, C.M. Gee ¹³⁶, A. Gekow ¹¹⁹, C. Gemme ^{57b}, M.H. Genest ⁶⁰, S. Gentile ^{75a,75b}, A.D. Gentry ¹¹², S. George ⁹⁵, W.F. George ²⁰, T. Geralis ⁴⁶, P. Gessinger-Befurt ³⁶, M.E. Geyik ¹⁷¹, M. Ghani ¹⁶⁷, M. Ghneimat ¹⁴¹, K. Ghorbanian ⁹⁴, A. Ghosal ¹⁴¹, A. Ghosh ¹⁶⁰, A. Ghosh ⁷, B. Giacobbe ^{23b}, S. Giagu ^{75a,75b}, T. Giani ¹¹⁴, P. Giannetti ^{74a}, A. Giannini ^{62a}, S.M. Gibson ⁹⁵, M. Gignac ¹³⁶, D.T. Gil ^{86b}, A.K. Gilbert ^{86a}, B.J. Gilbert ⁴¹, D. Gillberg ³⁴, G. Gilles ¹¹⁴, N.E.K. Gillwald ⁴⁸, L. Ginabat ¹²⁷, D.M. Gingrich ^{2,af}, M.P. Giordani ^{69a,69c}, P.F. Giraud ¹³⁵, G. Giugliarelli ^{69a,69c}, D. Giugni ^{71a}, F. Giuli ³⁶, I. Gkialas ^{9,j}, L.K. Gladilin ³⁷, C. Glasman ⁹⁹, G.R. Gledhill ¹²³, G. Glemža ⁴⁸, M. Glisic ¹²³, I. Gnesi ^{43b,f}, Y. Go ^{29,ai}, M. Goblirsch-Kolb ³⁶, B. Gocke ⁴⁹, D. Godin ¹⁰⁸, B. Gokturk ^{21a}, S. Goldfarb ¹⁰⁵, T. Golling ⁵⁶, M.G.D. Gololo ^{33g}, D. Golubkov ³⁷, J.P. Gombas ¹⁰⁷, A. Gomes ^{130a,130b}, G. Gomes Da Silva ¹⁴¹, A.J. Gomez Delegido ¹⁶³, R. Gonçalves ^{130a,130c}, G. Gonella ¹²³, L. Gonella ²⁰, A. Gongadze ^{149c}, F. Gonnella ²⁰, J.L. Gonski ⁴¹, R.Y. González Andana ⁵², S. González de la Hoz ¹⁶³, S. Gonzalez Fernandez ¹³, R. Gonzalez Lopez ⁹², C. Gonzalez Renteria ^{17a}, M.V. Gonzalez Rodrigues ⁴⁸, R. Gonzalez Suarez ¹⁶¹, S. Gonzalez-Sevilla ⁵⁶, G.R. Gonzalvo Rodriguez ¹⁶³, L. Goossens ³⁶, B. Gorini ³⁶, E. Gorini ^{70a,70b}, A. Gorišek ⁹³, T.C. Gosart ¹²⁸, A.T. Goshaw ⁵¹, M.I. Gostkin ³⁸, S. Goswami ¹²¹, C.A. Gottardo ³⁶, S.A. Gotz ¹⁰⁹, M. Goughri ^{35b}, V. Goumarre ⁴⁸, A.G. Goussiou ¹³⁸, N. Govender ^{33c}, I. Grabowska-Bold ^{86a}, K. Graham ³⁴, E. Gramstad ¹²⁵, S. Grancagnolo ^{70a,70b}, M. Grandi ¹⁴⁶, C.M. Grant ^{1,135}, P.M. Gravila ^{27f}, F.G. Gravili ^{70a,70b}, H.M. Gray ^{17a}, M. Greco ^{70a,70b}, C. Grefe ²⁴, I.M. Gregor ⁴⁸, P. Grenier ¹⁴³, S.G. Grewe ¹¹⁰, C. Grieco ¹³, A.A. Grillo ¹³⁶, K. Grimm ³¹, S. Grinstein ^{13,s}, J.-F. Grivaz ⁶⁶, E. Gross ¹⁶⁹, J. Grosse-Knetter ⁵⁵, C. Grud ¹⁰⁶, J.C. Grundy ¹²⁶, L. Guan ¹⁰⁶, W. Guan ²⁹, C. Gubbels ¹⁶⁴,

J.G.R. Guerrero Rojas [id](#)¹⁶³, G. Guerrieri [id](#)^{69a,69c}, F. Guescini [id](#)¹¹⁰, R. Gugel [id](#)¹⁰⁰, J.A.M. Guhit [id](#)¹⁰⁶, A. Guida [id](#)¹⁸, E. Guilloton [id](#)^{167,134}, S. Guindon [id](#)³⁶, F. Guo [id](#)^{14a,14e}, J. Guo [id](#)^{62c}, L. Guo [id](#)⁴⁸, Y. Guo [id](#)¹⁰⁶, R. Gupta [id](#)⁴⁸, R. Gupta [id](#)¹²⁹, S. Gurbuz [id](#)²⁴, S.S. Gurdasani [id](#)⁵⁴, G. Gustavino [id](#)³⁶, M. Guth [id](#)⁵⁶, P. Gutierrez [id](#)¹²⁰, L.F. Gutierrez Zagazeta [id](#)¹²⁸, M. Gutsche [id](#)⁵⁰, C. Gutschow [id](#)⁹⁶, C. Gwenlan [id](#)¹²⁶, C.B. Gwilliam [id](#)⁹², E.S. Haaland [id](#)¹²⁵, A. Haas [id](#)¹¹⁷, M. Habedank [id](#)⁴⁸, C. Haber [id](#)^{17a}, H.K. Hadavand [id](#)⁸, A. Hadeef [id](#)⁵⁰, S. Hadzic [id](#)¹¹⁰, A.I. Hagan [id](#)⁹¹, J.J. Hahn [id](#)¹⁴¹, E.H. Haines [id](#)⁹⁶, M. Haleem [id](#)¹⁶⁶, J. Haley [id](#)¹²¹, J.J. Hall [id](#)¹³⁹, G.D. Hallewell [id](#)¹⁰², L. Halser [id](#)¹⁹, K. Hamano [id](#)¹⁶⁵, M. Hamer [id](#)²⁴, G.N. Hamity [id](#)⁵², E.J. Hampshire [id](#)⁹⁵, J. Han [id](#)^{62b}, K. Han [id](#)^{62a}, L. Han [id](#)^{14c}, L. Han [id](#)^{62a}, S. Han [id](#)^{17a}, Y.F. Han [id](#)¹⁵⁵, K. Hanagaki [id](#)⁸⁴, M. Hance [id](#)¹³⁶, D.A. Hangal [id](#)^{41,ab}, H. Hanif [id](#)¹⁴², M.D. Hank [id](#)¹²⁸, R. Hankache [id](#)¹⁰¹, J.B. Hansen [id](#)⁴², J.D. Hansen [id](#)⁴², P.H. Hansen [id](#)⁴², K. Hara [id](#)¹⁵⁷, D. Harada [id](#)⁵⁶, T. Harenberg [id](#)¹⁷¹, S. Harkusha [id](#)³⁷, M.L. Harris [id](#)¹⁰³, Y.T. Harris [id](#)¹²⁶, J. Harrison [id](#)¹³, N.M. Harrison [id](#)¹¹⁹, P.F. Harrison [id](#)¹⁶⁷, N.M. Hartman [id](#)¹¹⁰, N.M. Hartmann [id](#)¹⁰⁹, Y. Hasegawa [id](#)¹⁴⁰, R. Hauser [id](#)¹⁰⁷, C.M. Hawkes [id](#)²⁰, R.J. Hawkings [id](#)³⁶, Y. Hayashi [id](#)¹⁵³, S. Hayashida [id](#)¹¹¹, D. Hayden [id](#)¹⁰⁷, C. Hayes [id](#)¹⁰⁶, R.L. Hayes [id](#)¹¹⁴, C.P. Hays [id](#)¹²⁶, J.M. Hays [id](#)⁹⁴, H.S. Hayward [id](#)⁹², F. He [id](#)^{62a}, M. He [id](#)^{14a,14e}, Y. He [id](#)¹⁵⁴, Y. He [id](#)⁴⁸, N.B. Heatley [id](#)⁹⁴, V. Hedberg [id](#)⁹⁸, A.L. Heggelund [id](#)¹²⁵, N.D. Hehir [id](#)^{94,*}, C. Heidegger [id](#)⁵⁴, K.K. Heidegger [id](#)⁵⁴, W.D. Heidorn [id](#)⁸¹, J. Heilman [id](#)³⁴, S. Heim [id](#)⁴⁸, T. Heim [id](#)^{17a}, J.G. Heinlein [id](#)¹²⁸, J.J. Heinrich [id](#)¹²³, L. Heinrich [id](#)^{110,ad}, J. Hejbal [id](#)¹³¹, L. Helary [id](#)⁴⁸, A. Held [id](#)¹⁷⁰, S. Hellesund [id](#)¹⁶, C.M. Helling [id](#)¹⁶⁴, S. Hellman [id](#)^{47a,47b}, R.C.W. Henderson [id](#)⁹¹, L. Henkelmann [id](#)³², A.M. Henriques Correia [id](#)³⁶, H. Herde [id](#)⁹⁸, Y. Hernández Jiménez [id](#)¹⁴⁵, L.M. Herrmann [id](#)²⁴, T. Herrmann [id](#)⁵⁰, G. Herten [id](#)⁵⁴, R. Hertenberger [id](#)¹⁰⁹, L. Hervas [id](#)³⁶, M.E. Hespig [id](#)¹⁰⁰, N.P. Hessey [id](#)^{156a}, H. Hibi [id](#)⁸⁵, E. Hill [id](#)¹⁵⁵, S.J. Hillier [id](#)²⁰, J.R. Hinds [id](#)¹⁰⁷, F. Hinterkeuser [id](#)²⁴, M. Hirose [id](#)¹²⁴, S. Hirose [id](#)¹⁵⁷, D. Hirschbuehl [id](#)¹⁷¹, T.G. Hitchings [id](#)¹⁰¹, B. Hiti [id](#)⁹³, J. Hobbs [id](#)¹⁴⁵, R. Hobincu [id](#)^{27e}, N. Hod [id](#)¹⁶⁹, M.C. Hodgkinson [id](#)¹³⁹, B.H. Hodgkinson [id](#)³², A. Hoecker [id](#)³⁶, D.D. Hofer [id](#)¹⁰⁶, J. Hofer [id](#)⁴⁸, T. Holm [id](#)²⁴, M. Holzbock [id](#)¹¹⁰, L.B.A.H. Hommels [id](#)³², B.P. Honan [id](#)¹⁰¹, J. Hong [id](#)^{62c}, T.M. Hong [id](#)¹²⁹, B.H. Hooberman [id](#)¹⁶², W.H. Hopkins [id](#)⁶, Y. Horii [id](#)¹¹¹, S. Hou [id](#)¹⁴⁸, A.S. Howard [id](#)⁹³, J. Howarth [id](#)⁵⁹, J. Hoya [id](#)⁶, M. Hrabovsky [id](#)¹²², A. Hrynevich [id](#)⁴⁸, T. Hryn'ova [id](#)⁴, P.J. Hsu [id](#)⁶⁵, S.-C. Hsu [id](#)¹³⁸, Q. Hu [id](#)^{62a}, Y.F. Hu [id](#)^{14a,14e}, S. Huang [id](#)^{64b}, X. Huang [id](#)^{14c}, X. Huang [id](#)^{14a,14e}, Y. Huang [id](#)¹³⁹, Y. Huang [id](#)^{14a}, Z. Huang [id](#)¹⁰¹, Z. Hubacek [id](#)¹³², M. Huebner [id](#)²⁴, F. Huegging [id](#)²⁴, T.B. Huffman [id](#)¹²⁶, C.A. Hugli [id](#)⁴⁸, M. Huhtinen [id](#)³⁶, S.K. Huiberts [id](#)¹⁶, R. Hulsken [id](#)¹⁰⁴, N. Huseynov [id](#)¹², J. Huston [id](#)¹⁰⁷, J. Huth [id](#)⁶¹, R. Hyneman [id](#)¹⁴³, G. Iacobucci [id](#)⁵⁶, G. Iakovidis [id](#)²⁹, I. Ibragimov [id](#)¹⁴¹, L. Iconomidou-Fayard [id](#)⁶⁶, P. Iengo [id](#)^{72a,72b}, R. Iguchi [id](#)¹⁵³, T. Iizawa [id](#)¹²⁶, Y. Ikegami [id](#)⁸⁴, N. Ilic [id](#)¹⁵⁵, H. Imam [id](#)^{35a}, M. Ince Lezki [id](#)⁵⁶, T. Ingebretsen Carlson [id](#)^{47a,47b}, G. Introzzi [id](#)^{73a,73b}, M. Iodice [id](#)^{77a}, V. Ippolito [id](#)^{75a,75b}, R.K. Irwin [id](#)⁹², M. Ishino [id](#)¹⁵³, W. Islam [id](#)¹⁷⁰, C. Issever [id](#)^{18,48}, S. Istin [id](#)^{21a,ak}, H. Ito [id](#)¹⁶⁸, J.M. Iturbe Ponce [id](#)^{64a}, R. Iuppa [id](#)^{78a,78b}, A. Ivina [id](#)¹⁶⁹, J.M. Izen [id](#)⁴⁵, V. Izzo [id](#)^{72a}, P. Jacka [id](#)^{131,132}, P. Jackson [id](#)¹, R.M. Jacobs [id](#)⁴⁸, B.P. Jaeger [id](#)¹⁴², C.S. Jagfeld [id](#)¹⁰⁹, G. Jain [id](#)^{156a}, P. Jain [id](#)⁵⁴, K. Jakobs [id](#)⁵⁴, T. Jakoubek [id](#)¹⁶⁹, J. Jamieson [id](#)⁵⁹, K.W. Janas [id](#)^{86a}, M. Javurkova [id](#)¹⁰³, F. Jeanneau [id](#)¹³⁵, L. Jeanty [id](#)¹²³, J. Jejelava [id](#)^{149a,z}, P. Jenni [id](#)^{54,g}, C.E. Jessiman [id](#)³⁴, S. Jézéquel [id](#)⁴, C. Jia [id](#)^{62b}, J. Jia [id](#)¹⁴⁵, X. Jia [id](#)⁶¹, X. Jia [id](#)^{14a,14e}, Z. Jia [id](#)^{14c}, S. Jiggins [id](#)⁴⁸, J. Jimenez Pena [id](#)¹³, S. Jin [id](#)^{14c}, A. Jinaru [id](#)^{27b}, O. Jinnouchi [id](#)¹⁵⁴, P. Johansson [id](#)¹³⁹, K.A. Johns [id](#)⁷, J.W. Johnson [id](#)¹³⁶, D.M. Jones [id](#)³², E. Jones [id](#)⁴⁸, P. Jones [id](#)³², R.W.L. Jones [id](#)⁹¹, T.J. Jones [id](#)⁹², H.L. Joos [id](#)^{55,36}, R. Joshi [id](#)¹¹⁹, J. Jovicevic [id](#)¹⁵, X. Ju [id](#)^{17a}, J.J. Junggeburch [id](#)¹⁰³, T. Junkermann [id](#)^{63a}, A. Juste Rozas [id](#)^{13,s}, M.K. Juzek [id](#)⁸⁷, S. Kabana [id](#)^{137e}, A. Kaczmarska [id](#)⁸⁷, M. Kado [id](#)¹¹⁰, H. Kagan [id](#)¹¹⁹, M. Kagan [id](#)¹⁴³, A. Kahn [id](#)⁴¹, A. Kahn [id](#)¹²⁸, C. Kahra [id](#)¹⁰⁰, T. Kaji [id](#)¹⁵³, E. Kajomovitz [id](#)¹⁵⁰, N. Kakati [id](#)¹⁶⁹, I. Kalaitzidou [id](#)⁵⁴, C.W. Kalderon [id](#)²⁹, A. Kamenshchikov [id](#)¹⁵⁵, N.J. Kang [id](#)¹³⁶, D. Kar [id](#)^{33g}, K. Karava [id](#)¹²⁶, M.J. Kareem [id](#)^{156b}, E. Karentzos [id](#)⁵⁴, I. Karkanias [id](#)¹⁵², O. Karkout [id](#)¹¹⁴, S.N. Karpov [id](#)³⁸,

Z.M. Karpova ³⁸, V. Kartvelishvili ⁹¹, A.N. Karyukhin ³⁷, E. Kasimi ¹⁵², J. Katzy ⁴⁸, S. Kaur ³⁴, K. Kawade ¹⁴⁰, M.P. Kawale ¹²⁰, C. Kawamoto ⁸⁸, T. Kawamoto ^{62a}, E.F. Kay ³⁶, F.I. Kaya ¹⁵⁸, S. Kazakos ¹⁰⁷, V.F. Kazanin ³⁷, Y. Ke ¹⁴⁵, J.M. Keaveney ^{33a}, R. Keeler ¹⁶⁵, G.V. Kehris ⁶¹, J.S. Keller ³⁴, A.S. Kelly ⁹⁶, J.J. Kempster ¹⁴⁶, K.E. Kennedy ⁴¹, P.D. Kennedy ¹⁰⁰, O. Kepka ¹³¹, B.P. Kerridge ¹⁶⁷, S. Kersten ¹⁷¹, B.P. Kerševan ⁹³, S. Keshri ⁶⁶, L. Keszeghova ^{28a}, S. Ketabchi Haghghat ¹⁵⁵, R.A. Khan ¹²⁹, M. Khandoga ¹²⁷, A. Khanov ¹²¹, A.G. Kharlamov ³⁷, T. Kharlamova ³⁷, E.E. Khoda ¹³⁸, M. Kholodenko ³⁷, T.J. Khoo ¹⁸, G. Khoriali ¹⁶⁶, J. Khubua ^{149b}, Y.A.R. Khwaira ⁶⁶, A. Kilgallon ¹²³, D.W. Kim ^{47a,47b}, Y.K. Kim ³⁹, N. Kimura ⁹⁶, M.K. Kingston ⁵⁵, A. Kirchhoff ⁵⁵, C. Kirfel ²⁴, F. Kirfel ²⁴, J. Kirk ¹³⁴, A.E. Kiryunin ¹¹⁰, C. Kitsaki ¹⁰, O. Kivernyk ²⁴, M. Klassen ^{63a}, C. Klein ³⁴, L. Klein ¹⁶⁶, M.H. Klein ¹⁰⁶, M. Klein ⁹², S.B. Klein ⁵⁶, U. Klein ⁹², P. Klimek ³⁶, A. Klimentov ²⁹, T. Klioutchnikova ³⁶, P. Kluit ¹¹⁴, S. Kluth ¹¹⁰, E. Kneringer ⁷⁹, T.M. Knight ¹⁵⁵, A. Knue ⁴⁹, R. Kobayashi ⁸⁸, D. Kobylanski ¹⁶⁹, S.F. Koch ¹²⁶, M. Kocian ¹⁴³, P. Kodyš ¹³³, D.M. Koeck ¹²³, P.T. Koenig ²⁴, T. Koffas ³⁴, O. Kolay ⁵⁰, I. Koletsou ⁴, T. Komarek ¹²², K. Köneke ⁵⁴, A.X.Y. Kong ¹, T. Kono ¹¹⁸, N. Konstantinidis ⁹⁶, P. Kontaxakis ⁵⁶, B. Konya ⁹⁸, R. Kopeliansky ⁶⁸, S. Koperny ^{86a}, K. Korcyl ⁸⁷, K. Kordas ^{152,e}, G. Koren ¹⁵¹, A. Korn ⁹⁶, S. Korn ⁵⁵, I. Korolkov ¹³, N. Korotkova ³⁷, B. Kortman ¹¹⁴, O. Kortner ¹¹⁰, S. Kortner ¹¹⁰, W.H. Kostecka ¹¹⁵, V.V. Kostyukhin ¹⁴¹, A. Kotskechagia ¹³⁵, A. Kotwal ⁵¹, A. Koulouris ³⁶, A. Kourkoumeli-Charalampidi ^{73a,73b}, C. Kourkoumelis ⁹, E. Kourlitis ^{110,ad}, O. Kovanda ¹⁴⁶, R. Kowalewski ¹⁶⁵, W. Kozanecki ¹³⁵, A.S. Kozhin ³⁷, V.A. Kramarenko ³⁷, G. Kramberger ⁹³, P. Kramer ¹⁰⁰, M.W. Krasny ¹²⁷, A. Krasznahorkay ³⁶, J.W. Kraus ¹⁷¹, J.A. Kremer ⁴⁸, T. Kresse ⁵⁰, J. Kretschmar ⁹², K. Kreul ¹⁸, P. Krieger ¹⁵⁵, S. Krishnamurthy ¹⁰³, M. Krivos ¹³³, K. Krizka ²⁰, K. Kroeninger ⁴⁹, H. Kroha ¹¹⁰, J. Kroll ¹³¹, J. Kroll ¹²⁸, K.S. Krowpman ¹⁰⁷, U. Kruchonak ³⁸, H. Krüger ²⁴, N. Krumnack ⁸¹, M.C. Kruse ⁵¹, O. Kuchinskaia ³⁷, S. Kuday ^{3a}, S. Kuehn ³⁶, R. Kuesters ⁵⁴, T. Kuhl ⁴⁸, V. Kukhtin ³⁸, Y. Kulchitsky ^{37,a}, S. Kuleshov ^{137d,137b}, M. Kumar ^{33g}, N. Kumari ⁴⁸, A. Kupco ¹³¹, T. Kupfer ⁴⁹, A. Kupich ³⁷, O. Kuprash ⁵⁴, H. Kurashige ⁸⁵, L.L. Kurchaninov ^{156a}, O. Kurdysh ⁶⁶, Y.A. Kurochkin ³⁷, A. Kurova ³⁷, M. Kuze ¹⁵⁴, A.K. Kvam ¹⁰³, J. Kvita ¹²², T. Kwan ¹⁰⁴, N.G. Kyriacou ¹⁰⁶, L.A.O. Laatu ¹⁰², C. Lacasta ¹⁶³, F. Lacava ^{75a,75b}, H. Lacker ¹⁸, D. Lacour ¹²⁷, N.N. Lad ⁹⁶, E. Ladygin ³⁸, B. Laforge ¹²⁷, T. Lagouri ^{137e}, F.Z. Lahbabi ^{35a}, S. Lai ⁵⁵, I.K. Lakomic ^{86a}, N. Lalloue ⁶⁰, J.E. Lambert ¹⁶⁵, S. Lammers ⁶⁸, W. Lampl ⁷, C. Lampoudis ^{152,e}, A.N. Lancaster ¹¹⁵, E. Lançon ²⁹, U. Landgraf ⁵⁴, M.P.J. Landon ⁹⁴, V.S. Lang ⁵⁴, R.J. Langenberg ¹⁰³, O.K.B. Langrekken ¹²⁵, A.J. Lankford ¹⁶⁰, F. Lanni ³⁶, K. Lantzs ²⁴, A. Lanza ^{73a}, A. Lapertosa ^{57b,57a}, J.F. Laporte ¹³⁵, T. Lari ^{71a}, F. Lasagni Manghi ^{23b}, M. Lassnig ³⁶, V. Latonova ¹³¹, A. Laudrain ¹⁰⁰, A. Laurier ¹⁵⁰, S.D. Lawlor ¹³⁹, Z. Lawrence ¹⁰¹, R. Lazaridou ¹⁶⁷, M. Lazzaroni ^{71a,71b}, B. Le ¹⁰¹, E.M. Le Boulicaut ⁵¹, B. Leban ⁹³, A. Lebedev ⁸¹, M. LeBlanc ¹⁰¹, F. Ledroit-Guillon ⁶⁰, A.C.A. Lee ⁹⁶, S.C. Lee ¹⁴⁸, S. Lee ^{47a,47b}, T.F. Lee ⁹², L.L. Leeuw ^{33c}, H.P. Lefebvre ⁹⁵, M. Lefebvre ¹⁶⁵, C. Leggett ^{17a}, G. Lehmann Miotto ³⁶, M. Leigh ⁵⁶, W.A. Leight ¹⁰³, W. Leinonen ¹¹³, A. Leisos ^{152,r}, M.A.L. Leite ^{83c}, C.E. Leitgeb ⁴⁸, R. Leitner ¹³³, K.J.C. Leney ⁴⁴, T. Lenz ²⁴, S. Leone ^{74a}, C. Leonidopoulos ⁵², A. Leopold ¹⁴⁴, C. Leroy ¹⁰⁸, R. Les ¹⁰⁷, C.G. Lester ³², M. Levchenko ³⁷, J. Levêque ⁴, D. Levin ¹⁰⁶, L.J. Levinson ¹⁶⁹, M.P. Lewicki ⁸⁷, D.J. Lewis ⁴, A. Li ⁵, B. Li ^{62b}, C. Li ^{62a}, C-Q. Li ¹¹⁰, H. Li ^{62a}, H. Li ^{62b}, H. Li ^{14c}, H. Li ^{14b}, H. Li ^{62b}, J. Li ^{62c}, K. Li ¹³⁸, L. Li ^{62c}, M. Li ^{14a,14e}, Q.Y. Li ^{62a}, S. Li ^{14a,14e}, S. Li ^{62d,62c,d}, T. Li ⁵, X. Li ¹⁰⁴, Z. Li ¹²⁶, Z. Li ¹⁰⁴, Z. Li ⁹², Z. Li ^{14a,14e}, S. Liang ^{14a,14e}, Z. Liang ^{14a}, M. Liberatore ¹³⁵, B. Liberti ^{76a}, K. Lie ^{64c}, J. Lieber Marin ^{83b}, H. Lien ⁶⁸, K. Lin ¹⁰⁷, R.E. Lindley ⁷, J.H. Lindon ², E. Lipeles ¹²⁸, A. Lipniacka ¹⁶,

A. Lister ¹⁶⁴, J.D. Little ⁴, B. Liu ^{14a}, B.X. Liu ¹⁴², D. Liu ^{62d,62c}, J.B. Liu ^{62a}, J.K.K. Liu ³²,
 K. Liu ^{62d,62c}, M. Liu ^{62a}, M.Y. Liu ^{62a}, P. Liu ^{14a}, Q. Liu ^{62d,138,62c}, X. Liu ^{62a}, Y. Liu ^{14d,14e},
 Y.L. Liu ^{62b}, Y.W. Liu ^{62a}, J. Llorente Merino ¹⁴², S.L. Lloyd ⁹⁴, E.M. Lobodzinska ⁴⁸,
 P. Loch ⁷, T. Lohse ¹⁸, K. Lohwasser ¹³⁹, E. Loiacono ⁴⁸, M. Lokajicek ^{131,*}, J.D. Lomas ²⁰,
 J.D. Long ¹⁶², I. Longarini ¹⁶⁰, L. Longo ^{70a,70b}, R. Longo ¹⁶², I. Lopez Paz ⁶⁷,
 A. Lopez Solis ⁴⁸, N. Lorenzo Martinez ⁴, A.M. Lory ¹⁰⁹, G. Löschcke Centeno ¹⁴⁶, O. Loseva ³⁷,
 X. Lou ^{47a,47b}, X. Lou ^{14a,14e}, A. Lounis ⁶⁶, J. Love ⁶, P.A. Love ⁹¹, G. Lu ^{14a,14e}, M. Lu ⁸⁰,
 S. Lu ¹²⁸, Y.J. Lu ⁶⁵, H.J. Lubatti ¹³⁸, C. Luci ^{75a,75b}, F.L. Lucio Alves ^{14c}, A. Lucotte ⁶⁰,
 F. Luehring ⁶⁸, I. Luise ¹⁴⁵, O. Lukianchuk ⁶⁶, O. Lundberg ¹⁴⁴, B. Lund-Jensen ¹⁴⁴,
 N.A. Luongo ⁶, M.S. Lutz ¹⁵¹, A.B. Lux ²⁵, D. Lynn ²⁹, H. Lyons ⁹², R. Lysak ¹³¹, E. Lytken ⁹⁸,
 V. Lyubushkin ³⁸, T. Lyubushkina ³⁸, M.M. Lyukova ¹⁴⁵, H. Ma ²⁹, K. Ma ^{62a}, L.L. Ma ^{62b},
 W. Ma ^{62a}, Y. Ma ¹²¹, D.M. Mac Donell ¹⁶⁵, G. Maccarrone ⁵³, J.C. MacDonald ¹⁰⁰,
 P.C. Machado De Abreu Farias ^{83b}, R. Madar ⁴⁰, W.F. Mader ⁵⁰, T. Madula ⁹⁶, J. Maeda ⁸⁵,
 T. Maeno ²⁹, H. Maguire ¹³⁹, V. Maiboroda ¹³⁵, A. Maio ^{130a,130b,130d}, K. Maj ^{86a},
 O. Majersky ⁴⁸, S. Majewski ¹²³, N. Makovec ⁶⁶, V. Maksimovic ¹⁵, B. Malaescu ¹²⁷,
 Pa. Malecki ⁸⁷, V.P. Maleev ³⁷, F. Malek ⁶⁰, M. Mali ⁹³, D. Malito ⁹⁵, U. Mallik ⁸⁰,
 S. Maltezos ¹⁰, S. Malyukov ³⁸, J. Mamuzic ¹³, G. Mancini ⁵³, G. Manco ^{73a,73b}, J.P. Mandalia ⁹⁴,
 I. Mandić ⁹³, L. Manhaes de Andrade Filho ^{83a}, I.M. Maniatis ¹⁶⁹, J. Manjarres Ramos ^{102,aa},
 D.C. Mankad ¹⁶⁹, A. Mann ¹⁰⁹, B. Mansoulie ¹³⁵, S. Manzoni ³⁶, L. Mao ^{62c}, X. Mapekula ^{33c},
 A. Marantis ^{152,r}, G. Marchiori ⁵, M. Marcisovsky ¹³¹, C. Marcon ^{71a}, M. Marinescu ²⁰,
 S. Marium ⁴⁸, M. Marjanovic ¹²⁰, E.J. Marshall ⁹¹, Z. Marshall ^{17a}, S. Marti-Garcia ¹⁶³,
 T.A. Martin ¹⁶⁷, V.J. Martin ⁵², B. Martin dit Latour ¹⁶, L. Martinelli ^{75a,75b}, M. Martinez ^{13,s},
 P. Martinez Agullo ¹⁶³, V.I. Martinez Outschoorn ¹⁰³, P. Martinez Suarez ¹³, S. Martin-Haugh ¹³⁴,
 V.S. Martoiu ^{27b}, A.C. Martyniuk ⁹⁶, A. Marzin ³⁶, D. Mascione ^{78a,78b}, L. Masetti ¹⁰⁰,
 T. Mashimo ¹⁵³, J. Masik ¹⁰¹, A.L. Maslennikov ³⁷, L. Massa ^{23b}, P. Massarotti ^{72a,72b},
 P. Mastrandrea ^{74a,74b}, A. Mastroberardino ^{43b,43a}, T. Masubuchi ¹⁵³, T. Mathisen ¹⁶¹,
 J. Matousek ¹³³, N. Matsuzawa ¹⁵³, J. Maurer ^{27b}, B. Maček ⁹³, D.A. Maximov ³⁷, R. Mazini ¹⁴⁸,
 I. Maznas ¹⁵², M. Mazza ¹⁰⁷, S.M. Mazza ¹³⁶, E. Mazzeo ^{71a,71b}, C. Mc Ginn ²⁹,
 J.P. Mc Gowan ¹⁰⁴, S.P. Mc Kee ¹⁰⁶, E.F. McDonald ¹⁰⁵, A.E. McDougall ¹¹⁴, J.A. Mcfayden ¹⁴⁶,
 R.P. McGovern ¹²⁸, G. Mchedlidze ^{149b}, R.P. Mckenzie ^{33g}, T.C. Mclachlan ⁴⁸,
 D.J. McLaughlin ⁹⁶, S.J. McMahon ¹³⁴, C.M. Mcpartland ⁹², R.A. McPherson ^{165,w},
 S. Mehlhase ¹⁰⁹, A. Mehta ⁹², D. Melini ¹⁵⁰, B.R. Mellado Garcia ^{33g}, A.H. Melo ⁵⁵,
 F. Meloni ⁴⁸, A.M. Mendes Jacques Da Costa ¹⁰¹, H.Y. Meng ¹⁵⁵, L. Meng ⁹¹, S. Menke ¹¹⁰,
 M. Mentink ³⁶, E. Meoni ^{43b,43a}, G. Mercado ¹¹⁵, C. Merlassino ^{69a,69c}, L. Merola ^{72a,72b},
 C. Meroni ^{71a,71b}, G. Merz ¹⁰⁶, O. Meshkov ³⁷, J. Metcalfe ⁶, A.S. Mete ⁶, C. Meyer ⁶⁸,
 J-P. Meyer ¹³⁵, R.P. Middleton ¹³⁴, L. Mijović ⁵², G. Mikenberg ¹⁶⁹, M. Mikestikova ¹³¹,
 M. Mikuž ⁹³, H. Mildner ¹⁰⁰, A. Milic ³⁶, C.D. Milke ⁴⁴, D.W. Miller ³⁹, L.S. Miller ³⁴,
 A. Milov ¹⁶⁹, D.A. Milstead ^{47a,47b}, T. Min ^{14c}, A.A. Minaenko ³⁷, I.A. Minashvili ^{149b}, L. Mince ⁵⁹,
 A.I. Mincer ¹¹⁷, B. Mindur ^{86a}, M. Mineev ³⁸, Y. Mino ⁸⁸, L.M. Mir ¹³, M. Miralles Lopez ¹⁶³,
 M. Mironova ^{17a}, A. Mishima ¹⁵³, M.C. Missio ¹¹³, A. Mitra ¹⁶⁷, V.A. Mitsou ¹⁶³,
 Y. Mitsumori ¹¹¹, O. Miu ¹⁵⁵, P.S. Miyagawa ⁹⁴, T. Mkrtchyan ^{63a}, M. Mlinarevic ⁹⁶,
 T. Mlinarevic ⁹⁶, M. Mlynarikova ³⁶, S. Mobius ¹⁹, P. Moder ⁴⁸, P. Mogg ¹⁰⁹,
 A.F. Mohammed ^{14a,14e}, S. Mohapatra ⁴¹, G. Mokgatitwane ^{33g}, L. Moleri ¹⁶⁹, B. Mondal ¹⁴¹,
 S. Mondal ¹³², K. Mönig ⁴⁸, E. Monnier ¹⁰², L. Monsonis Romero ¹⁶³, J. Montejo Berlingen ¹³,
 M. Montella ¹¹⁹, F. Montekali ^{77a,77b}, F. Monticelli ⁹⁰, S. Monzani ^{69a,69c}, N. Morange ⁶⁶,
 A.L. Moreira De Carvalho ^{130a}, M. Moreno Llácer ¹⁶³, C. Moreno Martinez ⁵⁶, P. Morettini ^{57b},
 S. Morgenstern ³⁶, M. Morii ⁶¹, M. Morinaga ¹⁵³, A.K. Morley ³⁶, F. Morodei ^{75a,75b},

L. Morvaj ³⁶, P. Moschovakos ³⁶, B. Moser ³⁶, M. Mosidze ^{149b}, T. Moskalets ⁵⁴,
 P. Moskvitina ¹¹³, J. Moss ^{31,1}, E.J.W. Moyses ¹⁰³, O. Mtintsilana ^{33g}, S. Muanza ¹⁰²,
 J. Mueller ¹²⁹, D. Muenstermann ⁹¹, R. Müller ¹⁹, G.A. Mullier ¹⁶¹, A.J. Mullin ³², J.J. Mullin ¹²⁸,
 D.P. Mungo ¹⁵⁵, D. Munoz Perez ¹⁶³, F.J. Munoz Sanchez ¹⁰¹, M. Murin ¹⁰¹, W.J. Murray ^{167,134},
 A. Murrone ^{71a,71b}, M. Muškinja ^{17a}, C. Mwewa ²⁹, A.G. Myagkov ^{37,a}, A.J. Myers ⁸,
 G. Myers ⁶⁸, M. Myska ¹³², B.P. Nachman ^{17a}, O. Nackenhorst ⁴⁹, A. Nag ⁵⁰, K. Nagai ¹²⁶,
 K. Nagano ⁸⁴, J.L. Nagle ^{29,ai}, E. Nagy ¹⁰², A.M. Nairz ³⁶, Y. Nakahama ⁸⁴, K. Nakamura ⁸⁴,
 K. Nakkalil ⁵, H. Nanjo ¹²⁴, R. Narayan ⁴⁴, E.A. Narayanan ¹¹², I. Naryshkin ³⁷, M. Naseri ³⁴,
 S. Nasri ¹⁵⁹, C. Nass ²⁴, G. Navarro ^{22a}, J. Navarro-Gonzalez ¹⁶³, R. Nayak ¹⁵¹, A. Nayaz ¹⁸,
 P.Y. Nechaeva ³⁷, F. Nechansky ⁴⁸, L. Nedic ¹²⁶, T.J. Neep ²⁰, A. Negri ^{73a,73b}, M. Negrini ^{23b},
 C. Nellist ¹¹⁴, C. Nelson ¹⁰⁴, K. Nelson ¹⁰⁶, S. Nemecek ¹³¹, M. Nessi ^{36,h}, M.S. Neubauer ¹⁶²,
 F. Neuhaus ¹⁰⁰, J. Neundorf ⁴⁸, R. Newhouse ¹⁶⁴, P.R. Newman ²⁰, C.W. Ng ¹²⁹, Y.W.Y. Ng ⁴⁸,
 B. Ngair ^{35e}, H.D.N. Nguyen ¹⁰⁸, R.B. Nickerson ¹²⁶, R. Nicolaidou ¹³⁵, J. Nielsen ¹³⁶,
 M. Niemeyer ⁵⁵, J. Niermann ^{55,36}, N. Nikiforou ³⁶, V. Nikolaenko ^{37,a}, I. Nikolic-Audit ¹²⁷,
 K. Nikolopoulos ²⁰, P. Nilsson ²⁹, I. Ninca ⁴⁸, H.R. Nindhito ⁵⁶, G. Ninio ¹⁵¹, A. Nisati ^{75a},
 N. Nishu ², R. Nisius ¹¹⁰, J-E. Nitschke ⁵⁰, E.K. Nkadimeng ^{33g}, T. Nobe ¹⁵³, D.L. Noel ³²,
 T. Nommensen ¹⁴⁷, M.B. Norfolk ¹³⁹, R.R.B. Norisam ⁹⁶, B.J. Norman ³⁴, M. Noury ^{35a},
 J. Novak ⁹³, T. Novak ⁴⁸, L. Novotny ¹³², R. Novotny ¹¹², L. Nozka ¹²², K. Ntekas ¹⁶⁰,
 N.M.J. Nunes De Moura Junior ^{83b}, E. Nurse ⁹⁶, J. Ocariz ¹²⁷, A. Ochi ⁸⁵, I. Ochoa ^{130a},
 S. Oerdek ⁴⁸, J.T. Offermann ³⁹, A. Ogrodnik ¹³³, A. Oh ¹⁰¹, C.C. Ohm ¹⁴⁴, H. Oide ⁸⁴,
 R. Oishi ¹⁵³, M.L. Ojeda ⁴⁸, M.W. O'Keefe ⁹², Y. Okumura ¹⁵³, L.F. Oleiro Seabra ^{130a},
 S.A. Olivares Pino ^{137d}, D. Oliveira Damazio ²⁹, D. Oliveira Goncalves ^{83a}, J.L. Oliver ¹⁶⁰,
 Ö.O. Öncel ⁵⁴, A.P. O'Neill ¹⁹, A. Onofre ^{130a,130e}, P.U.E. Onyisi ¹¹, M.J. Oreglia ³⁹,
 G.E. Orellana ⁹⁰, D. Orestano ^{77a,77b}, N. Orlando ¹³, R.S. Orr ¹⁵⁵, V. O'Shea ⁵⁹,
 L.M. Osojnak ¹²⁸, R. Ospanov ^{62a}, G. Otero y Garzon ³⁰, H. Otono ⁸⁹, P.S. Ott ^{63a},
 G.J. Ottino ^{17a}, M. Ouchrif ^{35d}, J. Ouellette ²⁹, F. Ould-Saada ¹²⁵, M. Owen ⁵⁹, R.E. Owen ¹³⁴,
 K.Y. Oyulmaz ^{21a}, V.E. Ozcan ^{21a}, F. Ozturk ⁸⁷, N. Ozturk ⁸, S. Ozturk ⁸², H.A. Pacey ¹²⁶,
 A. Pacheco Pages ¹³, C. Padilla Aranda ¹³, G. Padovano ^{75a,75b}, S. Pagan Griso ^{17a},
 G. Palacino ⁶⁸, A. Palazzo ^{70a,70b}, S. Palestini ³⁶, J. Pan ¹⁷², T. Pan ^{64a}, D.K. Panchal ¹¹,
 C.E. Pandini ¹¹⁴, J.G. Panduro Vazquez ⁹⁵, H.D. Pandya ¹, H. Pang ^{14b}, P. Pani ⁴⁸,
 G. Panizzo ^{69a,69c}, L. Paolozzi ⁵⁶, C. Papadatos ¹⁰⁸, S. Parajuli ⁴⁴, A. Paramonov ⁶,
 C. Paraskevopoulos ¹⁰, D. Paredes Hernandez ^{64b}, K.R. Park ⁴¹, T.H. Park ¹⁵⁵, M.A. Parker ³²,
 F. Parodi ^{57b,57a}, E.W. Parrish ¹¹⁵, V.A. Parrish ⁵², J.A. Parsons ⁴¹, U. Parzefall ⁵⁴,
 B. Pascual Dias ¹⁰⁸, L. Pascual Dominguez ¹⁵¹, E. Pasqualucci ^{75a}, S. Passaggio ^{57b}, F. Pastore ⁹⁵,
 P. Pasuwan ^{47a,47b}, P. Patel ⁸⁷, U.M. Patel ⁵¹, J.R. Pater ¹⁰¹, T. Pauly ³⁶, J. Pearkes ¹⁴³,
 M. Pedersen ¹²⁵, R. Pedro ^{130a}, S.V. Peleganchuk ³⁷, O. Penc ³⁶, E.A. Pender ⁵²,
 K.E. Pensi ¹⁰⁹, M. Penzin ³⁷, B.S. Peralva ^{83d}, A.P. Pereira Peixoto ⁶⁰, L. Pereira Sanchez ^{47a,47b},
 D.V. Perepelitsa ^{29,ai}, E. Perez Codina ^{156a}, M. Perganti ¹⁰, L. Perini ^{71a,71b,*}, H. Pernegger ³⁶,
 O. Perrin ⁴⁰, K. Peters ⁴⁸, R.F.Y. Peters ¹⁰¹, B.A. Petersen ³⁶, T.C. Petersen ⁴², E. Petit ¹⁰²,
 V. Petousis ¹³², C. Petridou ^{152,e}, A. Petrukhin ¹⁴¹, M. Pettee ^{17a}, N.E. Pettersson ³⁶,
 A. Petukhov ³⁷, K. Petukhova ¹³³, R. Pezoa ^{137f}, L. Pezzotti ³⁶, G. Pezzullo ¹⁷², T.M. Pham ¹⁷⁰,
 T. Pham ¹⁰⁵, P.W. Phillips ¹³⁴, G. Piacquadio ¹⁴⁵, E. Pianori ^{17a}, F. Piazza ¹²³, R. Piegai ³⁰,
 D. Pietreanu ^{27b}, A.D. Pilkington ¹⁰¹, M. Pinamonti ^{69a,69c}, J.L. Pinfeld ²,
 B.C. Pinheiro Pereira ^{130a}, A.E. Pinto Pinoargote ^{100,135}, L. Pintucci ^{69a,69c}, K.M. Piper ¹⁴⁶,
 A. Pirttikoski ⁵⁶, D.A. Pizzi ³⁴, L. Pizzimento ^{64b}, A. Pizzini ¹¹⁴, M.-A. Pleier ²⁹, V. Plesanovs ⁵⁴,
 V. Pleskot ¹³³, E. Plotnikova ³⁸, G. Poddar ⁴, R. Poettgen ⁹⁸, L. Poggioli ¹²⁷, I. Pokharel ⁵⁵,
 S. Polacek ¹³³, G. Polesello ^{73a}, A. Poley ^{142,156a}, R. Polifka ¹³², A. Polini ^{23b}, C.S. Pollard ¹⁶⁷,

Z.B. Pollock [ID119](#), V. Polychronakos [ID29](#), E. Pompa Pacchi [ID75a,75b](#), D. Ponomarenko [ID113](#), L. Pontecorvo [ID36](#), S. Popa [ID27a](#), G.A. Popeneciu [ID27d](#), A. Poreba [ID36](#), D.M. Portillo Quintero [ID156a](#), S. Pospisil [ID132](#), M.A. Postill [ID139](#), P. Postolache [ID27c](#), K. Potamianos [ID167](#), P.A. Potepa [ID86a](#), I.N. Potrap [ID38](#), C.J. Potter [ID32](#), H. Potti [ID1](#), T. Poulsen [ID48](#), J. Poveda [ID163](#), M.E. Pozo Astigarraga [ID36](#), A. Prades Ibanez [ID163](#), J. Pretel [ID54](#), D. Price [ID101](#), M. Primavera [ID70a](#), M.A. Principe Martin [ID99](#), R. Privara [ID122](#), T. Procter [ID59](#), M.L. Proffitt [ID138](#), N. Proklova [ID128](#), K. Prokofiev [ID64c](#), G. Proto [ID110](#), S. Protopopescu [ID29](#), J. Proudfoot [ID6](#), M. Przybycien [ID86a](#), W.W. Przygoda [ID86b](#), J.E. Puddefoot [ID139](#), D. Pudzha [ID37](#), D. Pyatiizbyantseva [ID37](#), J. Qian [ID106](#), D. Qichen [ID101](#), Y. Qin [ID101](#), T. Qiu [ID52](#), A. Quadt [ID55](#), M. Queitsch-Maitland [ID101](#), G. Quetant [ID56](#), R.P. Quinn [ID164](#), G. Rabanal Bolanos [ID61](#), D. Rafanoharana [ID54](#), F. Ragusa [ID71a,71b](#), J.L. Rainbolt [ID39](#), J.A. Raine [ID56](#), S. Rajagopalan [ID29](#), E. Ramakoti [ID37](#), I.A. Ramirez-Berend [ID34](#), K. Ran [ID48,14e](#), N.P. Rapheeha [ID33g](#), H. Rasheed [ID27b](#), V. Raskina [ID127](#), D.F. Rassloff [ID63a](#), S. Rave [ID100](#), B. Ravina [ID55](#), I. Ravinovich [ID169](#), M. Raymond [ID36](#), A.L. Read [ID125](#), N.P. Readioff [ID139](#), D.M. Rebuzzi [ID73a,73b](#), G. Redlinger [ID29](#), A.S. Reed [ID110](#), K. Reeves [ID26](#), J.A. Reidelsturz [ID171](#), D. Reikher [ID151](#), A. Rej [ID49](#), C. Rembser [ID36](#), A. Renardi [ID48](#), M. Renda [ID27b](#), M.B. Rendel [ID110](#), F. Renner [ID48](#), A.G. Rennie [ID160](#), A.L. Rescia [ID48](#), S. Resconi [ID71a](#), M. Ressegotti [ID57b,57a](#), S. Rettie [ID36](#), J.G. Reyes Rivera [ID107](#), E. Reynolds [ID17a](#), O.L. Rezanova [ID37](#), P. Reznicek [ID133](#), N. Ribaric [ID91](#), E. Ricci [ID78a,78b](#), R. Richter [ID110](#), S. Richter [ID47a,47b](#), E. Richter-Was [ID86b](#), M. Ridel [ID127](#), S. Ridouani [ID35d](#), P. Rieck [ID117](#), P. Riedler [ID36](#), E.M. Riefel [ID47a,47b](#), J.O. Rieger [ID114](#), M. Rijssenbeek [ID145](#), A. Rimoldi [ID73a,73b](#), M. Rimoldi [ID36](#), L. Rinaldi [ID23b,23a](#), T.T. Rinn [ID29](#), M.P. Rinnagel [ID109](#), G. Ripellino [ID161](#), I. Riu [ID13](#), P. Rivadeneira [ID48](#), J.C. Rivera Vergara [ID165](#), F. Rizatdinova [ID121](#), E. Rizvi [ID94](#), B.A. Roberts [ID167](#), B.R. Roberts [ID17a](#), S.H. Robertson [ID104,w](#), D. Robinson [ID32](#), C.M. Robles Gajardo [ID137f](#), M. Robles Manzano [ID100](#), A. Robson [ID59](#), A. Rocchi [ID76a,76b](#), C. Roda [ID74a,74b](#), S. Rodriguez Bosca [ID63a](#), Y. Rodriguez Garcia [ID22a](#), A. Rodriguez Rodriguez [ID54](#), A.M. Rodríguez Vera [ID156b](#), S. Roe [ID36](#), J.T. Roemer [ID160](#), A.R. Roepe-Gier [ID136](#), J. Roggel [ID171](#), O. Røhne [ID125](#), R.A. Rojas [ID103](#), C.P.A. Roland [ID127](#), J. Roloff [ID29](#), A. Romaniouk [ID37](#), E. Romano [ID73a,73b](#), M. Romano [ID23b](#), A.C. Romero Hernandez [ID162](#), N. Rompotis [ID92](#), L. Roos [ID127](#), S. Rosati [ID75a](#), B.J. Rosser [ID39](#), E. Rossi [ID126](#), E. Rossi [ID72a,72b](#), L.P. Rossi [ID57b](#), L. Rossini [ID54](#), R. Rosten [ID119](#), M. Rotaru [ID27b](#), B. Rottler [ID54](#), C. Rougier [ID102,aa](#), D. Rousseau [ID66](#), D. Rousso [ID32](#), A. Roy [ID162](#), S. Roy-Garand [ID155](#), A. Rozanov [ID102](#), Z.M.A. Rozario [ID59](#), Y. Rozen [ID150](#), X. Ruan [ID33g](#), A. Rubio Jimenez [ID163](#), A.J. Ruby [ID92](#), V.H. Ruelas Rivera [ID18](#), T.A. Ruggeri [ID1](#), A. Ruggiero [ID126](#), A. Ruiz-Martinez [ID163](#), A. Rummler [ID36](#), Z. Rurikova [ID54](#), N.A. Rusakovich [ID38](#), H.L. Russell [ID165](#), G. Russo [ID75a,75b](#), J.P. Rutherford [ID7](#), S. Rutherford Colmenares [ID32](#), K. Rybacki [ID91](#), M. Rybar [ID133](#), E.B. Rye [ID125](#), A. Ryzhov [ID44](#), J.A. Sabater Iglesias [ID56](#), P. Sabatini [ID163](#), H.F.W. Sadrozinski [ID136](#), F. Safai Tehrani [ID75a](#), B. Safarzadeh Samani [ID134](#), M. Safdari [ID143](#), S. Saha [ID165](#), M. Sahinsoy [ID110](#), A. Saibel [ID163](#), M. Saimpert [ID135](#), M. Saito [ID153](#), T. Saito [ID153](#), D. Salamani [ID36](#), A. Salnikov [ID143](#), J. Salt [ID163](#), A. Salvador Salas [ID151](#), D. Salvatore [ID43b,43a](#), F. Salvatore [ID146](#), A. Salzburger [ID36](#), D. Sammel [ID54](#), D. Sampsonidis [ID152,e](#), D. Sampsonidou [ID123](#), J. Sánchez [ID163](#), A. Sanchez Pineda [ID4](#), V. Sanchez Sebastian [ID163](#), H. Sandaker [ID125](#), C.O. Sander [ID48](#), J.A. Sandesara [ID103](#), M. Sandhoff [ID171](#), C. Sandoval [ID22b](#), D.P.C. Sankey [ID134](#), T. Sano [ID88](#), A. Sansoni [ID53](#), L. Santi [ID75a,75b](#), C. Santoni [ID40](#), H. Santos [ID130a,130b](#), S.N. Santpur [ID17a](#), A. Santra [ID169](#), K.A. Saoucha [ID116b](#), J.G. Saraiva [ID130a,130d](#), J. Sardain [ID7](#), O. Sasaki [ID84](#), K. Sato [ID157](#), C. Sauer [ID63b](#), F. Sauerburger [ID54](#), E. Sauvan [ID4](#), P. Savard [ID155,af](#), R. Sawada [ID153](#), C. Sawyer [ID134](#), L. Sawyer [ID97](#), I. Sayago Galvan [ID163](#), C. Sbarra [ID23b](#), A. Sbrizzi [ID23b,23a](#), T. Scanlon [ID96](#), J. Schaarschmidt [ID138](#), P. Schacht [ID110](#), U. Schäfer [ID100](#), A.C. Schaffer [ID66,44](#), D. Schaile [ID109](#), R.D. Schamberger [ID145](#), C. Scharf [ID18](#), M.M. Schefer [ID19](#), V.A. Schegelsky [ID37](#), D. Scheirich [ID133](#), F. Schenck [ID18](#), M. Schernau [ID160](#), C. Scheulen [ID55](#), C. Schiavi [ID57b,57a](#), E.J. Schioppa [ID70a,70b](#), M. Schioppa [ID43b,43a](#), B. Schlag [ID143,n](#), K.E. Schleicher [ID54](#),

S. Schlenker ³⁶, J. Schmeing ¹⁷¹, M.A. Schmidt ¹⁷¹, K. Schmieden ¹⁰⁰, C. Schmitt ¹⁰⁰,
 N. Schmitt ¹⁰⁰, S. Schmitt ⁴⁸, L. Schoeffel ¹³⁵, A. Schoening ^{63b}, P.G. Scholer ⁵⁴, E. Schopf ¹²⁶,
 M. Schott ¹⁰⁰, J. Schovancova ³⁶, S. Schramm ⁵⁶, F. Schroeder ¹⁷¹, T. Schroer ⁵⁶,
 H-C. Schultz-Coulon ^{63a}, M. Schumacher ⁵⁴, B.A. Schumm ¹³⁶, Ph. Schune ¹³⁵, A.J. Schuy ¹³⁸,
 H.R. Schwartz ¹³⁶, A. Schwartzman ¹⁴³, T.A. Schwarz ¹⁰⁶, Ph. Schwemling ¹³⁵,
 R. Schwienhorst ¹⁰⁷, A. Sciandra ¹³⁶, G. Sciolla ²⁶, F. Scuri ^{74a}, C.D. Sebastiani ⁹²,
 K. Sedlaczek ¹¹⁵, P. Seema ¹⁸, S.C. Seidel ¹¹², A. Seiden ¹³⁶, B.D. Seidlitz ⁴¹, C. Seitz ⁴⁸,
 J.M. Seixas ^{83b}, G. Sekhniaidze ^{72a}, S.J. Sekula ⁴⁴, L. Selem ⁶⁰, N. Semprini-Cesari ^{23b,23a},
 D. Sengupta ⁵⁶, V. Senthilkumar ¹⁶³, L. Serin ⁶⁶, L. Serkin ^{69a,69b}, M. Sessa ^{76a,76b},
 H. Severini ¹²⁰, F. Sforza ^{57b,57a}, A. Sfyrta ⁵⁶, E. Shabalina ⁵⁵, R. Shaheen ¹⁴⁴,
 J.D. Shahinian ¹²⁸, D. Shaked Renous ¹⁶⁹, L.Y. Shan ^{14a}, M. Shapiro ^{17a}, A. Sharma ³⁶,
 A.S. Sharma ¹⁶⁴, P. Sharma ⁸⁰, S. Sharma ⁴⁸, P.B. Shatalov ³⁷, K. Shaw ¹⁴⁶, S.M. Shaw ¹⁰¹,
 A. Shcherbakova ³⁷, Q. Shen ^{62c,5}, D.J. Sheppard ¹⁴², P. Sherwood ⁹⁶, L. Shi ⁹⁶, X. Shi ^{14a},
 C.O. Shimmin ¹⁷², J.D. Shinner ⁹⁵, I.P.J. Shipsey ¹²⁶, S. Shirabe ^{56,h}, M. Shiyakova ^{38,u},
 J. Shlomi ¹⁶⁹, M.J. Shochet ³⁹, J. Shojaii ¹⁰⁵, D.R. Shope ¹²⁵, B. Shrestha ¹²⁰, S. Shrestha ^{119,aj},
 E.M. Shrif ^{33g}, M.J. Shroff ¹⁶⁵, P. Sicho ¹³¹, A.M. Sickles ¹⁶², E. Sideras Haddad ^{33g},
 A. Sidoti ^{23b}, F. Siegert ⁵⁰, Dj. Sijacki ¹⁵, F. Sili ⁹⁰, J.M. Silva ²⁰, M.V. Silva Oliveira ²⁹,
 S.B. Silverstein ^{47a}, S. Simion ⁶⁶, R. Simoniello ³⁶, E.L. Simpson ⁵⁹, H. Simpson ¹⁴⁶,
 L.R. Simpson ¹⁰⁶, N.D. Simpson ⁹⁸, S. Simsek ⁸², S. Sindhu ⁵⁵, P. Sinervo ¹⁵⁵, S. Singh ¹⁵⁵,
 S. Sinha ⁴⁸, S. Sinha ¹⁰¹, M. Sioli ^{23b,23a}, I. Siral ³⁶, E. Sitnikova ⁴⁸, S.Yu. Sivoklov ^{37,*},
 J. Sjölin ^{47a,47b}, A. Skaf ⁵⁵, E. Skorda ²⁰, P. Skubic ¹²⁰, M. Slawinska ⁸⁷, V. Smakhtin ¹⁶⁹,
 B.H. Smart ¹³⁴, J. Smiesko ³⁶, S.Yu. Smirnov ³⁷, Y. Smirnov ³⁷, L.N. Smirnova ^{37,a},
 O. Smirnova ⁹⁸, A.C. Smith ⁴¹, E.A. Smith ³⁹, H.A. Smith ¹²⁶, J.L. Smith ⁹², R. Smith ¹⁴³,
 M. Smizanska ⁹¹, K. Smolek ¹³², A.A. Snesev ³⁷, S.R. Snider ¹⁵⁵, H.L. Snoek ¹¹⁴,
 S. Snyder ²⁹, R. Sobie ^{165,w}, A. Soffer ¹⁵¹, C.A. Solans Sanchez ³⁶, E.Yu. Soldatov ³⁷,
 U. Soldevila ¹⁶³, A.A. Solodkov ³⁷, S. Solomon ²⁶, A. Soloshenko ³⁸, K. Solovieva ⁵⁴,
 O.V. Solovyanov ⁴⁰, V. Solovyev ³⁷, P. Sommer ³⁶, A. Sonay ¹³, W.Y. Song ^{156b},
 J.M. Sonneveld ¹¹⁴, A. Sopczak ¹³², A.L. Sopio ⁹⁶, F. Sopkova ^{28b}, I.R. Sotarriva Alvarez ¹⁵⁴,
 V. Sothilingam ^{63a}, O.J. Soto Sandoval ^{137c,137b}, S. Sottocornola ⁶⁸, R. Soualah ^{116b},
 Z. Soumami ^{35e}, D. South ⁴⁸, N. Soybelman ¹⁶⁹, S. Spagnolo ^{70a,70b}, M. Spalla ¹¹⁰,
 D. Sperlich ⁵⁴, G. Spigo ³⁶, S. Spinali ⁹¹, D.P. Spiteri ⁵⁹, M. Spousta ¹³³, E.J. Staats ³⁴,
 A. Stabile ^{71a,71b}, R. Stamen ^{63a}, A. Stampekis ²⁰, M. Standke ²⁴, E. Stanecka ⁸⁷,
 M.V. Stange ⁵⁰, B. Stanislaus ^{17a}, M.M. Stanitzki ⁴⁸, B. Stapf ⁴⁸, E.A. Starchenko ³⁷,
 G.H. Stark ¹³⁶, J. Stark ^{102,aa}, D.M. Starko ^{156b}, P. Staroba ¹³¹, P. Starovoitov ^{63a}, S. Stärz ¹⁰⁴,
 R. Staszewski ⁸⁷, G. Stavropoulos ⁴⁶, J. Steentoft ¹⁶¹, P. Steinberg ²⁹, B. Stelzer ^{142,156a},
 H.J. Stelzer ¹²⁹, O. Stelzer-Chilton ^{156a}, H. Stenzel ⁵⁸, T.J. Stevenson ¹⁴⁶, G.A. Stewart ³⁶,
 J.R. Stewart ¹²¹, M.C. Stockton ³⁶, G. Stoica ^{27b}, M. Stolarski ^{130a}, S. Stonjek ¹¹⁰,
 A. Straessner ⁵⁰, J. Strandberg ¹⁴⁴, S. Strandberg ^{47a,47b}, M. Stratmann ¹⁷¹, M. Strauss ¹²⁰,
 T. Strebler ¹⁰², P. Strizenec ^{28b}, R. Ströhmer ¹⁶⁶, D.M. Strom ¹²³, R. Stroynowski ⁴⁴,
 A. Strubig ^{47a,47b}, S.A. Stucci ²⁹, B. Stugu ¹⁶, J. Stupak ¹²⁰, N.A. Styles ⁴⁸, D. Su ¹⁴³,
 S. Su ^{62a}, W. Su ^{62d}, X. Su ^{62a,66}, K. Sugizaki ¹⁵³, V.V. Sulin ³⁷, M.J. Sullivan ⁹²,
 D.M.S. Sultan ^{78a,78b}, L. Sultanaliyeva ³⁷, S. Sultansoy ^{3b}, T. Sumida ⁸⁸, S. Sun ¹⁰⁶, S. Sun ¹⁷⁰,
 O. Sunneborn Gudnadottir ¹⁶¹, N. Sur ¹⁰², M.R. Sutton ¹⁴⁶, H. Suzuki ¹⁵⁷, M. Svatos ¹³¹,
 M. Swiatlowski ^{156a}, T. Swirski ¹⁶⁶, I. Sykora ^{28a}, M. Sykora ¹³³, T. Sykora ¹³³, D. Ta ¹⁰⁰,
 K. Tackmann ^{48,t}, A. Taffard ¹⁶⁰, R. Tafirout ^{156a}, J.S. Tafoya Vargas ⁶⁶, E.P. Takeva ⁵²,
 Y. Takubo ⁸⁴, M. Talby ¹⁰², A.A. Talyshev ³⁷, K.C. Tam ^{64b}, N.M. Tamir ¹⁵¹, A. Tanaka ¹⁵³,
 J. Tanaka ¹⁵³, R. Tanaka ⁶⁶, M. Tanasini ^{57b,57a}, Z. Tao ¹⁶⁴, S. Tapia Araya ^{137f},

S. Tapprogge ¹⁰⁰, A. Tarek Abouelfadl Mohamed ¹⁰⁷, S. Tarem ¹⁵⁰, K. Tariq ^{14a}, G. Tarna ^{102,27b},
 G.F. Tartarelli ^{71a}, P. Tas ¹³³, M. Tasevsky ¹³¹, E. Tassi ^{43b,43a}, A.C. Tate ¹⁶², G. Tateno ¹⁵³,
 Y. Tayalati ^{35e,v}, G.N. Taylor ¹⁰⁵, W. Taylor ^{156b}, A.S. Tee ¹⁷⁰, R. Teixeira De Lima ¹⁴³,
 P. Teixeira-Dias ⁹⁵, J.J. Teoh ¹⁵⁵, K. Terashi ¹⁵³, J. Terron ⁹⁹, S. Terzo ¹³, M. Testa ⁵³,
 R.J. Teuscher ^{155,w}, A. Thaler ⁷⁹, O. Theiner ⁵⁶, N. Themistokleous ⁵², T. Theveneaux-Pelzer ¹⁰²,
 O. Thielmann ¹⁷¹, D.W. Thomas ⁹⁵, J.P. Thomas ²⁰, E.A. Thompson ^{17a}, P.D. Thompson ²⁰,
 E. Thomson ¹²⁸, Y. Tian ⁵⁵, V. Tikhomirov ^{37,a}, Yu.A. Tikhonov ³⁷, S. Timoshenko ³⁷,
 D. Timoshyn ¹³³, E.X.L. Ting ¹, P. Tipton ¹⁷², S.H. Tlou ^{33g}, A. Tnourji ⁴⁰, K. Todome ¹⁵⁴,
 S. Todorova-Nova ¹³³, S. Todt ⁵⁰, M. Togawa ⁸⁴, J. Tojo ⁸⁹, S. Tokár ^{28a}, K. Tokushuku ⁸⁴,
 O. Toldaiev ⁶⁸, R. Tombs ³², M. Tomoto ^{84,111}, L. Tompkins ^{143,n}, K.W. Topolnicki ^{86b},
 E. Torrence ¹²³, H. Torres ^{102,aa}, E. Torró Pastor ¹⁶³, M. Toscani ³⁰, C. Tosciri ³⁹, M. Tost ¹¹,
 D.R. Tovey ¹³⁹, A. Traeet ¹⁶, I.S. Trandafir ^{27b}, T. Trefzger ¹⁶⁶, A. Tricoli ²⁹, I.M. Trigger ^{156a},
 S. Trincaz-Duvoid ¹²⁷, D.A. Trischuk ²⁶, B. Trocmé ⁶⁰, C. Troncon ^{71a}, L. Truong ^{33c},
 M. Trzebinski ⁸⁷, A. Trzupiek ⁸⁷, F. Tsai ¹⁴⁵, M. Tsai ¹⁰⁶, A. Tsiamis ^{152,e}, P.V. Tsiareshka ³⁷,
 S. Tsigaridas ^{156a}, A. Tsirigotis ^{152,r}, V. Tsiskaridze ¹⁵⁵, E.G. Tskhadadze ^{149a},
 M. Tsopoulou ^{152,e}, Y. Tsujikawa ⁸⁸, I.I. Tsukerman ³⁷, V. Tsulaia ^{17a}, S. Tsuno ⁸⁴, K. Tsurii ¹¹⁸,
 D. Tsybychev ¹⁴⁵, Y. Tu ^{64b}, A. Tudorache ^{27b}, V. Tudorache ^{27b}, A.N. Tuna ⁶¹,
 S. Turchikhin ^{57b,57a}, I. Turk Cakir ^{3a}, R. Turra ^{71a}, T. Turtuvshin ^{38,x}, P.M. Tuts ⁴¹,
 S. Tzamarias ^{152,e}, P. Tzanis ¹⁰, E. Tzovara ¹⁰⁰, F. Ukegawa ¹⁵⁷, P.A. Ulloa Poblete ^{137c,137b},
 E.N. Umaka ²⁹, G. Unal ³⁶, M. Unal ¹¹, A. Undrus ²⁹, G. Unel ¹⁶⁰, J. Urban ^{28b},
 P. Urquijo ¹⁰⁵, P. Urrejola ^{137a}, G. Usai ⁸, R. Ushioda ¹⁵⁴, M. Usman ¹⁰⁸, Z. Uysal ^{21b},
 V. Vacek ¹³², B. Vachon ¹⁰⁴, K.O.H. Vadla ¹²⁵, T. Vafeiadis ³⁶, A. Vaitkus ⁹⁶, C. Valderanis ¹⁰⁹,
 E. Valdes Santurio ^{47a,47b}, M. Valente ^{156a}, S. Valentinetti ^{23b,23a}, A. Valero ¹⁶³,
 E. Valiente Moreno ¹⁶³, A. Vallier ^{102,aa}, J.A. Valls Ferrer ¹⁶³, D.R. Van Arneman ¹¹⁴,
 T.R. Van Daalen ¹³⁸, A. Van Der Graaf ⁴⁹, P. Van Gemmeren ⁶, M. Van Rijnbach ^{125,36},
 S. Van Stroud ⁹⁶, I. Van Vulpen ¹¹⁴, M. Vanadia ^{76a,76b}, W. Vandelli ³⁶, M. Vandenbroucke ¹³⁵,
 E.R. Vandewall ¹²¹, D. Vannicola ¹⁵¹, L. Vannoli ^{57b,57a}, R. Vari ^{75a}, E.W. Varnes ⁷,
 C. Varni ^{17b}, T. Varol ¹⁴⁸, D. Varouchas ⁶⁶, L. Varriale ¹⁶³, K.E. Varvell ¹⁴⁷, M.E. Vasile ^{27b},
 L. Vaslin ⁸⁴, G.A. Vasquez ¹⁶⁵, A. Vasyukov ³⁸, F. Vazeille ⁴⁰, T. Vazquez Schroeder ³⁶,
 J. Veatch ³¹, V. Vecchio ¹⁰¹, M.J. Veen ¹⁰³, I. Veliscek ¹²⁶, L.M. Veloce ¹⁵⁵, F. Veloso ^{130a,130c},
 S. Veneziano ^{75a}, A. Ventura ^{70a,70b}, S. Ventura Gonzalez ¹³⁵, A. Verbytskyi ¹¹⁰,
 M. Verducci ^{74a,74b}, C. Vergis ²⁴, M. Verissimo De Araujo ^{83b}, W. Verkerke ¹¹⁴,
 J.C. Vermeulen ¹¹⁴, C. Vernieri ¹⁴³, M. Vessella ¹⁰³, M.C. Vetterli ^{142,af}, A. Vgenopoulos ^{152,e},
 N. Viaux Maira ^{137f}, T. Vickey ¹³⁹, O.E. Vickey Boeriu ¹³⁹, G.H.A. Viehhauser ¹²⁶, L. Vignani ^{63b},
 M. Villa ^{23b,23a}, M. Villaplana Perez ¹⁶³, E.M. Villhauer ⁵², E. Vilucchi ⁵³, M.G. Vincter ³⁴,
 G.S. Virdee ²⁰, A. Vishwakarma ⁵², A. Visibile ¹¹⁴, C. Vittori ³⁶, I. Vivarelli ¹⁴⁶,
 E. Voevodina ¹¹⁰, F. Vogel ¹⁰⁹, J.C. Voigt ⁵⁰, P. Vokac ¹³², Yu. Volkotrub ^{86a}, J. Von Ahnen ⁴⁸,
 E. Von Toerne ²⁴, B. Vormwald ³⁶, V. Vorobel ¹³³, K. Vorobev ³⁷, M. Vos ¹⁶³, K. Voss ¹⁴¹,
 J.H. Vossebeld ⁹², M. Vozak ¹¹⁴, L. Vozdecky ⁹⁴, N. Vranjes ¹⁵, M. Vranjes Milosavljevic ¹⁵,
 M. Vreeswijk ¹¹⁴, R. Vuillermet ³⁶, O. Vujanovic ¹⁰⁰, I. Vukotic ³⁹, S. Wada ¹⁵⁷, C. Wagner ¹⁰³,
 J.M. Wagner ^{17a}, W. Wagner ¹⁷¹, S. Wahdan ¹⁷¹, H. Wahlberg ⁹⁰, M. Wakida ¹¹¹, J. Walder ¹³⁴,
 R. Walker ¹⁰⁹, W. Walkowiak ¹⁴¹, A. Wall ¹²⁸, T. Wamorkar ⁶, A.Z. Wang ¹³⁶, C. Wang ¹⁰⁰,
 C. Wang ^{62c}, H. Wang ^{17a}, J. Wang ^{64a}, R.-J. Wang ¹⁰⁰, R. Wang ⁶¹, R. Wang ⁶,
 S.M. Wang ¹⁴⁸, S. Wang ^{62b}, T. Wang ^{62a}, W.T. Wang ⁸⁰, W. Wang ^{14a}, X. Wang ^{14c},
 X. Wang ¹⁶², X. Wang ^{62c}, Y. Wang ^{62d}, Y. Wang ^{14c}, Z. Wang ¹⁰⁶, Z. Wang ^{62d,51,62c},
 Z. Wang ¹⁰⁶, A. Warburton ¹⁰⁴, R.J. Ward ²⁰, N. Warrack ⁵⁹, A.T. Watson ²⁰, H. Watson ⁵⁹,
 M.F. Watson ²⁰, E. Watton ^{59,134}, G. Watts ¹³⁸, B.M. Waugh ⁹⁶, C. Weber ²⁹, H.A. Weber ¹⁸,

M.S. Weber ¹⁹, S.M. Weber ^{63a}, C. Wei ^{62a}, Y. Wei ¹²⁶, A.R. Weidberg ¹²⁶, E.J. Weik ¹¹⁷, J. Weingarten ⁴⁹, M. Weirich ¹⁰⁰, C. Weiser ⁵⁴, C.J. Wells ⁴⁸, T. Wenaus ²⁹, B. Wendland ⁴⁹, T. Wengler ³⁶, N.S. Wenke¹¹⁰, N. Wermes ²⁴, M. Wessels ^{63a}, A.M. Wharton ⁹¹, A.S. White ⁶¹, A. White ⁸, M.J. White ¹, D. Whiteson ¹⁶⁰, L. Wickremasinghe ¹²⁴, W. Wiedenmann ¹⁷⁰, C. Wiel ⁵⁰, M. Wielers ¹³⁴, C. Wiglesworth ⁴², D.J. Wilbern¹²⁰, H.G. Wilkens ³⁶, D.M. Williams ⁴¹, H.H. Williams¹²⁸, S. Williams ³², S. Willocq ¹⁰³, B.J. Wilson ¹⁰¹, P.J. Windischhofer ³⁹, F.I. Winkel ³⁰, F. Winklmeier ¹²³, B.T. Winter ⁵⁴, J.K. Winter ¹⁰¹, M. Wittgen¹⁴³, M. Wobisch ⁹⁷, Z. Wolffs ¹¹⁴, J. Wollrath¹⁶⁰, M.W. Wolter ⁸⁷, H. Wolters ^{130a,130c}, A.F. Wongel ⁴⁸, E.L. Woodward ⁴¹, S.D. Worm ⁴⁸, B.K. Wosiek ⁸⁷, K.W. Woźniak ⁸⁷, S. Wozniowski ⁵⁵, K. Wraight ⁵⁹, C. Wu ²⁰, J. Wu ^{14a,14e}, M. Wu ^{64a}, M. Wu ¹¹³, S.L. Wu ¹⁷⁰, X. Wu ⁵⁶, Y. Wu ^{62a}, Z. Wu ¹³⁵, J. Wuerzinger ^{110,ad}, T.R. Wyatt ¹⁰¹, B.M. Wynne ⁵², S. Xella ⁴², L. Xia ^{14c}, M. Xia ^{14b}, J. Xiang ^{64c}, M. Xie ^{62a}, X. Xie ^{62a}, S. Xin ^{14a,14e}, A. Xiong ¹²³, J. Xiong ^{17a}, D. Xu ^{14a}, H. Xu ^{62a}, L. Xu ^{62a}, R. Xu ¹²⁸, T. Xu ¹⁰⁶, Y. Xu ^{14b}, Z. Xu ⁵², Z. Xu ^{14c}, B. Yabsley ¹⁴⁷, S. Yacoob ^{33a}, Y. Yamaguchi ¹⁵⁴, E. Yamashita ¹⁵³, H. Yamauchi ¹⁵⁷, T. Yamazaki ^{17a}, Y. Yamazaki ⁸⁵, J. Yan ^{62c}, S. Yan ¹²⁶, Z. Yan ²⁵, H.J. Yang ^{62c,62d}, H.T. Yang ^{62a}, S. Yang ^{62a}, T. Yang ^{64c}, X. Yang ³⁶, X. Yang ^{14a}, Y. Yang ⁴⁴, Y. Yang ^{62a}, Z. Yang ^{62a}, W-M. Yao ^{17a}, Y.C. Yap ⁴⁸, H. Ye ^{14c}, H. Ye ⁵⁵, J. Ye ^{14a}, S. Ye ²⁹, X. Ye ^{62a}, Y. Yeh ⁹⁶, I. Yeletsikh ³⁸, B.K. Yeo ^{17b}, M.R. Yexley ⁹⁶, P. Yin ⁴¹, K. Yorita ¹⁶⁸, S. Younas ^{27b}, C.J.S. Young ³⁶, C. Young ¹⁴³, C. Yu ^{14a,14e,ah}, Y. Yu ^{62a}, M. Yuan ¹⁰⁶, R. Yuan ^{62b}, L. Yue ⁹⁶, M. Zaazoua ^{62a}, B. Zabinski ⁸⁷, E. Zaid⁵², Z.K. Zak ⁸⁷, T. Zakareishvili ^{149b}, N. Zakharchuk ³⁴, S. Zambito ⁵⁶, J.A. Zamora Saa ^{137d,137b}, J. Zang ¹⁵³, D. Zanzi ⁵⁴, O. Zaplatilek ¹³², C. Zeitnitz ¹⁷¹, H. Zeng ^{14a}, J.C. Zeng ¹⁶², D.T. Zenger Jr ²⁶, O. Zenin ³⁷, T. Ženiš ^{28a}, S. Zenz ⁹⁴, S. Zerradi ^{35a}, D. Zerwas ⁶⁶, M. Zhai ^{14a,14e}, B. Zhang ^{14c}, D.F. Zhang ¹³⁹, J. Zhang ^{62b}, J. Zhang ⁶, K. Zhang ^{14a,14e}, L. Zhang ^{14c}, P. Zhang ^{14a,14e}, R. Zhang ¹⁷⁰, S. Zhang ¹⁰⁶, S. Zhang ⁴⁴, T. Zhang ¹⁵³, X. Zhang ^{62c}, X. Zhang ^{62b}, Y. Zhang ^{62c,5}, Y. Zhang ⁹⁶, Y. Zhang ^{14c}, Z. Zhang ^{17a}, Z. Zhang ⁶⁶, H. Zhao ¹³⁸, T. Zhao ^{62b}, Y. Zhao ¹³⁶, Z. Zhao ^{62a}, A. Zhemchugov ³⁸, J. Zheng ^{14c}, K. Zheng ¹⁶², X. Zheng ^{62a}, Z. Zheng ¹⁴³, D. Zhong ¹⁶², B. Zhou ¹⁰⁶, H. Zhou ⁷, N. Zhou ^{62c}, Y. Zhou⁷, C.G. Zhu ^{62b}, J. Zhu ¹⁰⁶, Y. Zhu ^{62c}, Y. Zhu ^{62a}, X. Zhuang ^{14a}, K. Zhukov ³⁷, V. Zhulanov ³⁷, N.I. Zimine ³⁸, J. Zinsser ^{63b}, M. Ziolkowski ¹⁴¹, L. Živković ¹⁵, A. Zoccoli ^{23b,23a}, K. Zoch ⁶¹, T.G. Zorbas ¹³⁹, O. Zormpa ⁴⁶, W. Zou ⁴¹, L. Zwalinski ³⁶.

¹Department of Physics, University of Adelaide, Adelaide; Australia.

²Department of Physics, University of Alberta, Edmonton AB; Canada.

³(^a)Department of Physics, Ankara University, Ankara; (^b)Division of Physics, TOBB University of Economics and Technology, Ankara; Türkiye.

⁴LAPP, Université Savoie Mont Blanc, CNRS/IN2P3, Annecy; France.

⁵APC, Université Paris Cité, CNRS/IN2P3, Paris; France.

⁶High Energy Physics Division, Argonne National Laboratory, Argonne IL; United States of America.

⁷Department of Physics, University of Arizona, Tucson AZ; United States of America.

⁸Department of Physics, University of Texas at Arlington, Arlington TX; United States of America.

⁹Physics Department, National and Kapodistrian University of Athens, Athens; Greece.

¹⁰Physics Department, National Technical University of Athens, Zografou; Greece.

¹¹Department of Physics, University of Texas at Austin, Austin TX; United States of America.

¹²Institute of Physics, Azerbaijan Academy of Sciences, Baku; Azerbaijan.

¹³Institut de Física d'Altes Energies (IFAE), Barcelona Institute of Science and Technology, Barcelona; Spain.

- ¹⁴(^a)Institute of High Energy Physics, Chinese Academy of Sciences, Beijing;^(b)Physics Department, Tsinghua University, Beijing;^(c)Department of Physics, Nanjing University, Nanjing;^(d)School of Science, Shenzhen Campus of Sun Yat-sen University;^(e)University of Chinese Academy of Science (UCAS), Beijing; China.
- ¹⁵Institute of Physics, University of Belgrade, Belgrade; Serbia.
- ¹⁶Department for Physics and Technology, University of Bergen, Bergen; Norway.
- ¹⁷(^a)Physics Division, Lawrence Berkeley National Laboratory, Berkeley CA;^(b)University of California, Berkeley CA; United States of America.
- ¹⁸Institut für Physik, Humboldt Universität zu Berlin, Berlin; Germany.
- ¹⁹Albert Einstein Center for Fundamental Physics and Laboratory for High Energy Physics, University of Bern, Bern; Switzerland.
- ²⁰School of Physics and Astronomy, University of Birmingham, Birmingham; United Kingdom.
- ²¹(^a)Department of Physics, Bogazici University, Istanbul;^(b)Department of Physics Engineering, Gaziantep University, Gaziantep;^(c)Department of Physics, Istanbul University, Istanbul; Türkiye.
- ²²(^a)Facultad de Ciencias y Centro de Investigaciones, Universidad Antonio Nariño, Bogotá;^(b)Departamento de Física, Universidad Nacional de Colombia, Bogotá; Colombia.
- ²³(^a)Dipartimento di Fisica e Astronomia A. Righi, Università di Bologna, Bologna;^(b)INFN Sezione di Bologna; Italy.
- ²⁴Physikalisches Institut, Universität Bonn, Bonn; Germany.
- ²⁵Department of Physics, Boston University, Boston MA; United States of America.
- ²⁶Department of Physics, Brandeis University, Waltham MA; United States of America.
- ²⁷(^a)Transilvania University of Brasov, Brasov;^(b)Horia Hulubei National Institute of Physics and Nuclear Engineering, Bucharest;^(c)Department of Physics, Alexandru Ioan Cuza University of Iasi, Iasi;^(d)National Institute for Research and Development of Isotopic and Molecular Technologies, Physics Department, Cluj-Napoca;^(e)University Politehnica Bucharest, Bucharest;^(f)West University in Timisoara, Timisoara;^(g)Faculty of Physics, University of Bucharest, Bucharest; Romania.
- ²⁸(^a)Faculty of Mathematics, Physics and Informatics, Comenius University, Bratislava;^(b)Department of Subnuclear Physics, Institute of Experimental Physics of the Slovak Academy of Sciences, Kosice; Slovak Republic.
- ²⁹Physics Department, Brookhaven National Laboratory, Upton NY; United States of America.
- ³⁰Universidad de Buenos Aires, Facultad de Ciencias Exactas y Naturales, Departamento de Física, y CONICET, Instituto de Física de Buenos Aires (IFIBA), Buenos Aires; Argentina.
- ³¹California State University, CA; United States of America.
- ³²Cavendish Laboratory, University of Cambridge, Cambridge; United Kingdom.
- ³³(^a)Department of Physics, University of Cape Town, Cape Town;^(b)iThemba Labs, Western Cape;^(c)Department of Mechanical Engineering Science, University of Johannesburg, Johannesburg;^(d)National Institute of Physics, University of the Philippines Diliman (Philippines);^(e)University of South Africa, Department of Physics, Pretoria;^(f)University of Zululand, KwaDlangezwa;^(g)School of Physics, University of the Witwatersrand, Johannesburg; South Africa.
- ³⁴Department of Physics, Carleton University, Ottawa ON; Canada.
- ³⁵(^a)Faculté des Sciences Ain Chock, Réseau Universitaire de Physique des Hautes Energies - Université Hassan II, Casablanca;^(b)Faculté des Sciences, Université Ibn-Tofail, Kénitra;^(c)Faculté des Sciences Semlalia, Université Cadi Ayyad, LPHEA-Marrakech;^(d)LPMR, Faculté des Sciences, Université Mohamed Premier, Oujda;^(e)Faculté des sciences, Université Mohammed V, Rabat;^(f)Institute of Applied Physics, Mohammed VI Polytechnic University, Ben Guerir; Morocco.
- ³⁶CERN, Geneva; Switzerland.
- ³⁷Affiliated with an institute covered by a cooperation agreement with CERN.

- ³⁸Affiliated with an international laboratory covered by a cooperation agreement with CERN.
- ³⁹Enrico Fermi Institute, University of Chicago, Chicago IL; United States of America.
- ⁴⁰LPC, Université Clermont Auvergne, CNRS/IN2P3, Clermont-Ferrand; France.
- ⁴¹Nevis Laboratory, Columbia University, Irvington NY; United States of America.
- ⁴²Niels Bohr Institute, University of Copenhagen, Copenhagen; Denmark.
- ⁴³(^a)Dipartimento di Fisica, Università della Calabria, Rende; (^b)INFN Gruppo Collegato di Cosenza, Laboratori Nazionali di Frascati; Italy.
- ⁴⁴Physics Department, Southern Methodist University, Dallas TX; United States of America.
- ⁴⁵Physics Department, University of Texas at Dallas, Richardson TX; United States of America.
- ⁴⁶National Centre for Scientific Research "Demokritos", Agia Paraskevi; Greece.
- ⁴⁷(^a)Department of Physics, Stockholm University; (^b)Oskar Klein Centre, Stockholm; Sweden.
- ⁴⁸Deutsches Elektronen-Synchrotron DESY, Hamburg and Zeuthen; Germany.
- ⁴⁹Fakultät Physik, Technische Universität Dortmund, Dortmund; Germany.
- ⁵⁰Institut für Kern- und Teilchenphysik, Technische Universität Dresden, Dresden; Germany.
- ⁵¹Department of Physics, Duke University, Durham NC; United States of America.
- ⁵²SUPA - School of Physics and Astronomy, University of Edinburgh, Edinburgh; United Kingdom.
- ⁵³INFN e Laboratori Nazionali di Frascati, Frascati; Italy.
- ⁵⁴Physikalisches Institut, Albert-Ludwigs-Universität Freiburg, Freiburg; Germany.
- ⁵⁵II. Physikalisches Institut, Georg-August-Universität Göttingen, Göttingen; Germany.
- ⁵⁶Département de Physique Nucléaire et Corpusculaire, Université de Genève, Genève; Switzerland.
- ⁵⁷(^a)Dipartimento di Fisica, Università di Genova, Genova; (^b)INFN Sezione di Genova; Italy.
- ⁵⁸II. Physikalisches Institut, Justus-Liebig-Universität Giessen, Giessen; Germany.
- ⁵⁹SUPA - School of Physics and Astronomy, University of Glasgow, Glasgow; United Kingdom.
- ⁶⁰LPSC, Université Grenoble Alpes, CNRS/IN2P3, Grenoble INP, Grenoble; France.
- ⁶¹Laboratory for Particle Physics and Cosmology, Harvard University, Cambridge MA; United States of America.
- ⁶²(^a)Department of Modern Physics and State Key Laboratory of Particle Detection and Electronics, University of Science and Technology of China, Hefei; (^b)Institute of Frontier and Interdisciplinary Science and Key Laboratory of Particle Physics and Particle Irradiation (MOE), Shandong University, Qingdao; (^c)School of Physics and Astronomy, Shanghai Jiao Tong University, Key Laboratory for Particle Astrophysics and Cosmology (MOE), SKLPPC, Shanghai; (^d)Tsung-Dao Lee Institute, Shanghai; (^e)School of Physics and Microelectronics, Zhengzhou University; China.
- ⁶³(^a)Kirchhoff-Institut für Physik, Ruprecht-Karls-Universität Heidelberg, Heidelberg; (^b)Physikalisches Institut, Ruprecht-Karls-Universität Heidelberg, Heidelberg; Germany.
- ⁶⁴(^a)Department of Physics, Chinese University of Hong Kong, Shatin, N.T., Hong Kong; (^b)Department of Physics, University of Hong Kong, Hong Kong; (^c)Department of Physics and Institute for Advanced Study, Hong Kong University of Science and Technology, Clear Water Bay, Kowloon, Hong Kong; China.
- ⁶⁵Department of Physics, National Tsing Hua University, Hsinchu; Taiwan.
- ⁶⁶IJCLab, Université Paris-Saclay, CNRS/IN2P3, 91405, Orsay; France.
- ⁶⁷Centro Nacional de Microelectrónica (IMB-CNM-CSIC), Barcelona; Spain.
- ⁶⁸Department of Physics, Indiana University, Bloomington IN; United States of America.
- ⁶⁹(^a)INFN Gruppo Collegato di Udine, Sezione di Trieste, Udine; (^b)ICTP, Trieste; (^c)Dipartimento Politecnico di Ingegneria e Architettura, Università di Udine, Udine; Italy.
- ⁷⁰(^a)INFN Sezione di Lecce; (^b)Dipartimento di Matematica e Fisica, Università del Salento, Lecce; Italy.
- ⁷¹(^a)INFN Sezione di Milano; (^b)Dipartimento di Fisica, Università di Milano, Milano; Italy.
- ⁷²(^a)INFN Sezione di Napoli; (^b)Dipartimento di Fisica, Università di Napoli, Napoli; Italy.
- ⁷³(^a)INFN Sezione di Pavia; (^b)Dipartimento di Fisica, Università di Pavia, Pavia; Italy.

- 74^(a) INFN Sezione di Pisa; ^(b) Dipartimento di Fisica E. Fermi, Università di Pisa, Pisa; Italy.
- 75^(a) INFN Sezione di Roma; ^(b) Dipartimento di Fisica, Sapienza Università di Roma, Roma; Italy.
- 76^(a) INFN Sezione di Roma Tor Vergata; ^(b) Dipartimento di Fisica, Università di Roma Tor Vergata, Roma; Italy.
- 77^(a) INFN Sezione di Roma Tre; ^(b) Dipartimento di Matematica e Fisica, Università Roma Tre, Roma; Italy.
- 78^(a) INFN-TIFPA; ^(b) Università degli Studi di Trento, Trento; Italy.
- 79 Universität Innsbruck, Department of Astro and Particle Physics, Innsbruck; Austria.
- 80 University of Iowa, Iowa City IA; United States of America.
- 81 Department of Physics and Astronomy, Iowa State University, Ames IA; United States of America.
- 82 Istinye University, Sariyer, Istanbul; Türkiye.
- 83^(a) Departamento de Engenharia Elétrica, Universidade Federal de Juiz de Fora (UFJF), Juiz de Fora; ^(b) Universidade Federal do Rio De Janeiro COPPE/EE/IF, Rio de Janeiro; ^(c) Instituto de Física, Universidade de São Paulo, São Paulo; ^(d) Rio de Janeiro State University, Rio de Janeiro; Brazil.
- 84 KEK, High Energy Accelerator Research Organization, Tsukuba; Japan.
- 85 Graduate School of Science, Kobe University, Kobe; Japan.
- 86^(a) AGH University of Krakow, Faculty of Physics and Applied Computer Science, Krakow; ^(b) Marian Smoluchowski Institute of Physics, Jagiellonian University, Krakow; Poland.
- 87 Institute of Nuclear Physics Polish Academy of Sciences, Krakow; Poland.
- 88 Faculty of Science, Kyoto University, Kyoto; Japan.
- 89 Research Center for Advanced Particle Physics and Department of Physics, Kyushu University, Fukuoka ; Japan.
- 90 Instituto de Física La Plata, Universidad Nacional de La Plata and CONICET, La Plata; Argentina.
- 91 Physics Department, Lancaster University, Lancaster; United Kingdom.
- 92 Oliver Lodge Laboratory, University of Liverpool, Liverpool; United Kingdom.
- 93 Department of Experimental Particle Physics, Jožef Stefan Institute and Department of Physics, University of Ljubljana, Ljubljana; Slovenia.
- 94 School of Physics and Astronomy, Queen Mary University of London, London; United Kingdom.
- 95 Department of Physics, Royal Holloway University of London, Egham; United Kingdom.
- 96 Department of Physics and Astronomy, University College London, London; United Kingdom.
- 97 Louisiana Tech University, Ruston LA; United States of America.
- 98 Fysiska institutionen, Lunds universitet, Lund; Sweden.
- 99 Departamento de Física Teórica C-15 and CIAFF, Universidad Autónoma de Madrid, Madrid; Spain.
- 100 Institut für Physik, Universität Mainz, Mainz; Germany.
- 101 School of Physics and Astronomy, University of Manchester, Manchester; United Kingdom.
- 102 CPPM, Aix-Marseille Université, CNRS/IN2P3, Marseille; France.
- 103 Department of Physics, University of Massachusetts, Amherst MA; United States of America.
- 104 Department of Physics, McGill University, Montreal QC; Canada.
- 105 School of Physics, University of Melbourne, Victoria; Australia.
- 106 Department of Physics, University of Michigan, Ann Arbor MI; United States of America.
- 107 Department of Physics and Astronomy, Michigan State University, East Lansing MI; United States of America.
- 108 Group of Particle Physics, University of Montreal, Montreal QC; Canada.
- 109 Fakultät für Physik, Ludwig-Maximilians-Universität München, München; Germany.
- 110 Max-Planck-Institut für Physik (Werner-Heisenberg-Institut), München; Germany.
- 111 Graduate School of Science and Kobayashi-Maskawa Institute, Nagoya University, Nagoya; Japan.
- 112 Department of Physics and Astronomy, University of New Mexico, Albuquerque NM; United States of

America.

¹¹³Institute for Mathematics, Astrophysics and Particle Physics, Radboud University/Nikhef, Nijmegen; Netherlands.

¹¹⁴Nikhef National Institute for Subatomic Physics and University of Amsterdam, Amsterdam; Netherlands.

¹¹⁵Department of Physics, Northern Illinois University, DeKalb IL; United States of America.

¹¹⁶^(a)New York University Abu Dhabi, Abu Dhabi; ^(b)University of Sharjah, Sharjah; United Arab Emirates.

¹¹⁷Department of Physics, New York University, New York NY; United States of America.

¹¹⁸Ochanomizu University, Otsuka, Bunkyo-ku, Tokyo; Japan.

¹¹⁹Ohio State University, Columbus OH; United States of America.

¹²⁰Homer L. Dodge Department of Physics and Astronomy, University of Oklahoma, Norman OK; United States of America.

¹²¹Department of Physics, Oklahoma State University, Stillwater OK; United States of America.

¹²²Palacký University, Joint Laboratory of Optics, Olomouc; Czech Republic.

¹²³Institute for Fundamental Science, University of Oregon, Eugene, OR; United States of America.

¹²⁴Graduate School of Science, Osaka University, Osaka; Japan.

¹²⁵Department of Physics, University of Oslo, Oslo; Norway.

¹²⁶Department of Physics, Oxford University, Oxford; United Kingdom.

¹²⁷LPNHE, Sorbonne Université, Université Paris Cité, CNRS/IN2P3, Paris; France.

¹²⁸Department of Physics, University of Pennsylvania, Philadelphia PA; United States of America.

¹²⁹Department of Physics and Astronomy, University of Pittsburgh, Pittsburgh PA; United States of America.

¹³⁰^(a)Laboratório de Instrumentação e Física Experimental de Partículas - LIP, Lisboa; ^(b)Departamento de Física, Faculdade de Ciências, Universidade de Lisboa, Lisboa; ^(c)Departamento de Física, Universidade de Coimbra, Coimbra; ^(d)Centro de Física Nuclear da Universidade de Lisboa, Lisboa; ^(e)Departamento de Física, Universidade do Minho, Braga; ^(f)Departamento de Física Teórica y del Cosmos, Universidad de Granada, Granada (Spain); ^(g)Departamento de Física, Instituto Superior Técnico, Universidade de Lisboa, Lisboa; Portugal.

¹³¹Institute of Physics of the Czech Academy of Sciences, Prague; Czech Republic.

¹³²Czech Technical University in Prague, Prague; Czech Republic.

¹³³Charles University, Faculty of Mathematics and Physics, Prague; Czech Republic.

¹³⁴Particle Physics Department, Rutherford Appleton Laboratory, Didcot; United Kingdom.

¹³⁵IRFU, CEA, Université Paris-Saclay, Gif-sur-Yvette; France.

¹³⁶Santa Cruz Institute for Particle Physics, University of California Santa Cruz, Santa Cruz CA; United States of America.

¹³⁷^(a)Departamento de Física, Pontificia Universidad Católica de Chile, Santiago; ^(b)Millennium Institute for Subatomic physics at high energy frontier (SAPHIR), Santiago; ^(c)Instituto de Investigación Multidisciplinario en Ciencia y Tecnología, y Departamento de Física, Universidad de La Serena; ^(d)Universidad Andres Bello, Department of Physics, Santiago; ^(e)Instituto de Alta Investigación, Universidad de Tarapacá, Arica; ^(f)Departamento de Física, Universidad Técnica Federico Santa María, Valparaíso; Chile.

¹³⁸Department of Physics, University of Washington, Seattle WA; United States of America.

¹³⁹Department of Physics and Astronomy, University of Sheffield, Sheffield; United Kingdom.

¹⁴⁰Department of Physics, Shinshu University, Nagano; Japan.

¹⁴¹Department Physik, Universität Siegen, Siegen; Germany.

¹⁴²Department of Physics, Simon Fraser University, Burnaby BC; Canada.

- ¹⁴³SLAC National Accelerator Laboratory, Stanford CA; United States of America.
- ¹⁴⁴Department of Physics, Royal Institute of Technology, Stockholm; Sweden.
- ¹⁴⁵Departments of Physics and Astronomy, Stony Brook University, Stony Brook NY; United States of America.
- ¹⁴⁶Department of Physics and Astronomy, University of Sussex, Brighton; United Kingdom.
- ¹⁴⁷School of Physics, University of Sydney, Sydney; Australia.
- ¹⁴⁸Institute of Physics, Academia Sinica, Taipei; Taiwan.
- ¹⁴⁹^(a)E. Andronikashvili Institute of Physics, Iv. Javakhishvili Tbilisi State University, Tbilisi; ^(b)High Energy Physics Institute, Tbilisi State University, Tbilisi; ^(c)University of Georgia, Tbilisi; Georgia.
- ¹⁵⁰Department of Physics, Technion, Israel Institute of Technology, Haifa; Israel.
- ¹⁵¹Raymond and Beverly Sackler School of Physics and Astronomy, Tel Aviv University, Tel Aviv; Israel.
- ¹⁵²Department of Physics, Aristotle University of Thessaloniki, Thessaloniki; Greece.
- ¹⁵³International Center for Elementary Particle Physics and Department of Physics, University of Tokyo, Tokyo; Japan.
- ¹⁵⁴Department of Physics, Tokyo Institute of Technology, Tokyo; Japan.
- ¹⁵⁵Department of Physics, University of Toronto, Toronto ON; Canada.
- ¹⁵⁶^(a)TRIUMF, Vancouver BC; ^(b)Department of Physics and Astronomy, York University, Toronto ON; Canada.
- ¹⁵⁷Division of Physics and Tomonaga Center for the History of the Universe, Faculty of Pure and Applied Sciences, University of Tsukuba, Tsukuba; Japan.
- ¹⁵⁸Department of Physics and Astronomy, Tufts University, Medford MA; United States of America.
- ¹⁵⁹United Arab Emirates University, Al Ain; United Arab Emirates.
- ¹⁶⁰Department of Physics and Astronomy, University of California Irvine, Irvine CA; United States of America.
- ¹⁶¹Department of Physics and Astronomy, University of Uppsala, Uppsala; Sweden.
- ¹⁶²Department of Physics, University of Illinois, Urbana IL; United States of America.
- ¹⁶³Instituto de Física Corpuscular (IFIC), Centro Mixto Universidad de Valencia - CSIC, Valencia; Spain.
- ¹⁶⁴Department of Physics, University of British Columbia, Vancouver BC; Canada.
- ¹⁶⁵Department of Physics and Astronomy, University of Victoria, Victoria BC; Canada.
- ¹⁶⁶Fakultät für Physik und Astronomie, Julius-Maximilians-Universität Würzburg, Würzburg; Germany.
- ¹⁶⁷Department of Physics, University of Warwick, Coventry; United Kingdom.
- ¹⁶⁸Waseda University, Tokyo; Japan.
- ¹⁶⁹Department of Particle Physics and Astrophysics, Weizmann Institute of Science, Rehovot; Israel.
- ¹⁷⁰Department of Physics, University of Wisconsin, Madison WI; United States of America.
- ¹⁷¹Fakultät für Mathematik und Naturwissenschaften, Fachgruppe Physik, Bergische Universität Wuppertal, Wuppertal; Germany.
- ¹⁷²Department of Physics, Yale University, New Haven CT; United States of America.
- ^a Also Affiliated with an institute covered by a cooperation agreement with CERN.
- ^b Also at An-Najah National University, Nablus; Palestine.
- ^c Also at Borough of Manhattan Community College, City University of New York, New York NY; United States of America.
- ^d Also at Center for High Energy Physics, Peking University; China.
- ^e Also at Center for Interdisciplinary Research and Innovation (CIRI-AUTH), Thessaloniki; Greece.
- ^f Also at Centro Studi e Ricerche Enrico Fermi; Italy.
- ^g Also at CERN, Geneva; Switzerland.
- ^h Also at Département de Physique Nucléaire et Corpusculaire, Université de Genève, Genève; Switzerland.

- i* Also at Departament de Fisica de la Universitat Autònoma de Barcelona, Barcelona; Spain.
- j* Also at Department of Financial and Management Engineering, University of the Aegean, Chios; Greece.
- k* Also at Department of Physics, Ben Gurion University of the Negev, Beer Sheva; Israel.
- l* Also at Department of Physics, California State University, Sacramento; United States of America.
- m* Also at Department of Physics, King's College London, London; United Kingdom.
- n* Also at Department of Physics, Stanford University, Stanford CA; United States of America.
- o* Also at Department of Physics, University of Fribourg, Fribourg; Switzerland.
- p* Also at Department of Physics, University of Thessaly; Greece.
- q* Also at Department of Physics, Westmont College, Santa Barbara; United States of America.
- r* Also at Hellenic Open University, Patras; Greece.
- s* Also at Institutio Catalana de Recerca i Estudis Avancats, ICREA, Barcelona; Spain.
- t* Also at Institut für Experimentalphysik, Universität Hamburg, Hamburg; Germany.
- u* Also at Institute for Nuclear Research and Nuclear Energy (INRNE) of the Bulgarian Academy of Sciences, Sofia; Bulgaria.
- v* Also at Institute of Applied Physics, Mohammed VI Polytechnic University, Ben Guerir; Morocco.
- w* Also at Institute of Particle Physics (IPP); Canada.
- x* Also at Institute of Physics and Technology, Ulaanbaatar; Mongolia.
- y* Also at Institute of Physics, Azerbaijan Academy of Sciences, Baku; Azerbaijan.
- z* Also at Institute of Theoretical Physics, Ilia State University, Tbilisi; Georgia.
- aa* Also at L2IT, Université de Toulouse, CNRS/IN2P3, UPS, Toulouse; France.
- ab* Also at Lawrence Livermore National Laboratory, Livermore; United States of America.
- ac* Also at National Institute of Physics, University of the Philippines Diliman (Philippines); Philippines.
- ad* Also at Technical University of Munich, Munich; Germany.
- ae* Also at The Collaborative Innovation Center of Quantum Matter (CICQM), Beijing; China.
- af* Also at TRIUMF, Vancouver BC; Canada.
- ag* Also at Università di Napoli Parthenope, Napoli; Italy.
- ah* Also at University of Chinese Academy of Sciences (UCAS), Beijing; China.
- ai* Also at University of Colorado Boulder, Department of Physics, Colorado; United States of America.
- aj* Also at Washington College, Chestertown, MD; United States of America.
- ak* Also at Yeditepe University, Physics Department, Istanbul; Türkiye.
- * Deceased